DOCUMENTING MODERN AND ANCIENT METHANE RELEASE FROM COLD SEEPS USING DEEP-SEA BENTHIC FORAMINIFERA

BY

SHELLEY ANNE DAY

A THESIS PRESENTED TO THE GRADUATE SCHOOL
OF THE UNIVERSITY OF FLORIDA IN PARTIAL FULFILLMENT
OF THE REQUIREMENTS FOR THE DEGREE OF
MASTER OF SCIENCE

UNIVERSITY OF FLORIDA

2003

ACKNOWLEDGMENTS

This research was funded by NOAA-NURP Grant numbers UAF98-0043 and FP007222. There are many people I wish to thank for their help and support on this project. First, I would like to thank my advisor, Dr. Jonathan Martin, for providing me with this research opportunity and his invaluable guidance and editorial assistance. I would also like to thank my other committee members, Dr. Anthony Randazzo, Dr. David Hodell and Dr. John Jaeger, for their time and advice. I thank Anthony Rathburn and Elena Pérez for contributing live foraminifera to this study, as well as assisting in identifying fossil foraminifera. In addition, I would like to thank Joris Gieskes for contributing pore water solute data. I thank Jason Curtis for his endless assistance in the stable isotope lab. Finally, I would like to thank my family for providing me with support and guidance throughout my life.

TABLE OF CONTENTS

page

LIST OF TABLES

LIST OF FIGURES

Abstract of Thesis Presented to the Graduate School
of the University of Florida in Partial Fulfillment of the
Requirements for the Degree of Master of Science

DOCUMENTING MODERN AND ANCIENT METHANE RELEASE FROM COLD SEEPS USING DEEP-SEA BENTHIC FORAMINIFERA

By

Shelley Anne Day

May 2003

Chair: Jonathan Martin
Major Department: Geological Sciences

Methane, which is a potent greenhouse gas and a highly reduced form of carbon, is a minor component of the atmosphere; however, large amounts of methane are stored in continental margin sediments as a component of pressure and temperature sensitive gas hydrates. Dissociation of these hydrates and the release of methane, which could have important climatic implications, have been inferred in the past based on the isotopic composition of fossil foraminifera in prior paleoceanographic studies. Little analogous data from modern seep sites exist to document the significance of released methane on foraminiferal isotopic composition.

Methane is commonly released from cold seep environments, which are ideal settings to investigate the relationship between methane and the isotopic composition of foraminifera. For this study the stable isotopic compositions of living (Rose Bengal stained) and fossil benthic foraminifera from active seepage sites in Monterey Bay (1000

m) and the Eel River Basin (~520 m) on the California margin were used along with pore water chemistry to assess the effects of methane on foraminiferal carbonate.

Live and fossil benthic foraminifera from these seep sites were found to have carbon isotopic compositions that are more variable than the same species of foraminifera previously measured from non-seep sites on the California and North Carolina margins. In general, the carbon isotopic values of the seep foraminifera were similar to or up to a few per mil lighter than the isotopic values of foraminifera found in non-seep sites. The isotopic values of the seep foraminifera, however, are far from equilibrium with the ambient dissolved inorganic carbon pool, which has carbon isotopic values as light as -45‰ in the upper 5 cm of the core. This disequilibrium could indicate that the foraminifera have specific microenvironments where calcification takes place, possibly near the surface or near burrows where seawater DIC ($\delta^{13}C_{DIC}$ approximately 0‰) would contribute more to the DIC pool. The isotopic composition of the DIC, which would vary with the episodic seepage of methane, does create variability in foraminiferal carbon isotope values.

In contrast with the large disequilibrium observed among foraminifera and $\delta^{13}C_{DIC}$ values in Monterey Bay, large negative carbon isotopic excursions, as light as -23‰, are seen in Eel River foraminifera. These light isotope ratios appear to result from postmortem precipitation of authigenic carbonate, which is in equilibrium with the $\delta^{13}C_{DIC}$, on the tests. Faster seepage rates or more profuse seepage at Eel River could cause authigenic carbonate precipitation to occur in Eel River and not Monterey Bay. Therefore, variability in the isotopic composition of conspecific foraminifera appears to be a better indication of methane release than absolute isotopic values.

CHAPTER 1
INTRODUCTION

Methane, which contains a highly reduced form of carbon, plays an important role in many of the biological and geochemical processes on Earth. Although methane is a minor component of the atmosphere, it has nevertheless received considerable attention due to its potential as a powerful greenhouse gas. The realization that large amounts of methane are stored subaqueously, frozen as "gas hydrates" within a temperature and pressure sensitive solid framework of water molecules, has led to suggestions that methane may have played an important role in the Earth's climatic history (Wefer et al., 1994; Dickens et al., 1995; Kennett et al., 1996). For instance, the abrupt warming which characterizes the first few decades of interglacials and interstadials is accompanied by rapid increases in atmospheric methane (Severinghaus et al., 1998).

Gas hydrates are temperature and pressure sensitive; therefore, the dissociation of gas hydrates would result from warmer climatic conditions and warmer waters or lower sea levels. Methane released from subaqueous gas hydrates could diffuse up through the sedimentary column, be oxidized by bacteria and contribute bicarbonate to the dissolved inorganic carbon pool and possibly be incorporated into foraminiferal tests. Using foraminifera as a proxy, Kennett et al. (2000) proposed that changes in thermohaline circulation over the past 60,000 years in the Santa Barbara Basin resulted in fluctuations in water temperature. In turn, variable water temperatures resulted in the periodic destabilization of gas hydrates, which contributed isotopically light carbon and heavy

oxygen to planktonic and benthic foraminifera living within the Santa Barbara Basin (Kennett et al., 2000).

If the isotopic values obtained from fossil foraminifera preserve ancient pore-water conditions, then the stratigraphic variation in these values would provide a record of methane seepage. In addition to the anomalously negative carbon isotopic compositions of fossilized benthic foraminifera suggested to result from gas hydrate dissociation (Kennett et al., 1996; 2000; Dickens et al., 1995; Wefer et al., 1994), diverse carbon isotopic compositions are reported for live and fossil benthic foraminifera inhabiting methane seep sites (Sen Gupta and Aharon, 1994; Rathburn et al., 2000). These recent studies (Rathburn et al., 2000; Williams et al., 2002) question the validity of a direct link between methane seepage and a light $\delta^{13}C$ foraminiferal test value. Seepage instead may be inferred based on the heterogeneity of carbon isotope values and the similarity of oxygen isotope values among numerous tests collected from identical depths (i.e., times of deposition). There is, however, a scarcity of analogous data available from modern (living) foraminifera to evaluate this hypothesis. Therefore, it is the intent of this work to show that the magnitude of the $\delta^{13}C$ of benthic foraminifera (live and fossil) alone does not reliably indicate methane and associated dissolved inorganic carbon (DIC) venting from marine sediments; however, when numerous foraminifera from areas of seepage are analyzed, methane venting is manifested in the heterogeneity of foraminiferal carbon isotope values among coexisting conspecific individuals.

The Correlation between Climate and Methane

In recent years, research focusing on the causes of global climate change, particularly global warming, has intensified. Greenhouse gases, such as carbon dioxide

and methane, which contribute to the global warming of the earth, are of particular concern. The effect that greenhouse gases have on the atmosphere not only depends on their concentrations but also on their residence times in the atmosphere and the width of their absorption bands. As a result of methane absorbing radiation in the wavelength band between 8000-12000 nm, where carbon dioxide is not an effective absorber, 1 kg of methane has the potential to absorb 21 times the infrared radiation as 1 kg of carbon dioxide (Houghton et al., 1990). Thus, the carbon cycle and climate change could be significantly affected by the release of methane. One of the major reservoirs of methane is believed to be in gas hydrates formed and trapped in continental margin settings (Kvenvolden, 1988).

Natural gas hydrates are formed when a rigid framework of water molecules freezes in the presence of sufficient natural gases; the water crystallizes in a cubic lattice and traps the gas molecules (MacDonald, 1990). Methane is the dominant gas found in most oceanic gas hydrates, representing greater than 98% of the total gas, although ethane, carbon dioxide, and hydrogen sulfide may also be significant in some regions (Dickens, 2001). According to Kvenvolden (1988), the amount of methane currently stored within subaqueous gas hydrates may be in excess of 10^{19} g of methane carbon. This estimation exceeds the amount of methane stored in all other reservoirs combined (Table 1-1).

The stability of gas hydrates is a function of temperature, pressure, salinity, and gas concentration, with hydrates commonly forming in the oceans where water depths are between 300 and 2000 meters and temperatures are less than 5° C (Kvenvolden, 1988). Hydrates form rapidly, within minutes, both in free seawater and in sediments based on

experiments conducted in the waters of Monterey Bay (Brewer et al., 1997); similarly, the hydrates dissociated rapidly during the experiment, first with bubbles being emitted from the sediments and then with continuing gas expansion, the dissociating hydrates ruptured the cylinders housing the experiment (Brewer et al., 1997). In natural settings, once the gas hydrates are no longer within the stability field, for example by changing ambient conditions (such as a pressure decrease due to the removal of overburden), the gases may migrate upward through the sedimentary column and reach the seafloor, depending upon the texture and porosity of the sediment. Such emissions of methane (and other gases) at ambient seafloor temperatures are often termed cold seeps.

Table 1-1. A list of the amount of organic carbon (g) stored in the various reservoirs.

Reservoir	**Amount of organic carbon (g)**
Gas hydrates	$>10^{19}$
All fossil fuel deposits	$5 \cdot 10^{18}$
Terrestrial soil, detritus, and peat	$1.96 \cdot 10^{18}$
Marine dissolved materials	$9.8 \cdot 10^{17}$
Terrestrial biota	$8.3 \cdot 10^{17}$
Atmosphere	$3.6 \cdot 10^{15}$
Marine biota	$3 \cdot 10^{15}$

Data from Kvenvolden (1988).

The methane emitted from cold seeps may be either biogenic or thermogenic in origin. Biogenic methane is produced in shallow sediments as a result of the microbial degradation of organic matter. Thermogenic methane results from the thermochemical dissociation of organic matter at high temperatures and depths (2-3 km). The two sources may be distinguished based on the carbon isotopic signature of the methane. In general, microbially produced methane is isotopically lighter than thermogenic methane, which is characterized by $\delta^{13}C$ values ranging from -50 to -20‰ (Whiticar, 1999). Biogenic

methane typically exhibits $\delta^{13}C$ values less than -50‰ (Whiticar, 1999). Regardless of its source, the $\delta^{13}C$ of methane is isotopically lighter than the inorganic forms of carbon dissolved in seawater, which have a $\delta^{13}C$ of approximately 0‰ PDB. Therefore, if isotopically light methane reaches the sediment-water interface, it would decrease the $\delta^{13}C$ of DIC after being oxidized in the pore waters. These light isotope ratios are retained in the authigenic carbonate minerals that form from the isotopically light DIC; however, it is unknown whether benthic foraminifera preserve these signatures. Inferring seepage based on benthic foraminiferal carbonate rather than authigenic carbonate would be valuable, as benthic foraminifera are characterized by a relatively short lifespan (on the order of years) and would provide a stratigraphic component, which may provide clues to the longevity of seepage.

Today the majority of natural atmospheric methane is produced as a result of bacterial decomposition in wetland environments (Blunier, 2000). It has been proposed, however, that during former periods of rapid climate change, large quantities of methane were released to the oceans and atmosphere as a result of the dissociation of gas hydrates (Wefer et al., 1994; Dickens et al., 1995; Kennett et al., 1996; 2000). For instance, off Peru, Dickens et al. (1995) attributed a –2 to –3‰ shift in benthic foraminiferal $\delta^{13}C$ and $\delta^{18}O$ in less than 10^4 years (during the late Paleocene) to the dissociation of hydrates, which were thought to have destabilized due to a 4ºC increase in bottom water temperature (Dickens et al., 1995). Additionally, in the Santa Barbara Basin, Kennett et al. (2000) attributed a large carbon isotopic excursion to hydrate destabilization; this excursion was characterized by interstadial benthic foraminifera being lighter by up to 4‰ relative to stadial foraminifera.

Methane and the Stable Isotopic Composition of Benthic Foraminifera

The flux of methane into the water column, and eventually the atmosphere, would be much greater were it not for the bacterial consumption of methane, which catalyzes inorganic methane oxidation. Methane that is migrating upward in the sedimentary column may be oxidized by either aerobic or anaerobic bacteria, known as methanotrophs, depending on the availability of free oxygen. Aerobic methanotrophs are able to use methane as an energy source through the production of carbon dioxide; these organisms are found living within the pores of sediments and in the tissues of benthic fauna associated with cold seeps (Cavagna et al., 1999). Alternatively, anaerobic methanotrophs interact with another microbial group, the hydrogen-oxidizing-sulfate-reducers, in order to drive the metabolic transformation of methane into bicarbonate (and sulfate into hydrogen sulfide) (DeLong, 2000). Another bacterial process occurs in the water column, where free-living methanotrophs oxidize methane; these organisms create carbon dioxide plumes, which when diluted with normal bottom waters can deplete the $\delta^{13}C_{DIC}$ by 4.5‰ (Aharon et al., 1992; LaRock et al., 1994).

The production of bicarbonate due to the activity of methanogens has a profound effect on the pore-water chemistry and possibly the isotopic composition of benthic foraminifera. Studies have shown that foraminifera found within seepage areas have more negative $\delta^{13}C$ signatures than foraminifera found within areas unaffected by seepage (Sen Gupta and Aharon, 1994). For instance, fossil benthic foraminifera from venting sites in the Gulf of Mexico had anomalously depleted $\delta^{13}C$ values (as light as –3.6‰), whereas fossil benthic foraminifera from non-seep sites displayed $\delta^{13}C$ values as heavy as 0.4 ‰ (Sen Gupta and Aharon, 1994).

Pore-water Chemistry, Vital Effects, and Foraminiferal Composition

In addition to ambient pore-water chemistry, taxon-specific "vital" effects and microhabitat effects also influence the geochemistry of benthic foraminiferal test carbonate (McCorkle et al., 1990). Vital effects, which are a result of physiological processes, can be divided into two categories: metabolic isotope effects and kinetic isotope effects. Metabolic effects result from the incorporation of respired, isotopically light carbon dioxide into the foraminiferal test, which results in a depletion of ^{13}C in the test (Grossman, 1987), whereas kinetic effects occur during periods of rapid chamber formation, when lighter isotopes of carbon and oxygen are preferentially incorporated (McConnaughey, 1989).

Microhabitat effects can be attributed to foraminifera living within the sediment at specific depths, where variations in the pore-water DIC may influence the $\delta^{13}C$ of the test. For instance, infaunal taxa display consistently lower $\delta^{13}C$ values than epifaunal taxa. Additionally, deep-dwelling species are consistently more depleted in ^{13}C than either shallow infaunal species or epifaunal species as a result of the decrease in the $\delta^{13}C$ of pore-water DIC with sediment depth (McCorkle et al., 1990). However, despite these recognized trends, for any particular species that displays a broad depth range within the sediment, the variability of $\delta^{13}C$ values is low, despite the depth at which the foraminiferan is found (Rathburn et al., 1996). While it has been proposed that the isotopic uniformity within a given species results from microenvironments, food preferences, or growth within a narrow depth range, the influence of pore-water chemistry on the isotopic composition of foraminiferal tests remains debatable (Rathburn et al., 1996; 2000).

Diagenesis

In addition to influencing the isotopic composition of live foraminifera, pore water chemistry may alter the isotopic composition of fossil foraminifera through diagenesis; contamination by biogenic calcite or post mortem calcite overgrowths is another plausible explanation for the negative $\delta^{13}C$ values observed in some fossil foraminifera. In marine settings, a consortium of bacteria produces bicarbonate while oxidizing organic matter and methane. Production of bicarbonate is enhanced at seep settings, where large quantities of methane are able to support a large population of bacteria. Carbonate precipitation may be enhanced by the production of bicarbonate, which would drive the reaction

$$Ca^{2+} + 2HCO_3^- \leftrightarrow CaCO_3 + H_2O + CO_2 \qquad (1)$$

to the right. Additionally, carbonate precipitation should be enhanced at the sulfate/methane boundary where localized anaerobic methane oxidation may produce a sharp increase in the alkalinity of the pore water (Blair and Aller, 1995).

Authigenic carbonate is present at Eel River and Monterey Bay seep sites (Stakes et al., 1999; Rathburn et al., 2000; this study). Thin sections of authigenic carbonates from Monterey Bay often contained pyrite framboids encased in high-Mg calcite filling the chambers of the *U. peregrina*, which are composed of low-Mg calcite (Stakes et al., 1999). Pristine *U. peregrina* tests, however, were also found in a groundmass of high-Mg calcite (Stakes et al., 1999). It is unknown whether fine-grained authigenic carbonates are being precipitated within the chambers of fossil foraminifera in unlithified sediments, such as those analyzed for this study. Although foraminifera designated for isotopic analysis are microscopically examined for calcite contamination and cleaned

ultrasonically, this technique may not detect authigenic carbonate grains that may be present inside some of the chambers of the test. If authigenic carbonate was contaminating foraminiferal tests, carbon and oxygen isotopic compositions would be expected to be widely variable in a large population of analyzed foraminifera.

The problem of diagenetic alteration can be approached through thermodynamics, by calculating saturation states. In thermodynamic modeling the chemical analysis of water is used to calculate the distribution of aqueous species. Saturation Indices (SI) determine whether a mineral should dissolve or precipitate. A positive saturation index for a mineral indicates that the pore water is oversaturated with respect to that mineral and thermodynamically, precipitation is favored. A negative value indicates that the pore water is undersaturated and dissolution of that mineral is thermodynamically favored. This technique assumes that the pore water composition has not changed from the time of deposition. With burial, however, the pore water should become increasingly saturated with respect to calcite through the diagenetic pathway shown by reaction (1).

Objective/Scope of Research

The primary objectives of this study are twofold: (1) to determine whether benthic foraminifera reliably record modern and historic sites of methane and associated DIC venting from cold seeps and (2) to determine how this record may be manifested in the isotopic composition of the foraminifera. While investigating this broad objective, the following more specific questions are addressed:

> 1. What is the relationship between the isotopic signature of foraminiferal carbonate and the isotopic signature of ambient pore-water in methane seep environments? What variations exist in the isotopic signatures of individual species within and between different seep settings? How do the stable isotopic signatures of benthic foraminifera from cold methane seeps compare to those generated in non-seep environments?

2. Does methane seepage create a distinct isotopic signature in benthic foraminiferal tests that may serve to map the extent and history of methane fluxes? If so, can isotopic signatures of fossil benthic foraminifera be used to identify the longevity and the extent of venting?

3. Within a given methane seep environment, do different species of benthic foraminifera have different carbon isotopic compositions? Are isotopic differences enhanced between epifaunal and infaunal species in methane seep environments?

Along with analyzing fossil benthic foraminiferal tests, this study also examines live (stained) deep-sea benthic foraminifera to determine the relationship between methane release and test composition, isotopic variability within a given species, and the variations in test composition generated by seep and non-seep environments. McCorkle et al. (1990) analyzed the isotopic composition of live foraminifera from both the Atlantic and Pacific Oceans. Their main objective, however, was to identify the relationship between microhabitats and the carbon isotopic composition of foraminiferal tests. One previous study published by Rathburn et al. (2000) researched the relationship between live foraminifera and methane seepage off the slope of the Eel River, California. However, the limited number of live foraminiferal specimens, the lack of $\delta^{13}C_{DIC}$ analyses, and the limited geographic coverage has left unanswered questions regarding methane release and foraminiferal test composition.

Study Areas

Monterey Bay

Monterey Bay provides an ideal location to investigate methane release from cold seeps (Figure 1-1). The bay is underlain by the Salinian block, which is an allochthonous granodiorite basement rock that has moved northward during the past 21 million years of activity along the San Andreas Fault (Page, 1970). The Salinian granodiorite, along with the San Simeon block, are the two major tectonic provinces within the bay (Greene et al.,

1993). The Miocene Monterey Formation, which along with its equivalents, are organic-rich marine sediments, the Late Miocene Santa Cruz mudstone, and the Miocene-Pliocene Purisma sandstone crop out offshore and along canyon walls (Greene et al., 1989). Numerous faults, including the San Gregorio and Monterey Bay Fault Zones, dissect the bay creating a dynamic environment characterized by fluid flow (Orange et al., 1999). Cold seeps have been found both as isolated communities along these major faults (Barry et al., 1996) or among isolated zones of active mud volcanism (Martin et al., 1997). Pore-water analyses obtained from push cores located within the cold seeps revealed methane concentrations up to 841 μM (Barry et al., 1997).

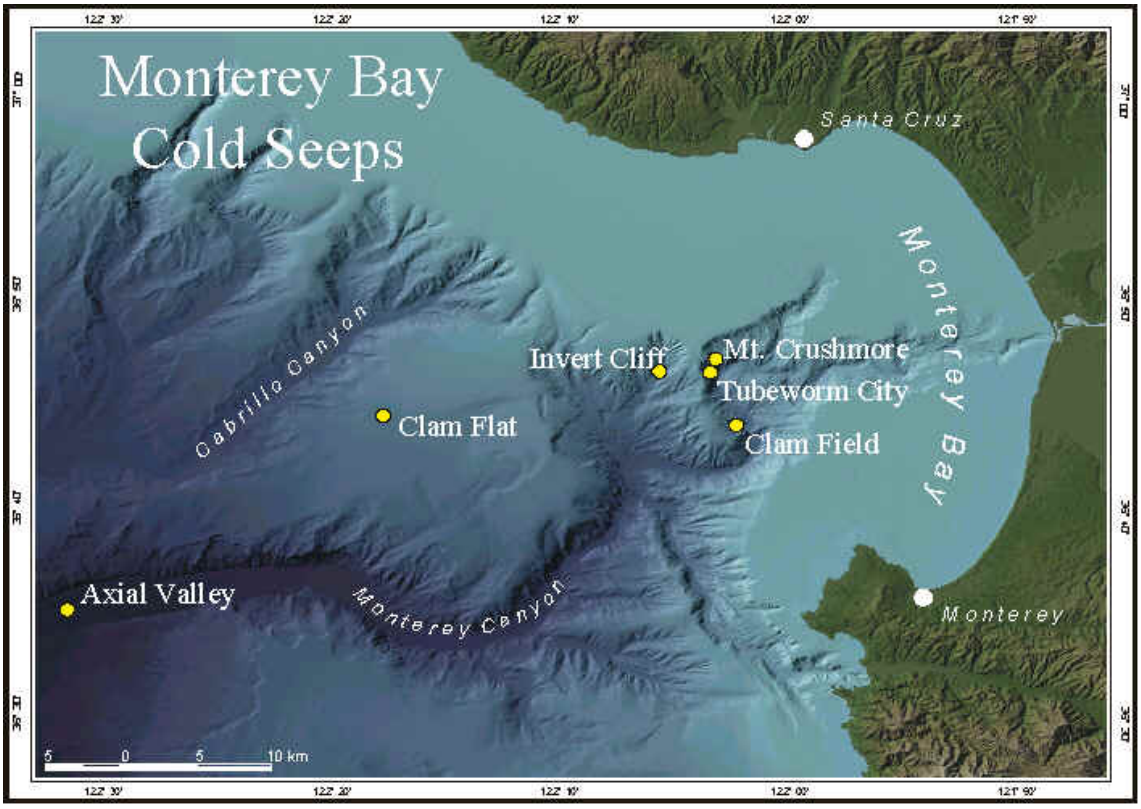

Figure 1-1. Map showing the location of Monterey Bay cold seeps, including Clam Flats and Invertebrate Cliffs, which were sampled in this study (taken from http://www.mbari.org/benthic/coldseeploc.htm).

At present in Monterey Bay, there are no known exposures of clathrates; however, discrete cold seeps sampled in the bay contain gaseous hydrocarbons and high molecular

weight aliphatic and aromatic hydrocarbons (Lorenson et al., 2002). Since no clathrates have been detected in Monterey Bay, fluid flow is instead likely the result of tectonic compression, with interstitial fluids migrating upward in the sedimentary column along faults (Lorenson et. al, 2002).

The methane seeping from Monterey Bay is likely to come from one of two sources. The organic-rich Monterey Formation provides a thermogenic source for the methane (Martin et al., 1997; Stakes et al., 1999), whereas the microbial reduction of carbon dioxide below the sulfate reduction zone provides a biologic source. Stakes et al. (1999) proposed that biological communities appear to be related to a deep source of reduced carbon, rather than a surficial source, based on the spatial arrangement of the communities. The isotopic composition of most sites however, points to a mixed origin for the methane (Martin et al., 1997).

Eel River

The Eel River Basin (Figure 1-2), which is part of a late Cenozoic forearc, extends approximately 210 km, from Cape Mendocino, California to Cape Sebastian, Oregon; the basin is bounded by the Cascadia subduction zone to the west, and the Mendocino Fracture Zone to south (Burger et al., 2002). The structural evolution of the basin continues today, as the convergence of the Gorda and North America plates continues; additionally, much of the deformation in the southern portion of the basin results from the continuing northward migration of the Mendocino Triple Junction (Furlong and Govers, 1999).

Although there are some similarities shared by Monterey Bay and the Eel River Basin, one major difference is the presence of gas hydrates in the Eel River Basin (Table 1-2). Kvenvolden and Field (1985) mapped the distribution of hydrates in the Eel River

basin using the location of the bottom-simulating reflector (BSR). The BSR is a characteristic seismic reflection, which results from the strong impedance contrast between hydrate bearing sediments and gas-filled pore spaces. Although BSRs may also result from changes in acoustic velocity resulting from diagenesis, the BSRs in the Eel River Basin are attributed to gas hydrates since they occur at the base of the gas hydrate stability field; additionally, the BSRs are found deeper in the sediment as water depth increases, which is characteristic of a gas hydrate, since diagenetic BSRs tend to become shallower as water depth increases (Kvenvolden and Field, 1985). Additionally, the recovery of hydrates containing biogenic gas from shallow cores, less than 6 meters deep, taken from areas showing bottom-simulating reflectors confirms both the indirect geophysical evidence and the geologic observations, such as active methane venting from sediments, for the presence of gas hydrates in the basin (Brooks et al., 1991).

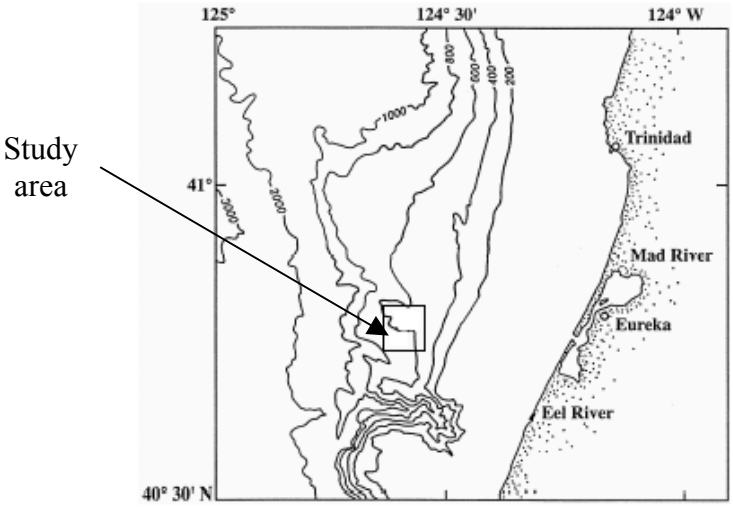

Figure 1-2. A map of the northern California margin showing a portion of the Eel River Basin, which was sampled for this study. Adapted from Rathburn et al. (2000).

Table 1-2. Some of the similarities and differences between the Monterey Bay and the Eel River basin.

	Monterey Bay	**Eel River**
Tectonics	Right-lateral strike slip	Convergent
Foraminiferal Assemblages	Similar to Eel River, with common species including *U. peregrina* and *E. pacifica*	Similar to Monterey Bay, with common species including *U. peregrina* and *E. pacifica*
Gas Hydrates	None found	Abundant
Average Sedimentation Rate	2.2 mm/yr for Monterey Bay shelf*	4 mm/yr for Eel River shelf**

*Lewis et al (2002) **Sommerfield and Nittrouer (1999)

CHAPTER 2
METHODS

Field Sampling

Monterey Bay

Samples from Monterey Bay were collected from two distinct sites during June of 2000. Samples from the first site were collected during Dive 1780 on June 22 from an area termed "Invertebrate Cliffs", located at 36º46.39´N 122º5.08´W. These samples were gathered using the R.V. *Point Lobos* and ROV *Ventana* in a water depth of approximately 955 meters. Cores were taken from four distinct areas within Invertebrate Cliffs (Table 2-1); three of these sites were located within an area influenced by methane seepage, based on the presence of clam communities and bacterial mats. The seep areas sampled were a whitish-gray bacterial mat, a yellow bacterial mat, and a clam community; the area had a concentric arrangement, with clams encircling the two bacterial communities (Figure 2-1). The last set of cores came from a reference site, which was located south of the clam community in an area of presumed non-seepage.

Three push cores, which were 7 cm in diameter and up to 20 cm in length, were collected from each of the four sites for the analyses of foraminifera and pore water. Additionally, two hydraulic piston cores, which were up to 45 cm in length, were taken for the analysis of fossil foraminifera; one core was taken in the clam community, and the other core was taken between the two bacterial mats.

Table 2-1. A listing of cores collected from Monterey Bay and their designated use.

DIVE	SITE	SITE DESRIPTION	CORE	DESIGNATED USE
1780	Invertebrate Cliffs	Whitish-gray bacterial mat	PC67	Live faunal analyses
			PC34	Pore water geochemistry
		Yellow bacterial mat	PC31*	Pore water geochemistry
		Between the two bacterial mats	HPC 2	Live faunal analyses
		Clams	PC30*	Faunal analyses
			PC79*	Pore water geochemistry
			HPC5*	Faunal analyses (fossil)
1781	Clam Flats	Reference (5 m N. of clam bed)	PC71	Live faunal analyses
			PC38*	Pore water geochemistry
		Clam bed	PC31*	Live faunal analyses
			PC80*	Pore water geochemistry
		Bacterial mat	PC30	Live faunal analyses
			PC28	Pore water geochemistry
		Reference (4 m. from Mat)	PC34	Live faunal analyses
			PC72	Pore water geochemistry

* Results from these cores will be presented in detail in this thesis.

Figure 2-1. A picture of the seepage area sampled from Invertebrate Cliffs located at approximately 955 meters water depth (Dive 1780).

On June 23, a second area, Clam Flats, located at 36º44.7´N 122º16.6´W, was sampled. During Dive 1781, cores were collected from a bacterial mat located at a water

depth of approximately 1000 meters. Reference cores were collected four meters from the bacterial mats. Live clam beds, as well as a reference area located five meters due north of the clam bed were sampled. Once again, three push cores were taken from each site for isotopic and faunal analyses (Table 2-1). A complete description of this site is provided by Barry et al. (1996).

Eel River

Eel River samples were collected August 21, 2001, during Dive 2052. Four distinct areas were visited for sampling purposes: a bacterial mat (40º47.058´N 124º35.729´W), a clam bed (2 m north of 40º47.080´N 124º35.700´W, a site marked by active bubbling (40º47.2001´N 124º35.7251´W), and a reference area (40º47.1717´N 124º35.6970´W) (Table 2-2). The approximate water depth for all cores was 520 meters.

Table 2-2. The location and designated use of Eel River cores.

DIVE	SITE	SITE DESCRIPTION	CORE	DESIGNATED USE
2052	Eel River Basin	Bacterial mat	Long Core 5	Faunal analyses (fossil)
			PC16	Pore water geochemistry
		Clams	Long Core 4	Faunal analyses (fossil)
			PC8	Pore water geochemistry
		Bubble site	Long Core 2	Faunal analyses (fossil)
			PC19	Pore water geochemistry

Foraminiferal Preparation and Analyses

Live Foraminifera Preparation

For all sites, push cores designated for live foraminiferal analysis were vertically subsampled at 0.5-cm increments down to 3 cm and at 1-cm intervals down to 10 cm within the sediments. Following procedures outlined by Rathburn and Corliss (1994), each subsample was preserved in 200 ml of 4% buffered formaldehyde; in the laboratory 65 ml of Rose Bengal stain solution was added to foraminiferal samples and allowed to

remain staining the samples for at least one week. Samples were then washed and sieved with nested 63 and 150 μm mesh sieves. Stained benthic foraminifera, which were believed to be alive at the time of collection, were then wet-picked from the >150 μm fraction, sorted, and identified. As a convention in this paper, the use of the term "live" will refer to Rose Bengal stained (i.e., those foraminifera containing at least one stained chamber) foraminifera, which were presumed to be alive at the time of collection (Table 2-3). The term "fossil" will refer to those foraminifera subjected to the Rose Bengal stain, containing no stained chambers, which were presumed to be dead at the time of collection. Additionally, all foraminifera collected from cores not treated with Rose Bengal stain will be referred to as fossil (?), since it is unknown whether these foraminifera were alive or dead at the time of collection.

Foraminifera are commonly found living up to 10 cm below the seafloor (Jorrisen, 1999). In addition, Corliss (1985) found the deeper infaunal species *Globobulimina pacifica*, which is tolerant to low oxygen conditions, living at sediment depths down to 15 cm below the seafloor. Unless associated with a burrow, shallower infaunal foraminifera most likely are not living below 10 cm sediment depth. Live foraminifera from Monterey Bay were not found at high abundances below 5 cm sediment depth. All foraminifera designated for analysis were microscopically examined and cleaned using an ultrasonic bath.

The Rose Bengal Staining Technique

The Rose Bengal technique was first introduced in 1952 by Walton; it is the most prevalent technique in the literature pertaining to the identification of live foraminifera. The stain functions by absorbing onto the surface of the protoplasm, staining it a bright

red. As a result of the protoplasm filling the test and inhibiting the penetration of the stain, often only one or two of the newest chambers of the foraminifera are visibly stained (Boltovskoy and Wright, 1976).

Table 2-3. List of terms used in this paper to describe foraminifera.

Term	Definition (as used in this paper)
Live	Those foraminifera subjected to the Rose Bengal stain, which contain at least one brightly stained red or pink chamber. Believed to be alive at the time of collection (or at least recently)
Fossil	Those foraminifera subjected to the Rose Bengal stain, which contain no stained chambers. Believed to be dead at the time of collection.
Fossil (?)	Those foraminifera not subjected to the Rose Bengal stain, some of which, from the upper portion of the cores, could have been living at the time of collection.

The manner in which Rose Bengal works has resulted in one of its major criticisms: since the stain adheres to proteins, any algae or nematode occupying a fossil foraminiferal test will also be visibly stained. Additionally, even after death, the protoplasm may still absorb stain; however, the time required for the disintegration of protoplasm appears short in oxic environments (Jorrisen, 1999). In anoxic environments, however, the degradation of the protoplasm can take weeks or months and theoretically tens of years and could adsorb the Rose Bengal stain during this period (Bernhard, 1988; Corliss and Emerson, 1990).

Notwithstanding these restrictions, Rose Bengal is the most practical technique available for dealing with large quantities of foraminifera (Rathburn et al., 2000). Additionally, since the technique is commonly used, data are available for comparison. Finally, unlike other stains, it is known that Rose Bengal does not affect the isotopic signature of the foraminifera.

Fossil Foraminifera Preparation

Hydraulic piston cores and long cores designated for fossil foraminiferal analyses were vertically subsampled at 1-cm intervals. In the laboratory, the subsamples were sonicated (if necessary), washed and wet-sieved using nested 63 and 125 μm mesh sieves. Samples were washed onto filter paper and dried in the oven at 60ºC.

The >125 μm fraction designated for picking was split using a microsplitter (if the sample needed to be reduced into a manageable volume) and weighed. The foraminifera were then picked, counted, and identified.

Foraminiferal Isotope Analyses

All foraminifera, stained and unstained, used for isotopic analyses were stripped of organic matter by soaking in 15% hydrogen peroxide for 20 minutes; this procedure was followed by a methanol rinse. Live foraminifera had been sonicated following identification, however, fossil (?) foraminifera had not been previously sonicated and therefore to remove debris, fossil (?) foraminifera were sonicated in methanol (following the removal of hydrogen peroxide). Due to differences in the strengths of the tests, *Epistominella pacifica, Bulimina mexicana,* and *Globobulimina pacifica* were sonicated for 3 minutes at 30% power, while *Uvigerina peregrina* was sonicated at full power for 2 minutes. Following the methanol rinse, fossil (?) *G. pacifica* were broken to aid in removing debris from within the test; they were then cleaned using water and a fine-tipped paint brush. Fossil (?) *G. pacifica* was the only species analyzed where debris could be seen within the test, perhaps due to the transparency of the test walls. All samples were dried in the oven at 60º C.

The foraminifera were reacted at 73° C with anhydrous phosphoric acid in a Kiel III device connected to a Finnigan MAT 252 isotope ratio mass spectrometer. The purpose of the Kiel device is to limit the number of specimens required for accurate analyses, which aids in determining the isotopic variation within individual species. Foraminifera were analyzed for both $\delta^{13}C$ and $\delta^{18}O$, whenever a sufficient number of specimens were present to generate enough gas for the mass spectrometer. Typically, enough gas was liberated when at least 20 μg of foraminiferal tests were used, which corresponded to between one and six tests per analysis, depending upon the species analyzed. Whenever possible single tests were analyzed to better assess variability within a species. With very large specimens of *U. peregrina* or *G. pacifica*, tests had to be broken in half. Data is reported in the standard delta notation relative to the Pee Dee Belemnite (PDB) standard. The precision, based on analyzing replicates of the NBS-19 standard, averaged ±0.04 ‰ for $\delta^{18}O$ and ±0.08‰ for $\delta^{13}C$.

Pore-water DIC Analysis

Carbon Isotopes

Standards were prepared in order to determine both the accuracy and precision of the pore-water DIC extraction technique. Two standards, with concentrations of 400 μg/g $KHCO_3$ and 750 μg/g $KHCO_3$, were prepared. The $KHCO_3$ was analyzed as a solid and yields a $\delta^{13}C$ value of –23.91‰. One standard was extracted for every five samples, with the concentration of the standard used alternating between 400 μg/g and 750 μg/g $KHCO_3$. The $\delta^{13}C$ of the standards averaged –23.37±0.20 ‰ (1σ). Sample data have been corrected for the offset between the solid and dissolved standards.

Pore-water samples designated for carbon isotopic analyses ($\delta^{13}C$) were injected and stored in pre-evacuated vacutainers. Five milliliters of standard solution (either 400 µg/g or 750µg/g $KHCO_3$) was injected into pre-evacuated vacutainers. Prior to analysis, the samples and standards were acidified with approximately 100 µL of concentrated H_3PO_4 to reduce the pH. The carbon dioxide, which evolved from the acidified pore-waters, was extracted from the vacutainers by puncturing the septum with a hypodermic needle attached to a vacuum line (Martin et al., 1997). The gas, which is cryogenically cleaned of contaminants, was stored in 5-mm glass tubes, which were flame-sealed. The gas was then analyzed for $\delta^{13}C$ using an automatic cracker system attached to a VG Prism II mass spectrometer.

Pore Water Solutes

Analyses of pore water solutes, excluding DIC, were performed on board of the ship. Pore fluids were separated from the sediments using centrifugation. Chemical analyses were performed for the following constituents: alkalinity, sulfate, sulfide, calcium, magnesium, ammonium, phosphate, silicate, and nitrate. The chemical analyses performed on board followed the methods used aboard the JOIDES Resolution (Gieskes et al., 1991).

SEM Analysis

Selected specimens of *Epistominella pacifica* and *Uvigerina peregrina* were taken from Monterey Bay and Eel River sites. The purpose of the SEM analysis was to determine whether any recrystallization or overgrowths could be seen on the outside of the tests. Samples were chosen from three general depths within the core (whenever

possible): near the sediment-water interface, the middle of the core, and the bottom of the core (Table 2-4).

Foraminifera were mounted onto stubs using double-sided tape. Prior to SEM analysis, the stubs were coated with a thin layer of a gold-palladium film, designed to make the samples conduct electricity and minimize the buildup of charge on the surface of the test. The foraminifera were analyzed using a JSM 6400 SEM at the Major Analytical Instrumentation Center (MAIC) at the University of Florida. Two pictures of each specimen were taken: an overall view of the test and a close-up of the test.

Table 2-4. Foraminifera used for SEM analysis.

SITE	CORE	SPECIES	DEPTH	STATUS
Monterey Bay-Invertebrate Cliffs	1780 HPC5	*Epistominella pacifica*	0.5 16.5 27.5	Fossil (?)
		Uvigerina peregrina	15.5 21.5 29.5	
	1780 PC30	*Uvigerina peregrina*	0.5	Live
	1780 PC67	*Epistominella smithi*	0.5	
Monterey Bay-Clam Flats	1780 HPC5	*Uvigerina peregrina*	0.5 15.5	Fossil (?)
			24.5	
Eel River-Bubble Site	Long Core 2	*Epistominella pacifica*	10.5	Fossil (?)
Eel River-Clam Bed	Long Core 4	*Epistominella pacifica*	1.5 11.5 18.5	
		Uvigerina peregrina	12.5 17.5	
Eel River - Bacterial Mat	Long Core 5	*Epistominella pacifica*	0.5 12.5	Fossil (?)
		Uvigerina peregrina	1.5 15.5 25.5	
Eel River Reference Site	Long Core 1	*Epistominella pacifica*	4.5	Fossil (?)

CHAPTER 3
RESULTS

Pore Fluid Geochemistry

Monterey Bay

Pore water chemistry is distinctly different in the two clam beds sampled: Invertebrate Cliffs (1780 PC 79) and Clam Flats (1781 PC 80) (Appendix A). For instance, the calcium concentrations at Invertebrate Cliffs show virtually no change down core, whereas the calcium concentrations at Clam Flats show variation with sediment depth, decreasing more than 4 mM in the first 8 cm of the core (Figure 3-1). The Clam Flats site also has significantly higher sulfide concentrations, with pore water values at Clam Flats being up to 118 times higher than Invertebrate Cliffs (Figure 3-2). There are also similar differences between the cores' alkalinity gradients. Changes in sulfide and alkalinity likely correspond to sulfate reduction in the sediment (Figure 3-3).

The carbon isotopic compositions also differ between the dive sites. The $\delta^{13}C_{DIC}$ value from Clam Flats is approximately seven times lighter in the first centimeter of the core than the $\delta^{13}C_{DIC}$ of Invertebrate Cliffs. The DIC from Invertebrate Cliffs is found to be no lighter than –9‰ in the 12 cm of pore water analyzed, whereas Clam Flats $\delta^{13}C_{DIC}$ remains lighter than -40‰ from 2 cm on to the bottom of the core (16 cm) (Figure 3-4). Oxidation of marine organic carbon ($\delta^{13}C_{DIC}$ of -25‰) cannot account for the isotopically light DIC found at Clam Flats. Although no bottom waters were collected from the

dives, supernatant fluid was extracted from the tops of cores designated for pore water analyses and analyzed for $\delta^{13}C_{DIC}$ (Table 3-1).

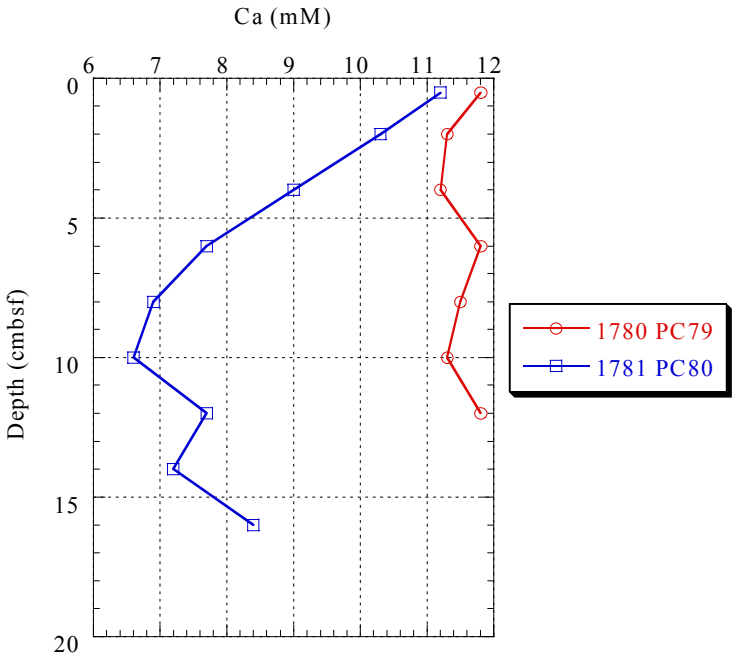

Figure 3-1. Pore water calcium profiles for Monterey Bay clam beds (Dive 1780 PC79, Invertebrate Cliffs and Dive 1781 PC80, Clam Flats).

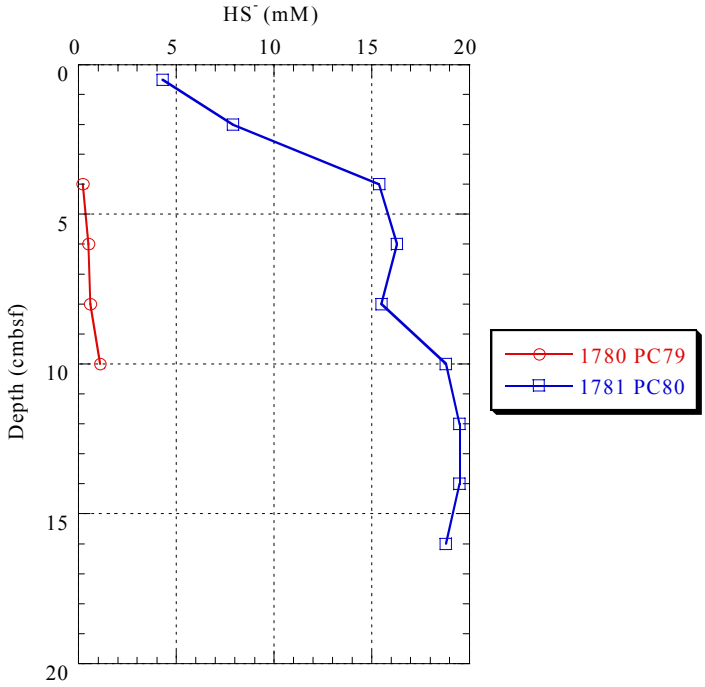

Figure 3-2. Pore water sulfide (HS^-) profiles for Monterey Bay clam beds (Dive 1780 PC79, Invertebrate Cliffs and Dive 1781 PC80, Clam Flats).

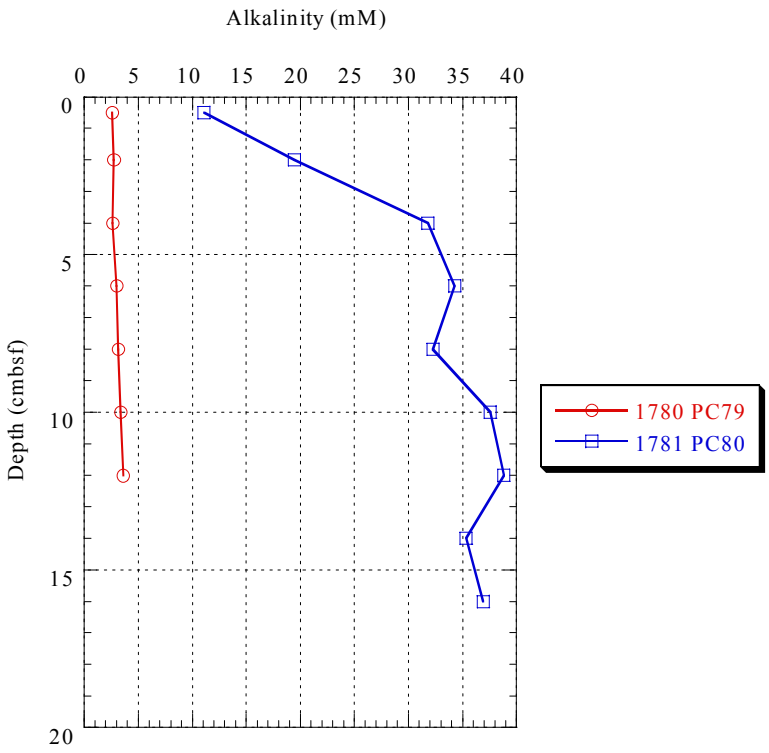

Figure 3-3. Pore water alkalinity profiles from Monterey Bay clam beds (Dive 1780 PC79, Invertebrate Cliffs and Dive 1781 PC80, Clam Flats).

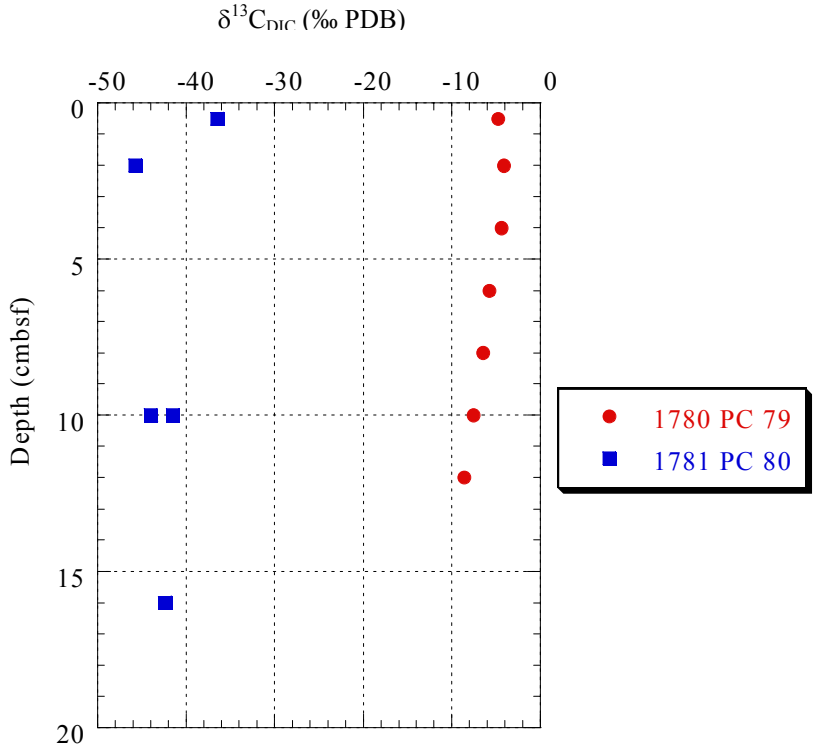

Figure 3-4. The $\delta^{13}C_{DIC}$ profile of pore water from Monterey Bay clam beds (Dive 1780 PC79, Invertebrate Cliffs and 1781 PC80, Clam Flats).

Table 3-1. The $\delta^{13}C_{DIC}$ values of supernatant fluids taken from the tops of cores designated for pore water analyses.

Location	Dive number	Core	Site Description	$\delta^{13}C_{DIC}$ value (‰)
Monterey Bay	1780	PC31	Yellow bacterial mat	-3.72
	1781	PC38	Reference (clam bed)	-3.93
Eel River Basin	2052	PC8	Clam bed	-5.72
	2052	PC16	Bacterial mat	-5.18

Eel River

The various sites sampled from Eel River: a bacterial mat, a clam bed, and a bubble site, all exhibit similar pore water trends (Appendix A). For example, all of the Eel River cores reveal an overall decrease in calcium concentration with depth, with approximately similar gradients (Figure 3-5). All cores display similar bisulfide ion and sulfate trends, although gradients differ; the bisulfide ion concentration increase more rapidly with depth for PC19 (the bubble site) than for either PC8 (clams) or PC16, a bacterial mat (Figure 3-6). The bubble site also has the steepest decreasing gradient for sulfate, with complete consumption of sulfate by 10.5 cm (Figure 3-7). Additionally, all cores have an increase in alkalinity with depth (Figure 3-8). The clam bed (PC8) and the bacterial mat (PC16) have similar $\delta^{13}C_{DIC}$ gradients, with both cores having core- top supernatant fluid $\delta^{13}C_{DIC}$ values of approximately -5‰ (Figure 3-9, Table 3-1). The bubble site (PC19) has initially lighter $\delta^{13}C_{DIC}$ values, with a value of approximately -18‰ at 0.5 cm sediment depth. Within the top five centimeters of the core the $\delta^{13}C_{DIC}$ values begin to be lighter than that of oxidized marine organic carbon (~ -22‰) (Figure 3-9).

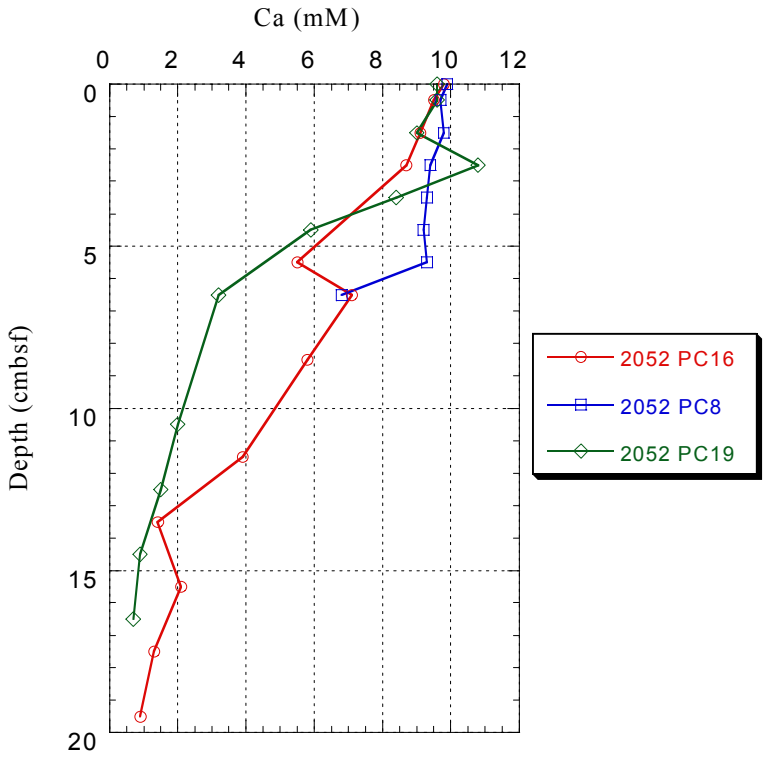

Figure 3-5. Calcium pore water profiles for Eel River Dive 2052: PC16 (bacterial mat), PC8 (clam bed), and PC19 (bubble site).

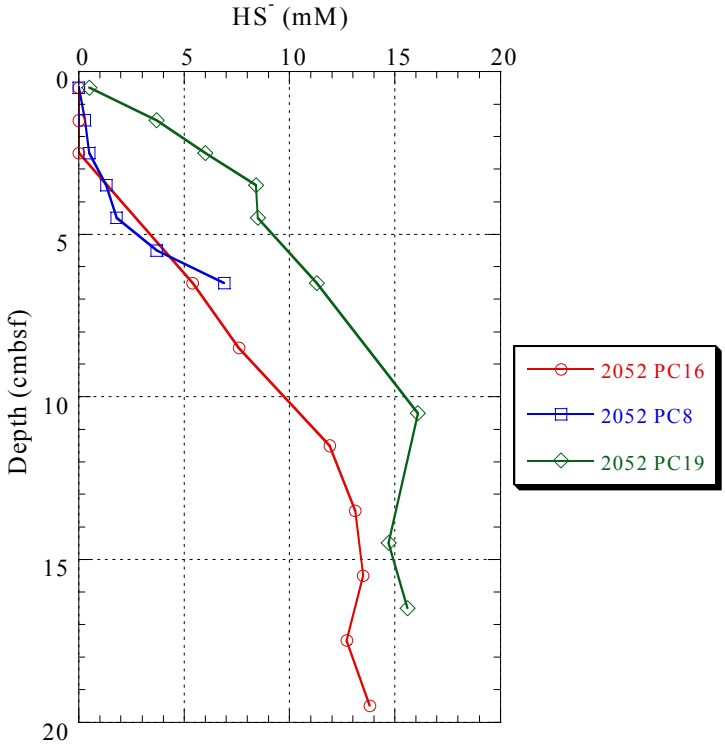

Figure 3-6. Pore water sulfide profiles for Eel River Dive 2052: PC16 (bacterial mat), PC 8 (clam bed) and PC19 (bubble site).

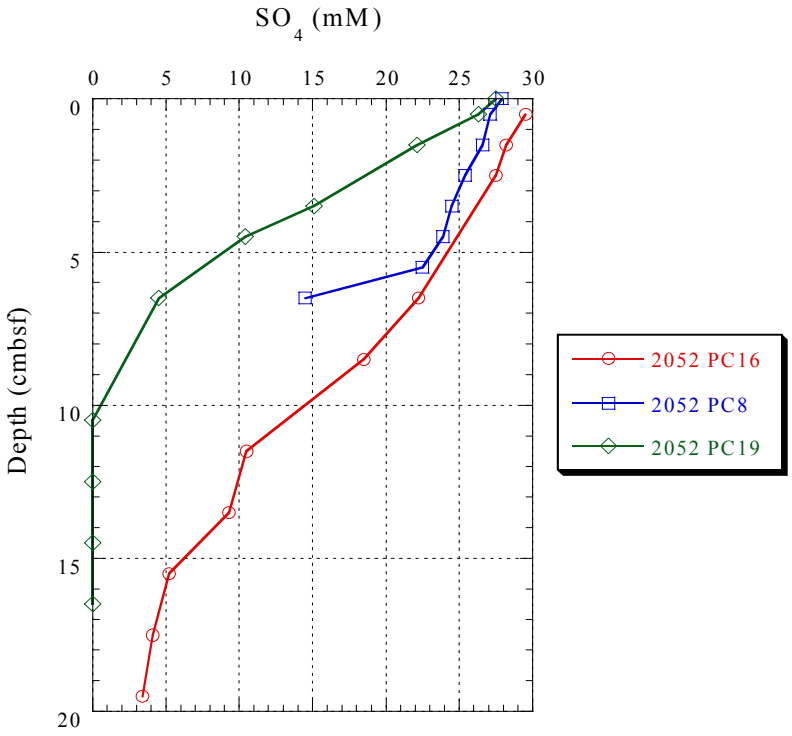

Figure 3-7. Sulfate ion pore water profiles from Eel River Dive 2052: PC16 (bacterial mat), PC 8 (clam bed) and PC19 (bubble site).

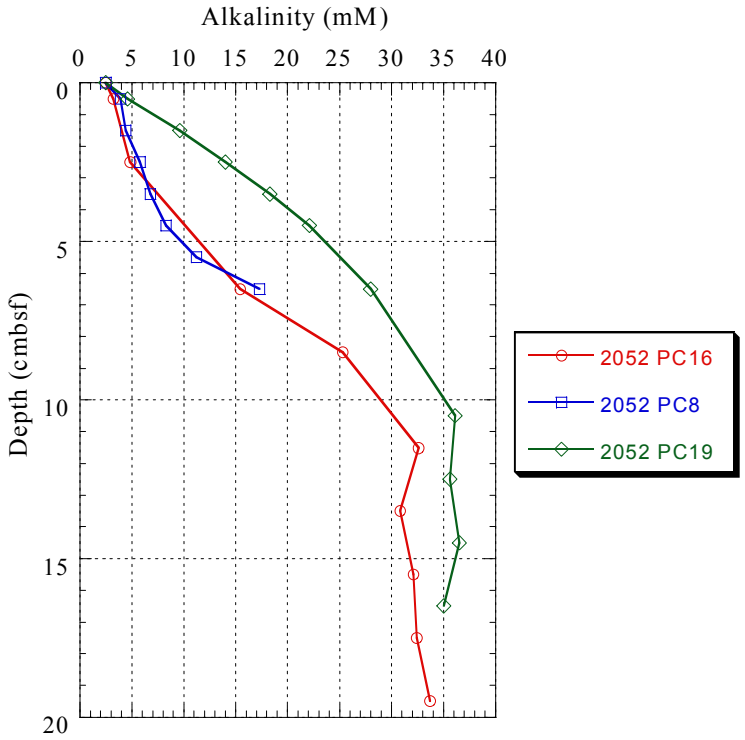

Figure 3-8. Pore water alkalinities for Eel River Dive 2052: PC8 (clam bed), PC16 (bacterial mat), and PC19 (bubble site).

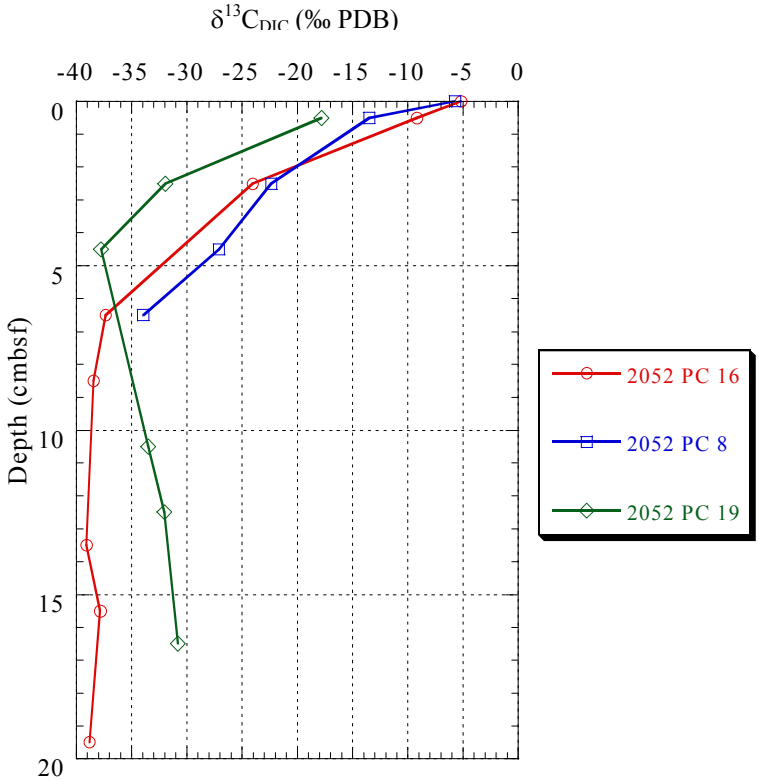

Figure 3-9. Pore water $\delta^{13}C_{DIC}$ for Eel River Dive 2052 PC16 (bacterial mat), PC8 (clam bed) and PC19 (bubble site).

Stable Isotopic Signatures of Foraminiferal Carbonate

Monterey Bay

Carbon isotopes

The foraminifera from Invertebrate Cliffs display a range of $\delta^{13}C$ values (Table 3-2, Appendix B). Sediments at the Invertebrate Cliffs clam bed (1780 PC30) contain live *U. peregrina* with $\delta^{13}C$ values ranging from -0.04 to -0.85 ‰, over the entire length of the core, while the $\delta^{13}C$ of fossil (?) *U. peregrina* from HPC5 (Invertebrate Cliffs clam bed) varies from 0.01 to -1.05 ‰ (Figure 3-10). Additionally, when the $\delta^{13}C$ values of individual live *U. peregrina* from within the same depth interval are compared, variations up to 0.55 ‰ are observed at 0.5 cm and 4.5 cm. A smaller range of $\delta^{13}C$ values is evident in other species; for instance, live specimens of *E. pacifica* range from –0.50 to

–0.79 ‰ over the length of the core, PC30, whereas fossil (?) *E. pacifica* from HPC5 vary between –0.13 to –1.16 ‰ over the entire length of the core (Figure 3-11). Live *B. mexicana* range between –0.70 and –0.92 ‰ within PC30 and fossil (?) specimens from HPC5 vary between –0.52 and –1.04 ‰ (Figure 3-12). Most species of fossil (?) foraminifera have a wider carbon isotopic range compared to their living counterparts. *G. pacifica* is the only species sampled from Invertebrate Cliffs where live $\delta^{13}C$ values have a broader range compared to fossil (?) $\delta^{13}C$ values (Figure 3-13). For most species from Invertebrate Cliffs, however, the number of fossil (?) tests analyzed greatly surpasses the number of live tests analyzed, possibly contributing to the greater variation in the fossil (?) isotopic composition relative to the live composition (Table 3-2).

Table 3-2. A statistical comparison of Monterey Bay foraminifera

Dive No./ Core No.	Species	Status	n	Mean $\delta^{13}C$	$\pm\sigma$ ($\delta^{13}C$)	Min (‰)	Max (‰)	Mean $\delta^{18}O$	$\pm\sigma$ ($\delta^{18}O$)	Min (‰)	Max (‰)
1780 PC30	*B. mexicana*	Live	9	-0.80	0.08	-0.92	-0.70	3.28	0.04	3.2	3.36
		Fossil	1	-0.83	N/A	N/A	N/A	3.33	N/A	N/A	N/A
		Fossil (?)*	17	-0.75	0.16	-1.04	-0.52	3.47	0.24	3.05	3.94
	E. pacifica	Live	12	-0.65	0.10	-0.79	-.50	3.18	0.07	3.09	3.30
		Fossil (?)*	70	-0.45	0.15	-1.16	-0.13	3.28	0.17	2.31	3.60
	U. peregrina	Live	27	-0.50	0.18	-0.85	-0.04	3.06	0.18	2.59	3.40
		Fossil	2	-0.80	0.21	-0.95	-0.65	3.13	0.10	3.06	3.20
		Fossil (?)*	33	-0.59	0.29	-1.05	0.01	3.25	0.13	3.06	3.73
	G. pacifica	Live	25	-1.38	0.48	-2.23	-0.41	3.32	0.07	3.23	3.49
		Fossil (?)*	24	-1.04	0.22	-1.69	-0.61	3.40	0.11	3.26	3.71
1781 PC31	*B. mexicana*	Live	3	-1.09	0.07	-1.17	-1.03	3.44	0.31	3.22	3.80
		Fossil	5	-1.43	0.48	-2.24	-1.04	4.74	0.09	4.65	4.89
	E. pacifica	Live	4	-0.96	0.04	-0.98	-0.92	4.25	0.73	3.15	4.66
		Fossil	4	-1.15	0.06	-1.20	-1.09	4.61	0.03	4.59	4.65
	U. peregrina	Live	37	-0.91	0.45	-2.05	-0.10	3.20	0.16	3.04	4.04
		Fossil	15	-1.41	0.31	-2.03	-1.03	4.65	0.10	4.49	4.83
	G. pacifica	Live	3	-3.97	0.54	-4.56	-3.49	3.30	0.11	3.20	3.42

*Indicates foraminifera are from 1780 HPC5. **Statistical analyses were unavailable as only one isotopic value was obtained for these specific foraminifera.

No systematic variations in the carbon isotopic patterns can be discerned for Invertebrate Cliffs (Dive 1780 PC30). Isotopic values fluctuate randomly, but generally remain around the same isotopic values throughout the length of the core.

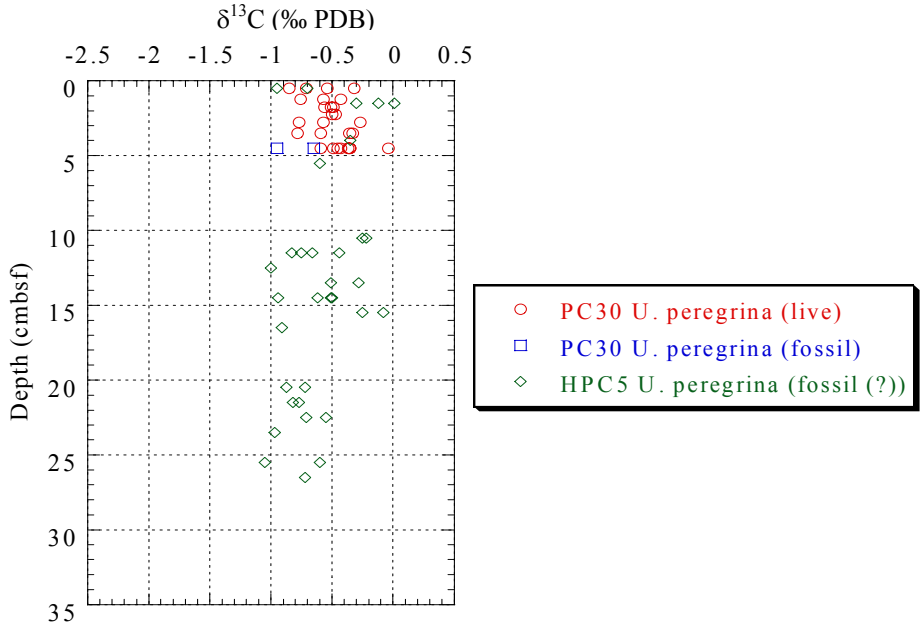

Figure 3-10. Dive 1780 HPC5 and PC30 (Invertebrate Cliffs clam bed) *Uvigerina peregrina* $\delta^{13}C$ vs. depth.

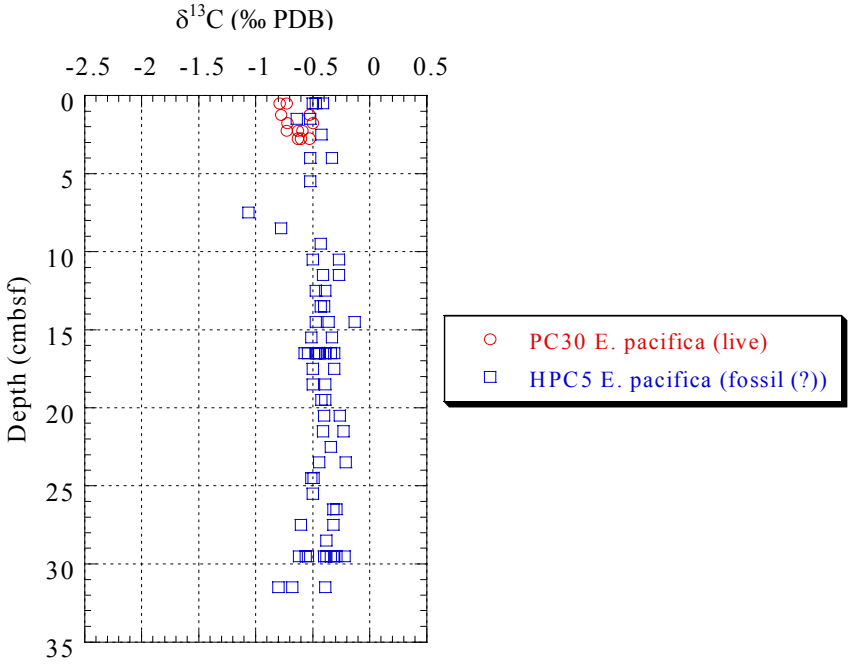

Figure 3-11. Dive 1780 HPC5 and PC30 (Invertebrate Cliffs clam bed) *Epistominella pacifica* $\delta^{13}C$ vs. depth.

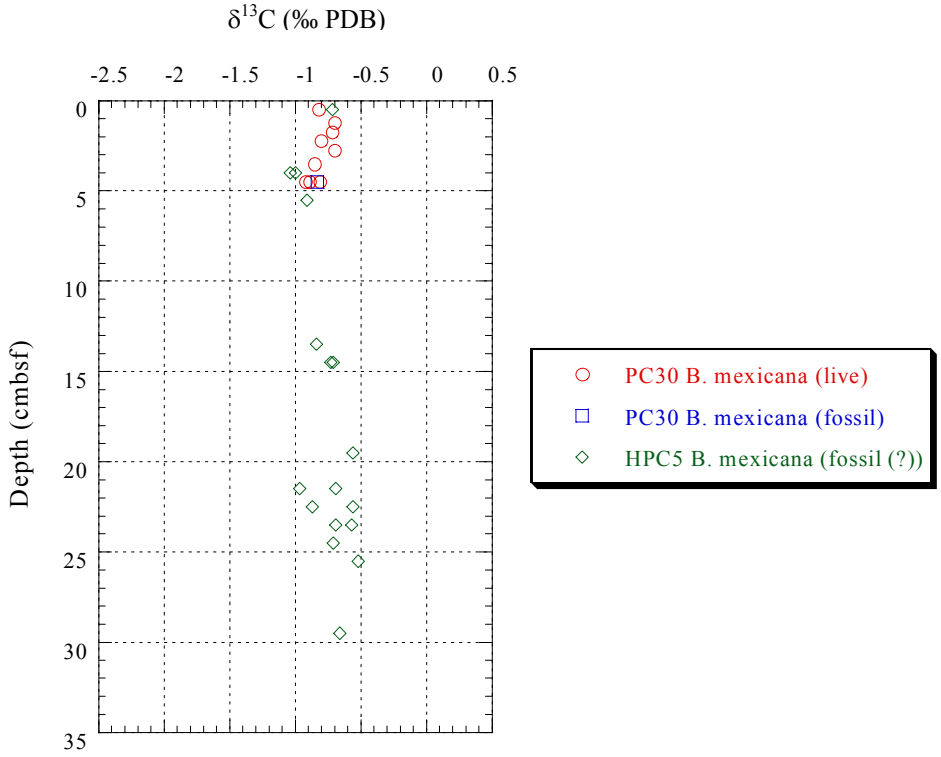

Figure 3-12. Dive 1780 HPC5 and PC30 (Invertebrate Cliffs clam bed): *Bulimina mexicana* $\delta^{13}C$ vs. depth.

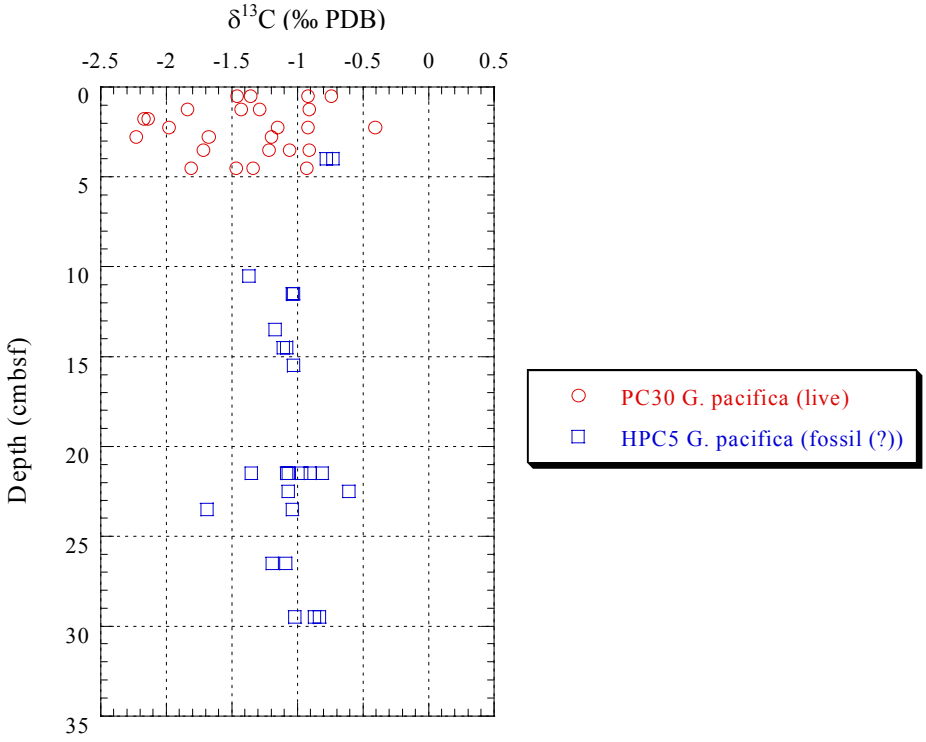

Figure 3-13. Dive 1780 (Invertebrate Cliffs clam bed) HPC5 and PC30 *Globobulimina pacifica* $\delta^{13}C$ vs. depth.

Variable carbon isotope values are also observed at the Clam Flats site (Dive 1781 PC31), with the $\delta^{13}C$ of live *U. peregrina* ranging from –0.10 to –2.05‰ (Figure 3-14); this large variation is observed between individuals within the same depth interval (2-2.5 cm). The carbon isotopic range of fossil *U. peregrina* is smaller than the range found for live specimens, with values lying between –1.03 and –2.03 ‰. *U. peregrina* is the most abundant species of foraminifera from Clam Flats; however, the $\delta^{13}C$ of other foraminiferal species at the Clam Flats site used for comparison purposes with other cores is presented (Figure 3-15). These other species, including the shallow infaunal species *E. pacifica* and *B. mexicana* fall within the range of values found for *U. peregrina*. Live *E. pacifica* varies between –0.92 and –0.98 ‰, while fossil specimens of *E. pacifica* range from –1.09 to –1.20 ‰. Live *B. mexicana* vary from –1.03 to –1.17 ‰, while their fossil conspecifics vary between –1.04 and –2.24 ‰ over the length of the core. The isotopic values of live *G. pacifica*, a deeper infaunal species, which vary between –3.49 and –4.56 ‰, is slightly lighter than values obtained from *U. peregrina*. The last species presented, *Planulina species*, which is an epifaunal foraminiferan, has carbon isotopic values ranging between –0.22 and +0.45 ‰, which is slightly heavier than most of *U. peregrina's* isotopic values.

From the data available, there is no systematic variation in carbon isotopes with depth for PC31 (Clam Flats). No discernible disparities exist between live and fossil conspecifics. When looking at the length of the core, fossil *U. peregrina* fall within the isotopic range found for live *U. peregrina* (Figure 3-14). Both *E. pacifica* and *B. mexicana* also have similar ranges for live and fossil conspecifics over the length of the core (Figure 3-15).

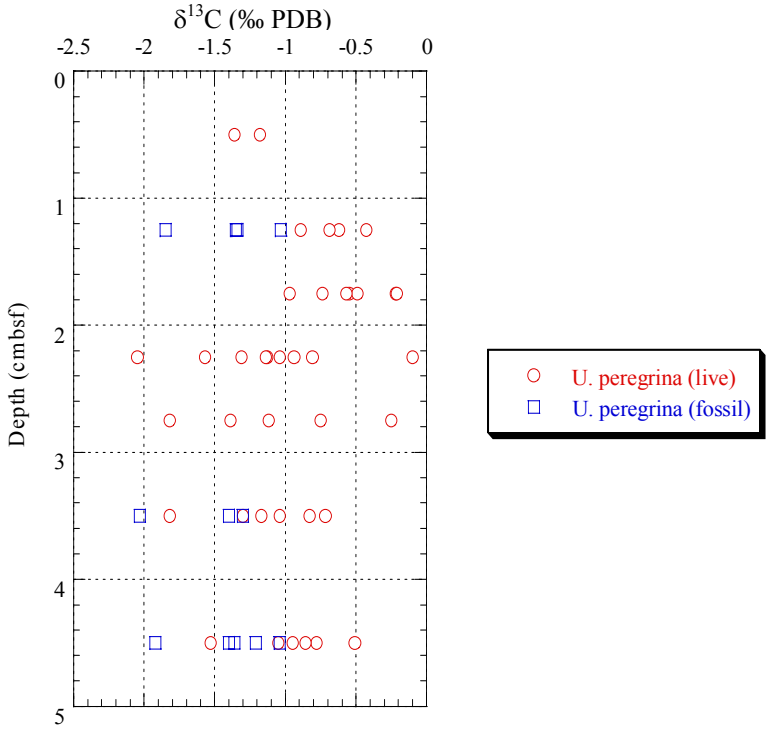

Figure 3-14. Dive 1781 PC31 (Clam Flats clam bed) *Uvigerina peregrina* $\delta^{13}C$ vs. depth

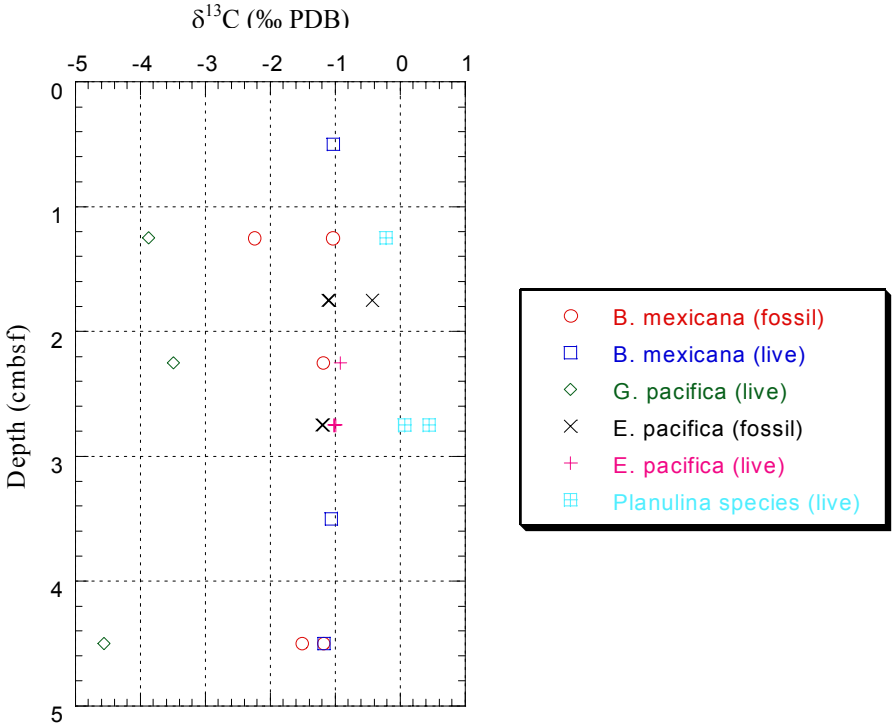

Figure 3-15. Dive 1781 PC31 Clam Flats (clam bed): *Epistominella pacifica*, *Bulimina mexicana*, *Globobulimina pacifica*, and *Planulina species* $\delta^{13}C$ vs. depth.

Oxygen isotopes

Oxygen isotopes also vary for a given species of benthic foraminifera; however, similar to carbon isotopes, no down-core trends occur. *E. pacifica* and *B. mexicana* from 1780 PC30 (Invertebrate Cliffs) both have a slightly larger variation in fossil (?) $\delta^{18}O$ than in live $\delta^{18}O$ (Figure 3-16, 3-17). *U. peregrina* was the only species analyzed from 1780 PC30 that has greater $\delta^{18}O$ variability for live specimens compared to fossil (?) specimens (Figure 3-18). Live *G. pacifica*, which shows the largest variation in $\delta^{13}C$ (σ = 0.54 ‰) has a relatively narrow range of $\delta^{18}O$ values, varying up to 0.22 ‰ within 1780 PC30 (Figure 3-19). The oxygen isotopes do not vary appreciably from live to fossil conspecifics found at the same depth within the core (Figures 3-16, 3-17, 3-18, and 3-19).

When live and fossil foraminifera from Clam Flats are compared to each other, they have for the most part different $\delta^{18}O$ signatures (Table 3-2, Figure 3-20). For the entire core, the average $\delta^{18}O$ value for fossil *U. peregrina* (n=15) is 4.65 ± 0.10 ‰. Alternatively, the live *U. peregrina* (n=37) have a mean of 3.20 ± 0.16 ‰ over the length of PC31. Unlike these differences in $\delta^{18}O$, the carbon isotopic values for live and fossil *U. peregrina* show some overlap in value, even though mean $\delta^{13}C$ values are lighter for fossil specimens (Table 3-2, Figure 3-15). Similar offsets are seen in other species from Clam Flats (1781 PC31) (Table 3-2).

Eel River

Carbon isotopes

No live foraminiferal data are available from Eel River, however fossil (?) foraminifera were analyzed for all Eel River sites (Appendix B). Long core 5, which

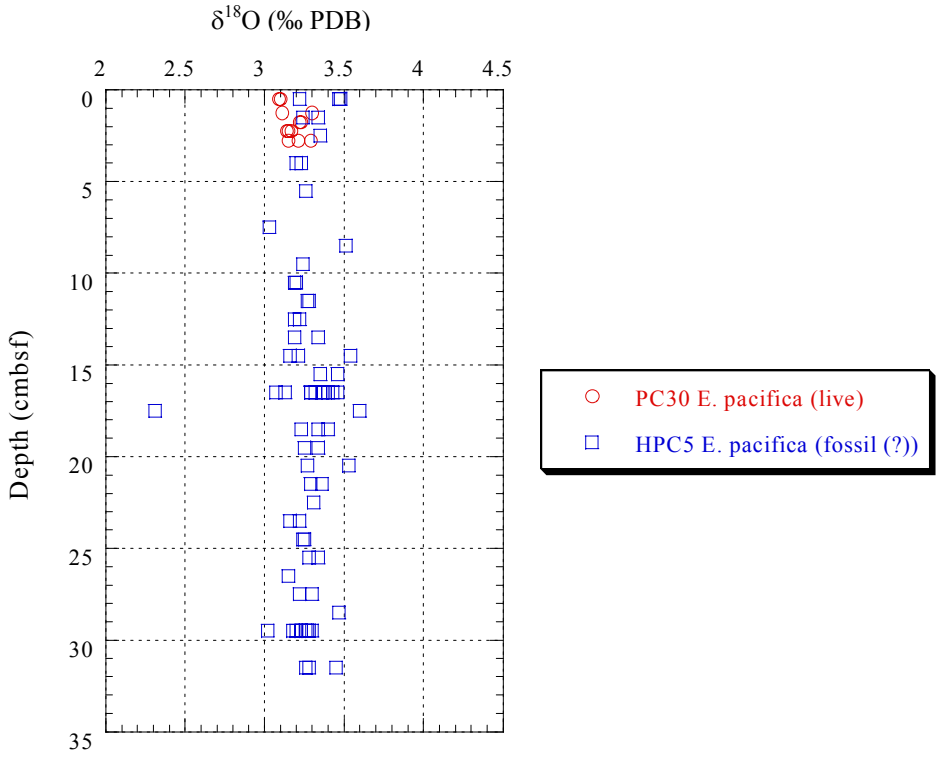

Figure 3-16. Dive 1780 HPC 5 and PC30 (Invertebrate Cliffs clam bed) *Epistominella pacifica* $\delta^{18}O$ vs. depth.

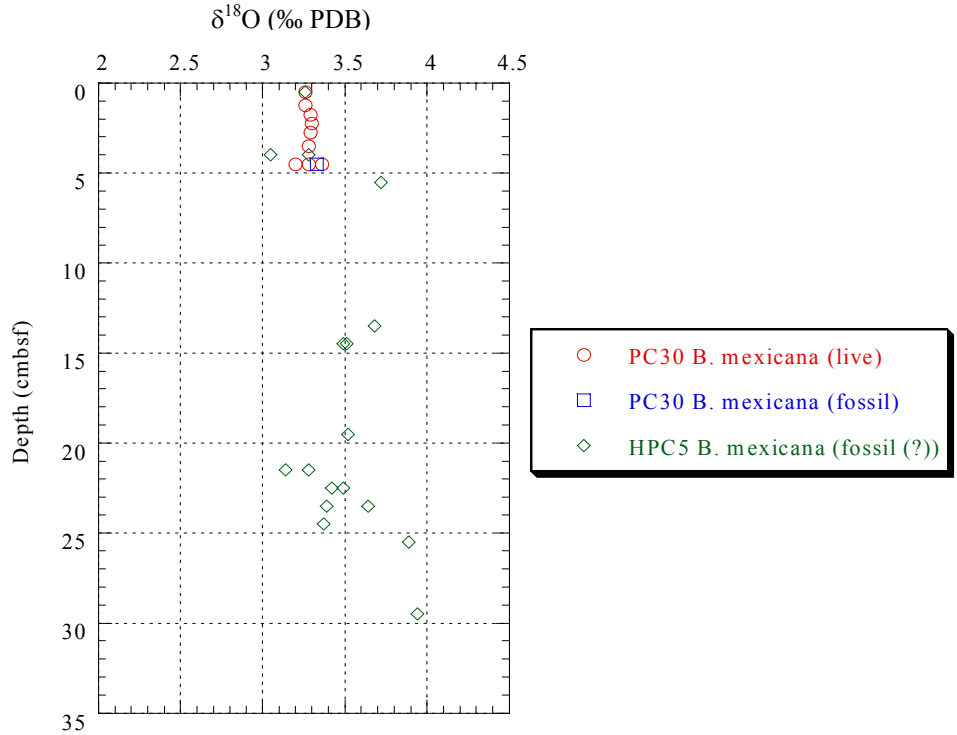

Figure 3-17. Dive 1780 HPC5 and PC30 (Invertebrate Cliffs clam bed) *Bulimina mexicana* $\delta^{18}O$ vs. depth.

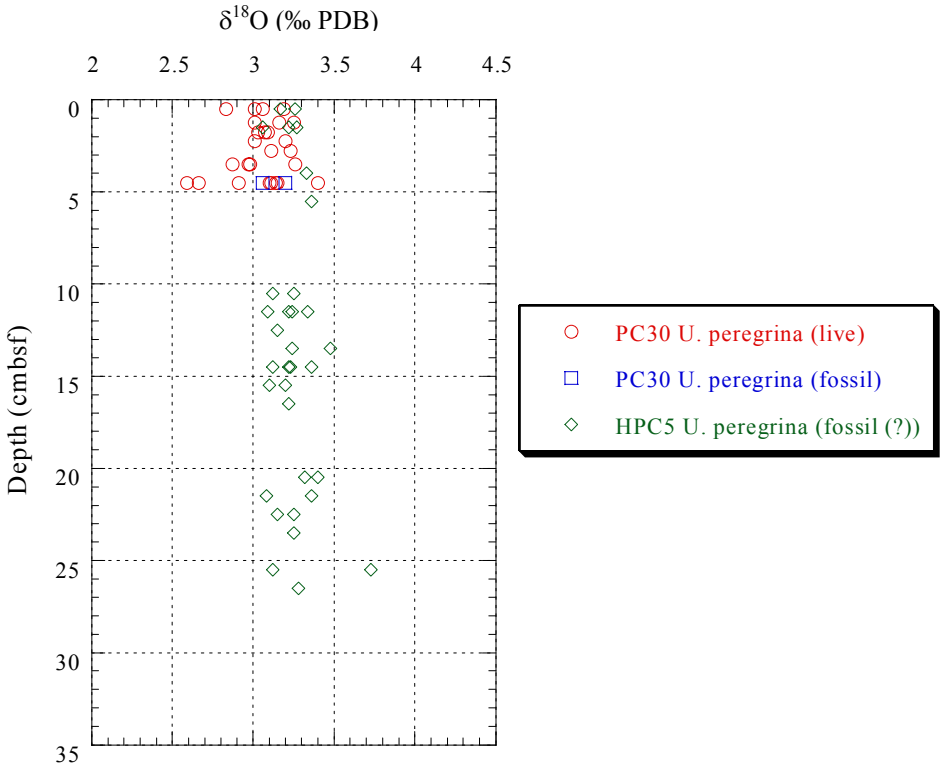

Figure 3-18. Dive 1780 (Invertebrate Cliffs clam bed) HPC5 and PC30: *Uvigerina peregrina* $\delta^{18}O$ vs. depth.

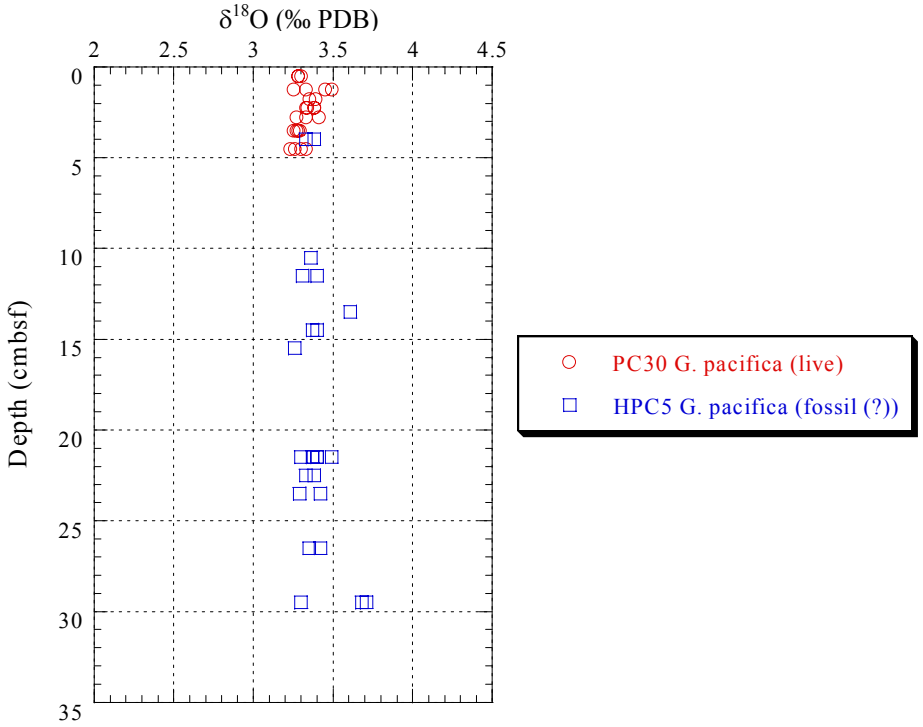

Figure 3-19. Dive 1780 (Invertebrate Cliffs clam bed) HPC5 and PC30 *Globobulimina pacifica* $\delta^{18}O$ vs. depth.

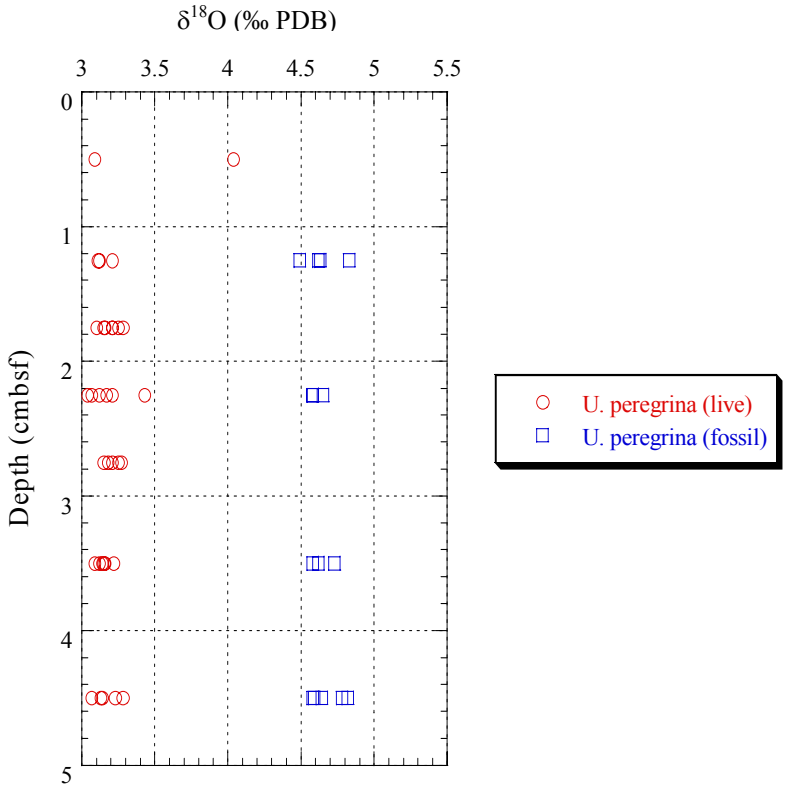

Figure 3-20. Dive 1781 PC31 (Clam Flats clam bed) *Uvigerina peregrina* $\delta^{18}O$ vs. depth.

was collected from a bacterial mat, contains fossil (?) *U. peregrina* that have a mean $\delta^{13}C$ value of –1.49 ± 2.10 ‰ (Table 3-3, Figure 3-21). If, however, three of the outlying values are excluded, specifically – 4.48, -6.97 and –11.59‰, the mean $\delta^{13}C$ value increases to –0.93 ± 0.28‰. Fossil (?) *E. pacifica* isotope values range from –1.01 to –0.32 ‰ (Figure 3-21). The other two cores, Long core 4 and Long core 2 contain foraminifera with extreme ranges in $\delta^{13}C$ values. For instance, Long core 4, which was taken in a clam bed, contains *U. peregrina* specimens with $\delta^{13}C$ values ranging from –0.46 to –7.13‰ (Figure 3-22). Even more extreme, the $\delta^{13}C$ of *E. pacifica* ranges from –0.65 to –19.46 ‰, with the lightest of values occurring rather shallowly at 1.5 cm. However, the majority of the foraminifera from Long core 4 have a $\delta^{13}C$ value of

approximately 2‰ or heavier (Figure 3-22). In contrast, Long core 2 (from the bubble site) has more variable $\delta^{13}C$ values than LC4 (Figure 3-23). For example, out of a sample set that includes 33 *U. peregrina* data points, the range in $\delta^{13}C$ values is from –0.65 to –23.22‰ (Figure 3-23), with a mean $\delta^{13}C$ of –6.70‰, and a standard deviation (σ) of 7.00‰ (Table 3-3). *B. mexicana* and *E. pacifica* show similar variability. The variation in $\delta^{13}C$ for all cores is unsystematic with depth.

Table 3-3. A statistical comparison of fossil (?) foraminifera from Eel River Basin.

Dive Number and Core Number	Species	n	Mean $\delta^{13}C$	$\pm\sigma$ ($\delta^{13}C$)	Min (‰)	Max (‰)	Mean $\delta^{18}O$	$\pm\sigma$ ($\delta^{18}O$)	Min (‰)	Max (‰)
2052 Long Core 2	*U. peregrina*	33	-6.70	7.00	-23.22	-0.65	3.60	0.61	2.14	4.76
	E. pacifica	18	-3.46	4.99	-15.24	-0.16	3.36	0.46	2.76	4.03
	B. mexicana	15	-12.73	6.12	-21.13	-0.71	4.05	0.19	3.83	4.51
2052 Long Core 4	*U. peregrina*	32	-1.37	1.55	-7.13	-0.46	3.56	0.34	2.81	4.05
	E. pacifica	20	-2.94	4.52	-19.46	-0.65	3.70	0.28	3.08	4.30
2052 Long Core 5	*U. peregrina*	36	-1.49	2.10	-11.59	-0.41	3.70	0.17	2.99	3.97
	E. pacifica	17	-0.75	0.20	-1.01	-0.32	3.67	0.14	3.37	3.97

Oxygen isotopes

Variable $\delta^{18}O$ values accompany the wide range of $\delta^{13}C$ values for Eel River cores. The bubble site (LC2), which has the most variable $\delta^{13}C$ values, also has the widest range of $\delta^{18}O$ values, ranging from 2.14 to 4.76‰ throughout the core (Figure 3-24, Table 3-3). The majority of foraminiferal $\delta^{18}O$ values from long core 4 (clams) are between 3 and 4‰ (Figure 3-25); likewise, the majority of foraminifera from long core 5 (bacterial mat) have $\delta^{18}O$ values between 3.5 and 3.9‰ (Figure 3-26). No down core trends in variability could be distinguished for any of the Eel River cores.

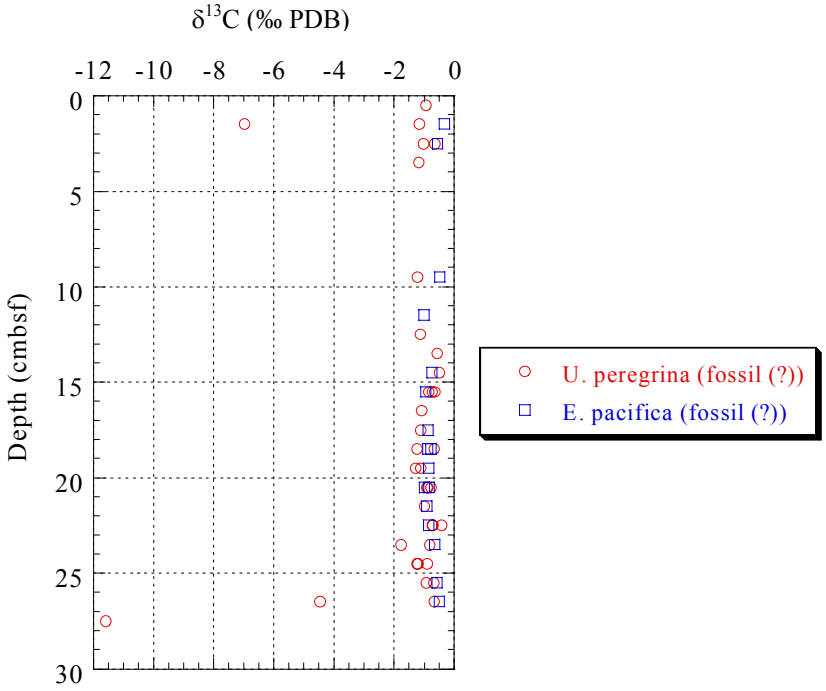

Figure 3-21. Dive 2052 long core 5 (bacterial mat): *Uvigerina peregrina* and *Epistominella pacifica* $\delta^{13}C$ vs. depth.

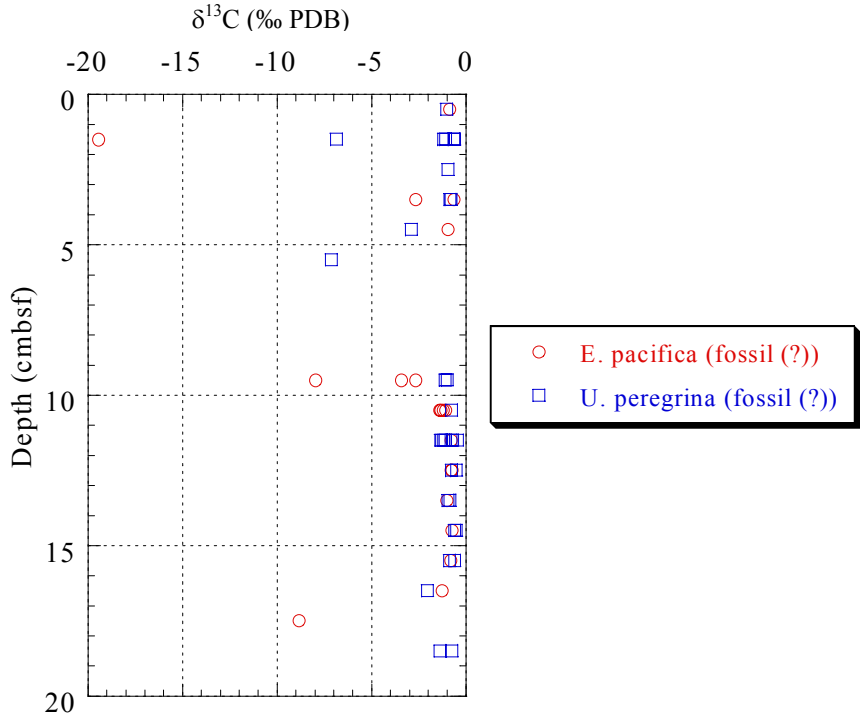

Figure 3-22. Dive 2052 Long core 4 (clam bed): *Epistominella pacifica* and *Uvigerina peregrina* $\delta^{13}C$ vs. depth.

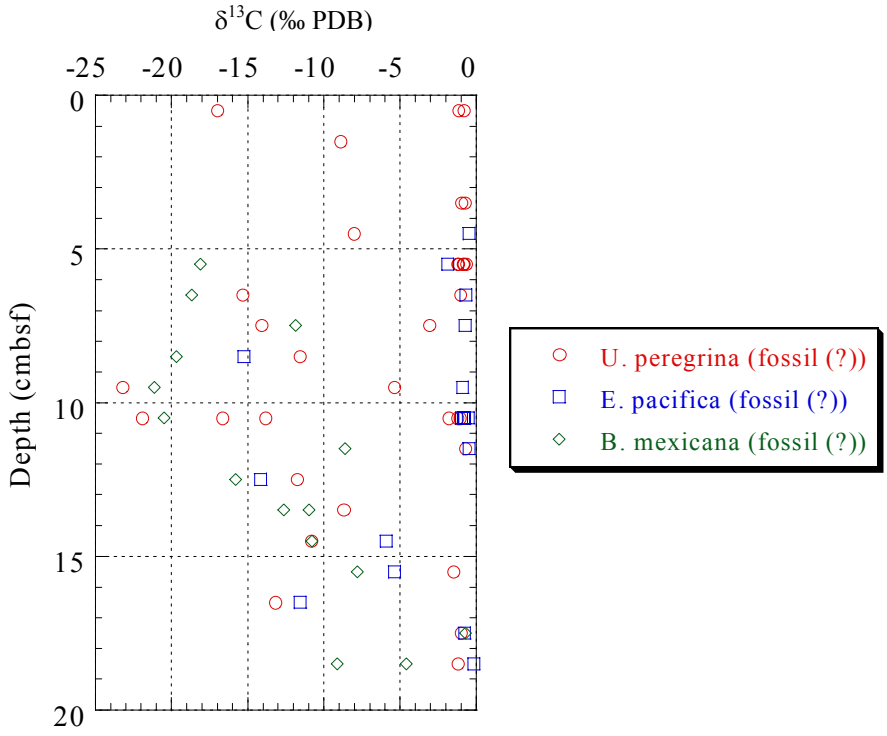

Figure 3-23. Dive 2052 Long core 2 (bubble site): *Uvigerina peregrina*, *Epistominella pacifica*, and *Bulimina mexicana* $\delta^{13}C$ vs. depth.

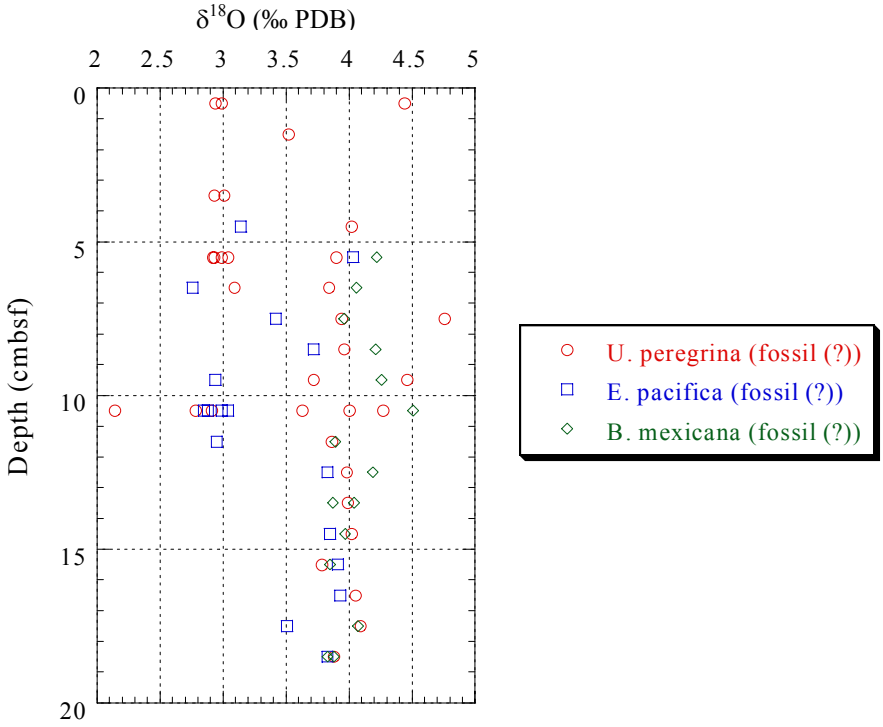

Figure 3-24. Dive 2052 long core 2 (bubble site): *Uvigerina peregrina*, *Bulimina mexicana* and *Epistominella pacifica* $\delta^{18}O$ vs. depth.

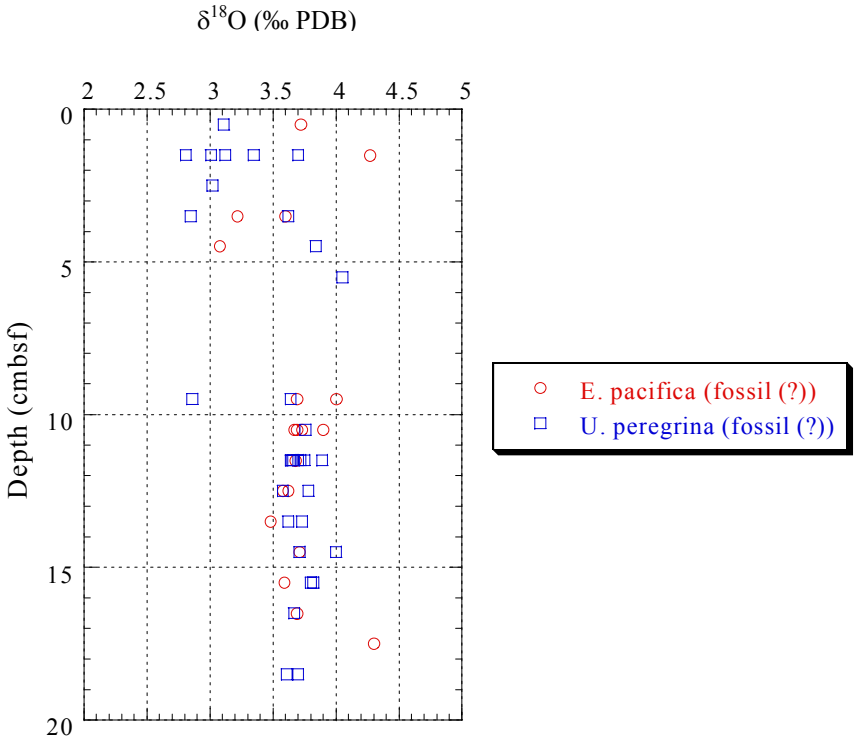

Figure 3-25. Dive 2052 long core 4 (clam bed): *Epistominella pacifica* and *Uvigerina peregrina* $\delta^{18}O$ vs. depth.

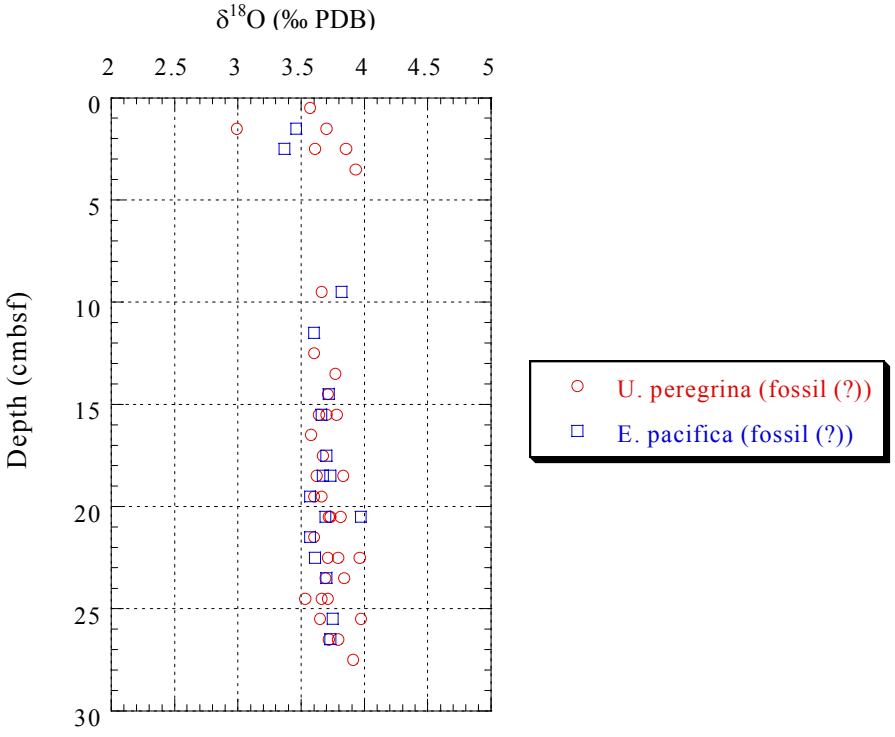

Figure 3-26. Dive 2052 Long Core 5 (bacterial mat): *Uvigerina peregrina* and *Epistominella pacifica* $\delta^{18}O$ vs. depth.

Scanning Electron Microscope (SEM) Micrographs

No evidence of recrystallization or overgrowths is visible from the micrographs taken from Monterey Bay's Invertebrate Cliffs or Clam Flats (Appendix C, Figure 3-28 and Figure 3-29). This observation was consistent with the isotopic composition of the foraminifera, which did not have unusually light carbon signatures.

Some of the foraminifera photographed from Eel River appear to be diagenetically altered (Appendix C, Figure 3-30). The photographed specimens are from 2052 long core 4, the clam bed, however, it is likely other Eel River cores also contain recrystallized foraminifera or foraminifera containing authigenic carbonate, based on the light carbon isotopic signatures present in some foraminifera.

(a)

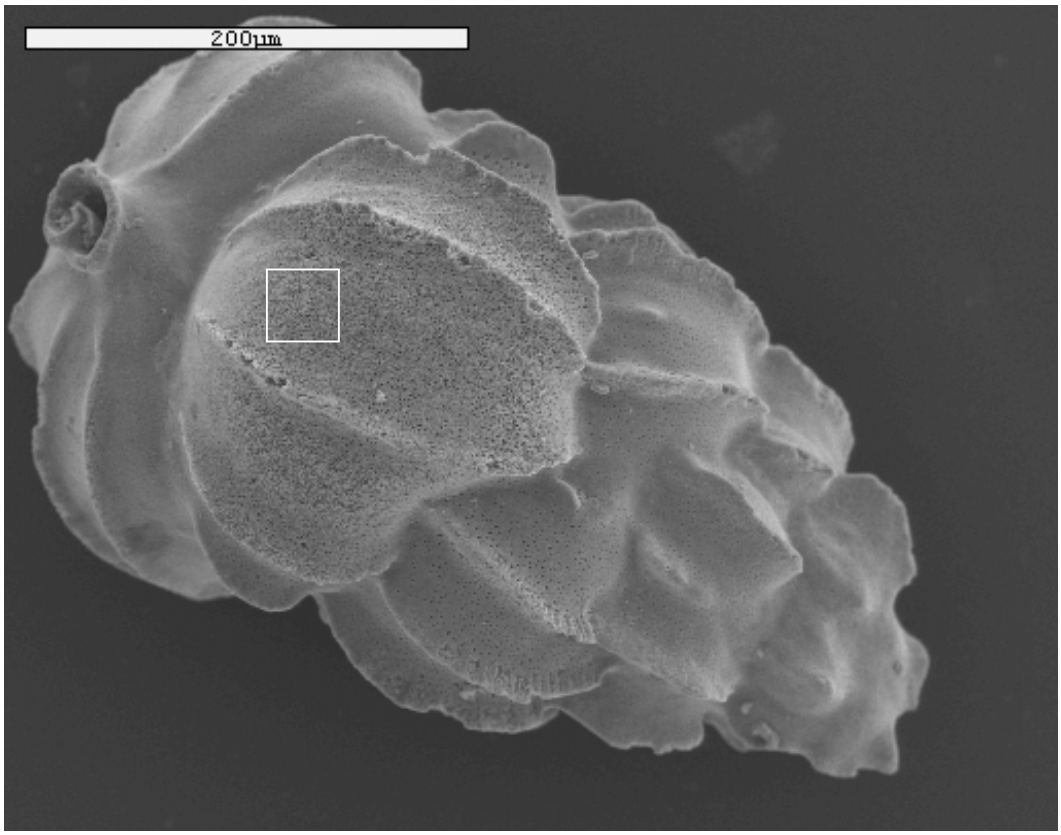

(b)

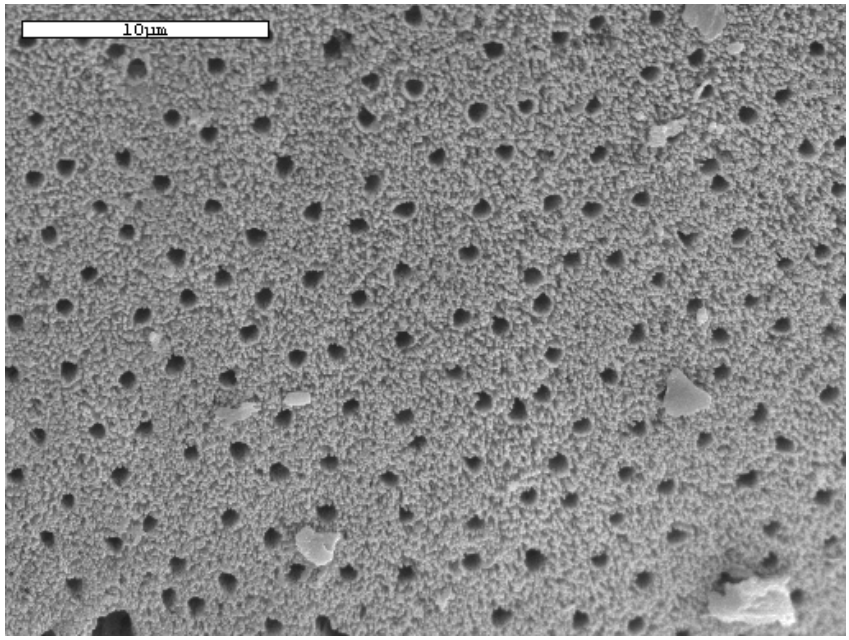

Figure 3-27 (a, b). A scanning electron micrograph of an *Uvigerina peregrina* from Monterey Bay's Invertebrate Cliffs clam bed. This specimen was taken from 21-22 cm and was not cleaned before analysis. (a) An overall shot of the test. (b) A close up of the test from the region identified in (a).

(a).

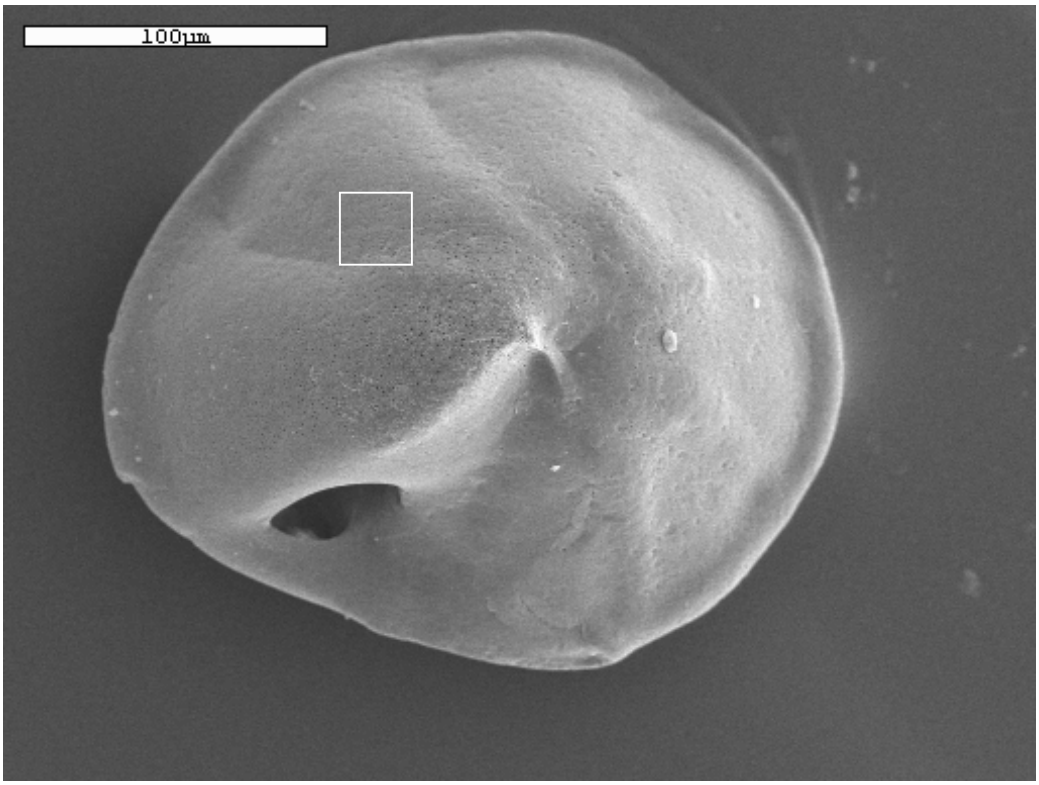

(b).

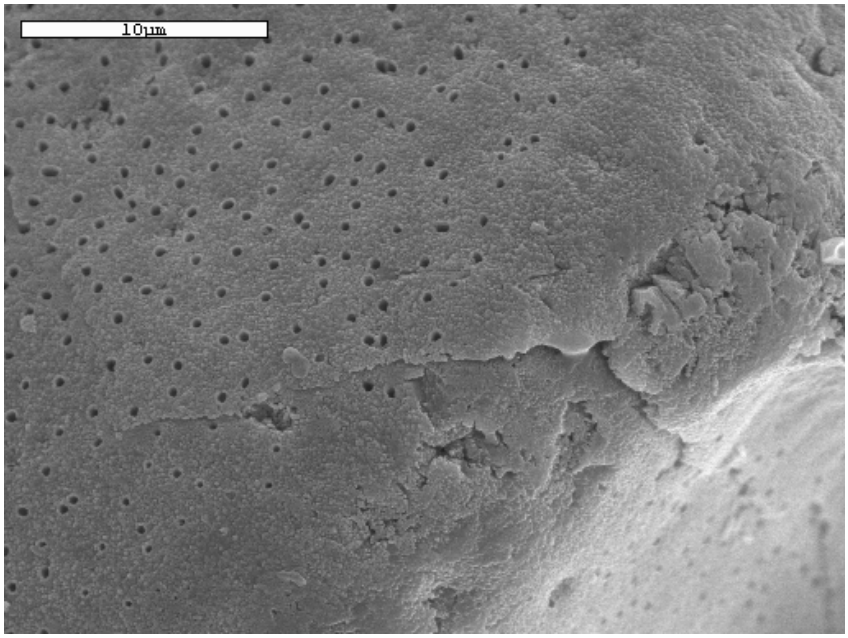

Figure 3-28. A scanning electron micrograph of an *Epistominella pacifica* from Monterey Bay's Invertebrate Cliffs clam bed. Specimen was taken from 27-28 cm depth. Specimen was cleaned before analysis. (a). An overall view of the test. (b). A close-up of the test from the region identified in (a).

(a)

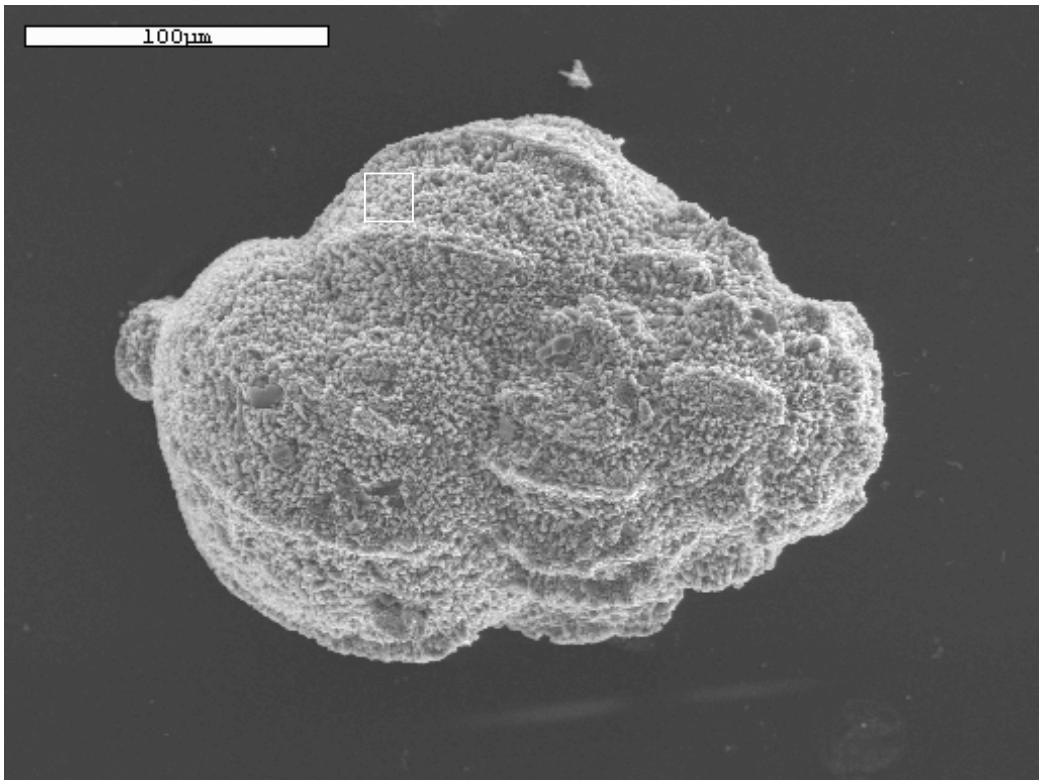

(b).

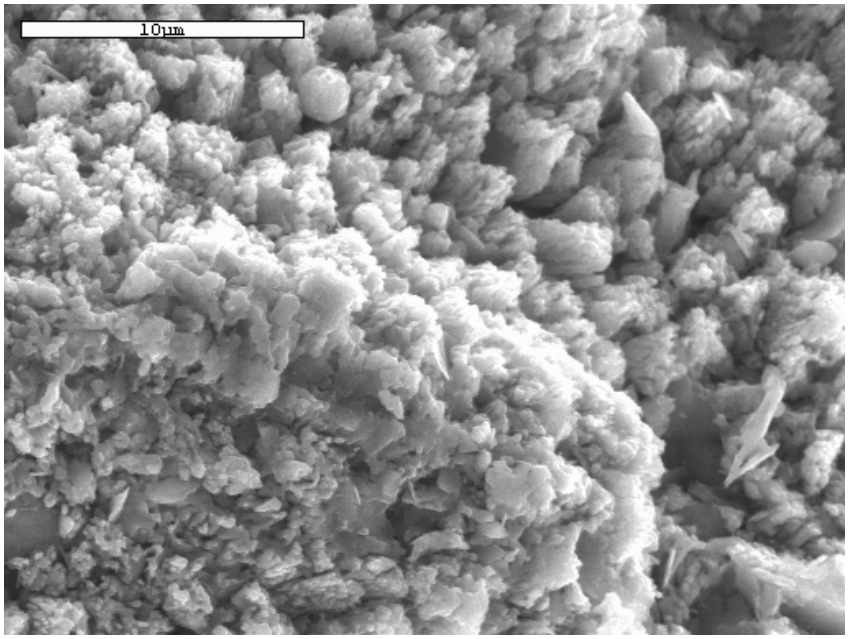

Figure 3-29 (a,b). A scanning electron micrograph of a *U. peregrina* from Eel River's long core 4 (clam bed). Specimen was taken from 8-9 cm depth and was cleaned prior to analysis. (a) An overall view of the test. (b). A close-up of the region identified in (a).

CHAPTER 4
DISCUSSION

Although cold seep locations and foraminiferal distributions are well documented, previous research reporting the isotopic compositions of seep foraminifera is scarce. Previous studies have shown that seep-inhabiting foraminifera have no special adaptations that enable them to inhabit seep sites (Bernhard et al., 2001), where sulfide and methane concentrations can reach potentially toxic levels. Some seep inhabiting species, however, do appear to have variable carbon isotopic values (Sen Gupta et al., 1997; Rathburn et al., 2000); pore water was not collected during either of these prior studies (Sen Gupta et al., 1997; Rathburn et al., 2000), so the relationship between pore water $\delta^{13}C_{DIC}$ and the $\delta^{13}C$ of foraminiferal carbonate was not analyzed.

The Effects of Methane on Pore Water Composition

The DIC in pore waters is a mixture of three end-members: seawater DIC, which has a $\delta^{13}C$ approximating 0‰ PDB, oxidized organic matter ($\delta^{13}C$ = -25‰), and oxidized methane, which has $\delta^{13}C$ values typically between –25 and -50‰ (Whiticar, 1999). The relative amounts of marine organic matter oxidation and seawater present in the subsurface will influence the pore water composition; if enough seawater is present within the sediments, it could increase the $\delta^{13}C_{DIC}$ enough to conceal an isotopically light methane signature. Pore water composition is altered by the activity of clams, which intensify the downward mixing of relatively heavy seawater and pore water, leading to a

heavier $\delta^{13}C_{DIC}$ signature. For example, in dense *Calyptogena* clam beds, the flux of seawater resulting from bioirrigation caused by bivalves was found to exceed the upward advection of pore fluids by several orders of magnitude at Aleutian cold seeps (Wallman et al., 1997).

Bacterial activity occurring within the sediment will also alter pore water composition. For instance, the microbial breakdown of organic matter, by a reaction similar to:

$$2CH_2O + SO_4^{2-} \rightarrow HCO_3^- + H_2S, \qquad (2)$$

will result in increased alkalinity and increased sulfide concentrations within pore waters. Bicarbonate produced from the microbial reduction of organic matter would yield $\delta^{13}C$ values of approximately –25 ‰. In addition to the above reaction, anaerobic methane oxidation often occurs at cold seep environments and also leads to increases in alkalinity. Anaerobic methane oxidation consumes sulfate and methane by the net reaction:

$$CH_4 + SO_4^{2-} \rightarrow HCO_3^- + HS^- + H_2O \qquad (3)$$

(Reeburgh, 1976). Since bicarbonate is a product, and the dominant component of the DIC at a neutral pH, the $\delta^{13}C_{DIC}$ should record the isotopically light carbon signature inherited from the methane.

The Invertebrate Cliffs clam bed (1780 PC30) shows little indication of the occurrence of methane oxidation, based on $\delta^{13}C_{DIC}$, alkalinity, and bisulfide ion profiles. Pore water $\delta^{13}C_{DIC}$ values are heavier than -8.6‰ in the upper 12 cm of the sediment column, and sulfide and alkalinity profiles show virtually no changes over the length of the core, with values remaining around 1 mM and 3 mM, respectively. Alternatively, pore waters at Clam Flats show light $\delta^{13}C_{DIC}$ values, high alkalinity and downcore

increases in sulfide. The presence of $\delta^{13}C$ values less than -25‰ confirms the presence of methane and its subsequent oxidation in the pore water.

The differences in the pore water compositions at Invertebrate Cliffs and Clam Flats could have a variety of causes. For instance, the Invertebrate Cliffs clam bed may have lower seepage rates or if seepage is episodic, it is possible that seepage had occurred more recently at Clam Flats, leading to isotopically lighter DIC and increased alkalinity and sulfide concentrations compared to Invertebrate Cliffs. Additionally, higher rates of bioirrigation could mask the isotopically light seep signature of Invertebrate Cliffs. Furthermore, a different methane source (possibly more thermogenic methane, which is isotopically heavier than biogenic methane), could account for some of the disparity between the two sites. Most likely, however, it is a combination of these processes that may have masked the isotopically light methane signature of the Invertebrate Cliffs seep.

Like the Clam Flats clam bed, all of the Eel River cores show a down core increase in alkalinity coupled with an increase in sulfide. The mixing of bicarbonate from marine organic carbon and the bicarbonate in seawater cannot account for the light $\delta^{13}C$ displayed by the pore water from the Eel River cores, which decrease below -25‰ (Figure 3-9). Methane oxidation must be occurring in the subsurface. In addition, the microbial activity responsible for methane and organic matter oxidation, which increase alkalinity, could initiate the precipitation of authigenic carbonate; this could explain the decreasing calcium concentrations with sediment depth.

Pore Water, Methane, and the Isotopic Composition of Foraminiferal Tests

The carbon isotopic composition of foraminifera differs from that which would be produced by direct precipitation from solution due to the processes of biogenic carbonate

formation. These differences between abiotic carbonate formation and biogenic carbonate formation are generally characterized as "vital effects". According to Grossman (1987), the source for most foraminiferal carbonate is inorganic carbon-oxygen compounds; however, isotopically light carbon-oxygen compounds resulting from both metabolic activities within the organism, as well as organic matter, may also contribute to calcification of the test (Grossman, 1987). Foraminifera inhabiting seep sites would, at least periodically, be inhabiting isotopically light pore waters, depending on the relative contributions of methane oxidation, sea water DIC, and marine organic matter.

The heterogeneous nature of methane release along with variations in the timing of test calcification could create intraspecific isotopic variations in foraminiferal carbonate. For instance, the Green Canyon area in the Gulf of Mexico displays a wide range of conspecific foraminiferal $\delta^{13}C$ values compared to non-seep areas. However, Rose Bengal stained foraminifera at this site are sparse (i.e., most individuals were dead at the time of collection), therefore only unstained tests were analyzed. These tests may have been influenced by diagenetic processes. Sen Gupta and Aharon (1994) report variations up to 1.9 ‰ in the carbon isotopic composition of unstained *U. peregrina* from the upper centimeter of a core at a Gulf of Mexico hydrocarbon seep.

Diagenesis as a Contributing Factor to Isotopically Light Foraminiferal Carbonate

Although methane appears to create variability in the carbon isotopic composition of foraminifera, it does not appear to explain the negative isotopic excursions seen in some fossil foraminifera. Other factors, such as diagenesis, may have influenced the isotopic composition of these foraminifera. Depending upon the composition (and the

saturation state) of the pore fluids, fossil foraminifera could either be recrystallized or become sites of authigenic carbonate precipitation. This would not only create variability in fossil foraminiferal tests, but would also create more negative carbon isotopic compositions, since these carbonates would be in isotopic equilibrium with pore fluids, unlike the foraminiferal carbonate precipitated during the life of the foraminifera.

Instead of hydrate destabilization, which was the theory proposed by Kennett et al (2000) to explain variations in foraminiferal test carbonate during the Pleistocene, Stott et al. (2002) proposed that in the modern Santa Barbara Basin, changes in the flux and oxidation of organic carbon associated with variations in productivity and habitat depth generate variation in the isotopic composition of live benthic foraminifera.

The $\delta^{13}C$ of pore waters sampled were isotopically heavier than –18 ‰ in the upper 4.2 meters of sediment at the Santa Barbara basin center and slightly heavier at the basin slope (Stott et al., 2002). These pore water values show little evidence of an influence by methane, which today enters the basin through cold seep environments (Stott et al., 2002). Foraminifera inhabiting these pore waters, specifically *Buliminella tenuata*, an infaunal foraminifera, had carbon isotopic values that approximated pore water $\delta^{13}C_{DIC}$ values at 3 to 4 mm, which is where they are believed to calcify their tests (Stott et al., 2002); carbon isotopic values for *B. tenuata* were around –3 ‰ (Stott et al., 2002).

Stott et al. (2000) reported that increases in the rates of carbon oxidation led to a –1.5 ‰ shift in the average $\delta^{13}C$ of *B. tenuata* between the early 1900s and the 1960s. Because today these foraminifera seem to accurately record pore water $\delta^{13}C_{DIC}$, Stott et al. (2002) suggested that as productivity in the North Pacific varied due to climatic

changes during the Pleistocene, so did the pore water $\delta^{13}C$ and the foraminiferal carbonate values. This theory may be applicable to non-seep sites in the modern Santa Barbara Basin; however, no seep sites were sampled to determine the isotopic variability of Santa Barbara seep foraminifera.

Diagenesis was also listed as a possible contributing factor to the negative carbon isotopic compositions of Pleistocene foraminifera from the Santa Barbara basin, which Kennett et al. (2000) found to vary up to 5‰ between stadials and interstadials. Reimers et al. (1996) found that the pore waters become supersaturated with respect to calcite below 2 cm, which could affect the down core carbonate record through secondary calcite precipitation.

For this study, although foraminiferal tests were microscopically examined for evidence of diagenesis before analysis, authigenic carbonate grains could have been present within the chambers of some of the tests. Many diagenetic processes may influence fossil tests. For instance, the bacterial decomposition of biological tissue, such as the protoplasm of foraminifera, under anoxic conditions generates ammonia and carbon dioxide, which lead to increased alkalinity (Berner, 1980). Additionally, if the bacterial reduction of sulfate is occurring within the sediment, alkalinity will increase further. As a consequence of these reactions, the degree of saturation with respect to carbonate minerals does increase. Depending on the degree of saturation, specifically whether supersaturation is reached, authigenic carbonate may be precipitated. This initial carbonate precipitation may function as a nucleus for continued growth, assuming that supersaturation is maintained (Berner, 1980).

The bacterial decomposition of the protoplasm, however, is probably more important for the formation of authigenic iron minerals, such as pyrite, because of the production of sulfide resulting from the reduction of sulfate, than for authigenic carbonate formation (Berner, 1980). Iron is probably readily available in the reducing pore waters and siliciclastic sediments of the seeps. Some of the authigenic carbonates from Monterey Bay analyzed by Stakes et al. (1999) contained fossil foraminifera whose chambers were concentrically filled with pyrite framboids encased in high-Mg calcite. However, pyrite formation is not solely associated with diagenetic processes, as it may also form in the tests of live foraminifera due to anaerobic bacterial activity occurring within the organism (Seigle, 1973).

Diagenesis in the Eel River Basin

Methane seepage alone cannot account for all of the isotopic variability seen in Eel River basin foraminifera. The fossil (?) foraminifera from Eel River sites had carbon isotopic compositions up to 21.3‰ lighter than Monterey Bay foraminifera and oxygen compositions, which were heavier than Monterey Bay by up to 0.72‰; this excludes the fossil foraminifera from Clam Flats, which had, in general, heavier oxygen isotopes than Eel River foraminifera (Table 4-1).

Table 4-1. A comparison of the mean $\delta^{13}C$ and $\delta^{18}O$ values of *U. peregrina* from Invertebrate Cliffs (1780 PC30), Clam Flats (1781 PC31), and Eel River (2052 LC2, LC4, and LC5).

Dive and Core No.	Site Description	Mean $\delta^{13}C$	σ ($\delta^{13}C$)	Mean $\delta^{18}O$	σ ($\delta^{18}O$)
1780 PC30 (fossil ?)	Clam bed	-0.59	0.29	3.25	0.13
1781 PC31 (fossil)	Clam bed	-1.41	0.31	4.65	0.10
2052 LC 2 (fossil ?)	Bubble site	-6.70	7.00	3.60	0.61
2052 LC 4 (fossil ?)	Clam bed	-1.37	1.55	3.56	0.34
2052 LC 5 (fossil ?)	Bacterial mat	-1.30	1.91	3.70	0.17

Using the geochemical modeling program PHREEQC (Parkhurst and Appelo, 1999), saturation indices were calculated for the Eel River cores; due to the lack of necessary parameters (such as pH, magnesium, or sulfate), saturation states could not be calculated for Monterey Bay. PHREEQC is a computer program that is designed to perform a wide variety of low-temperature aqueous geochemical calculations including speciation and saturation-index calculations (Parkhurst and Appelo, 1999). There are, however, a couple of problems encountered when using PHREEQC for seawater calculations. First, PHREEQC uses an ionic-strength term in the Debye Hückel expressions in an attempt to extend the limit of applicability of this model for seawater ionic strengths (~ 0.7 molal); the applicability of the model may fail if ionic strengths are high (> ~1.0 molal) (Parkhurst and Appelo, 1999). Another problem encountered with the calculations is the inability to introduce pressure as a variable in the modeling, which could have an effect on mineral formation at water depths of 500 to 1000 meters.

The bubble site (PC19) was characterized by the most positive saturation indices compared with the other Eel River sites, with dolomite more oversaturated compared to calcite or aragonite (Figure 4-1). Long core 2, which contains foraminifera from the bubble site, also had the most variable foraminiferal carbon values, with $\delta^{13}C$ values ranging from –23.22 to –0.49‰. The saturation indices calculated for long core 4 (clam bed) were also all positive, with dolomite being the most oversaturated, with saturation indices up to 2.42, followed by calcite, then aragonite (Figure 4-2). The first sample of long core 5 (bacterial mat), 0.5 cm, was undersaturated with respect to calcite and aragonite. However, all depths below 0.5 cm were oversaturated with respect to dolomite, calcite, and aragonite (Figure 4-3).

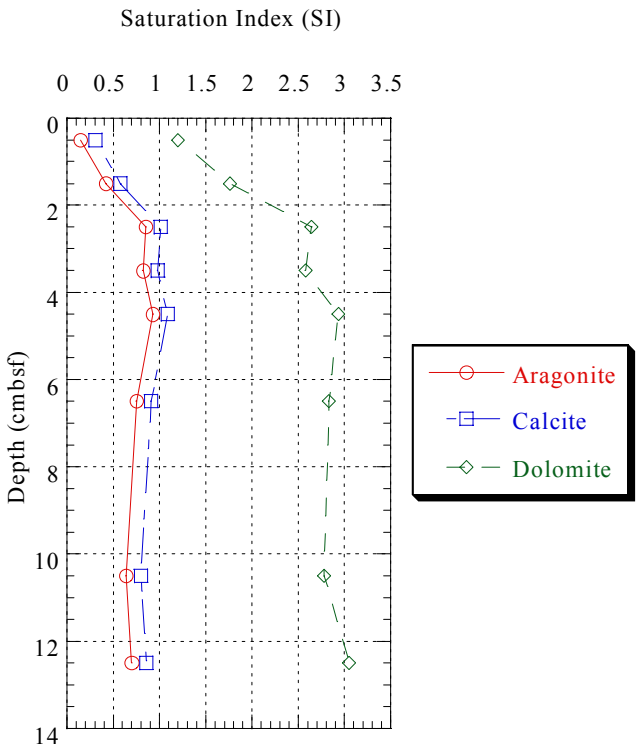

Figure 4-1. A plot of the saturation indices (SI) versus depth for the bubble site (PC19, which corresponds to the foraminifera from long core 2).

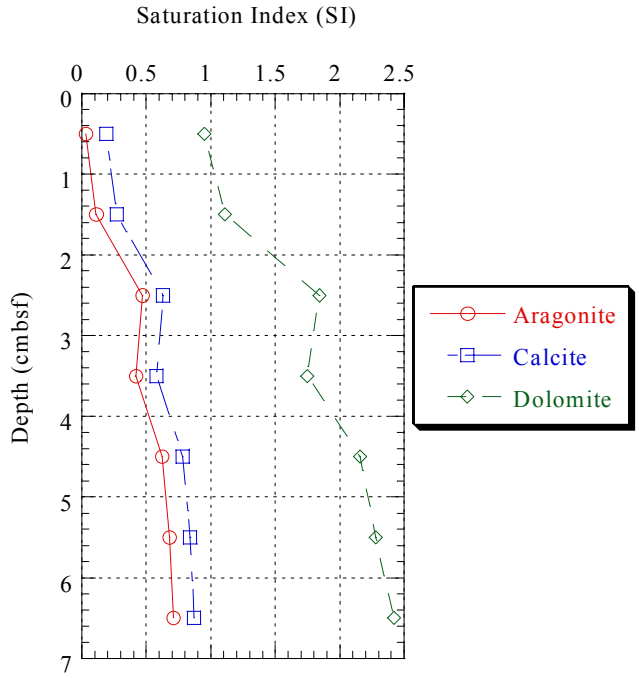

Figure 4-2. A plot of the saturation indices (SI) versus depth for PC8 (clam bed, which corresponds to the foraminifera from long core 4).

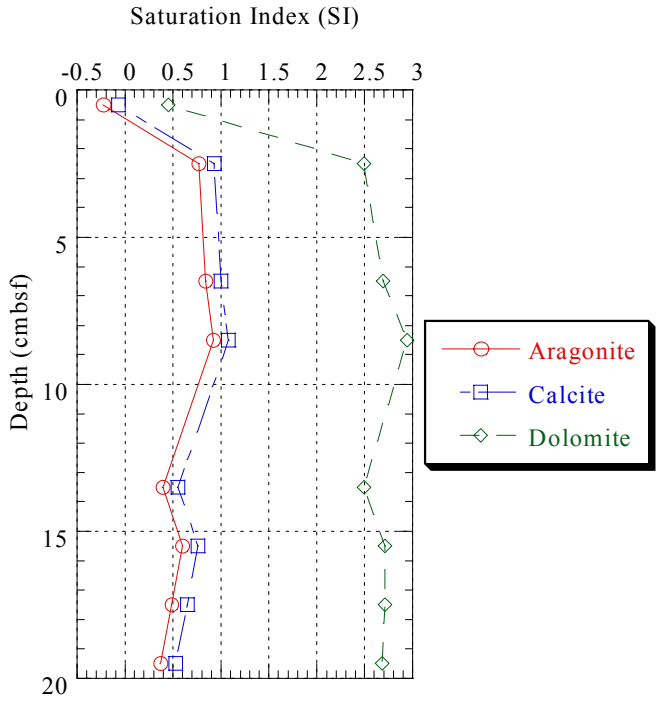

Figure 4-3. A plot of the saturation indices (SI) versus depth for PC16 (bacterial mat, which corresponds to the foraminifera from long core 5).

Based on the values and the ranges of isotopes (carbon and oxygen) seen in fossil (?) foraminifera from Eel River and the model-predicted saturation indices, it is likely that secondary calcite precipitation is masking variability created by methane seepage. If venting is episodic, during times of cessation of seepage the saturation of pore fluids is likely to change from that of supersaturated to saturated (and possibly undersaturated), which would cause authigenic carbonate precipitation to either cease or in the case of undersaturation, could cause dissolution to occur. However, when seepage does begin, the composition of pore fluids will once again be altered based on the relative amounts of DIC contributed by seawater, organic matter oxidation, and methane oxidation. If supersaturation occurs, precipitation will preferentially occur on foraminifera, which had prior mineral growth, leading to increased variation in isotopic composition. In this way variations as large as those seen in Long core 2, where at the most extreme $\delta^{13}C$ values

reach –23.22 ‰ at 9.5 cm depth and just a centimeter below this a *U. peregrina* has a $\delta^{13}C$ signature of –1.05 ‰, can be generated.

Although saturation states were not calculated for Monterey Bay, based upon the isotopic composition of the foraminifera, it is unlikely that diagenesis is affecting the fossil foraminifera. In addition to no foraminifera having extremely light isotopes, such as those seen in Eel River, the standard deviations for both carbon and oxygen isotopes are relatively small (Table 3-2), with maximum standard deviations (σ) of 0.48 and 0.29, for $\delta^{13}C$ and $\delta^{18}O$, respectively. If diagenesis were occurring, standard deviations should be larger, due to variations in pore fluid composition and the possibility of multiple periods of precipitation. Considering that live foraminifera from Monterey Bay, which would not be affected by diagenetic processes, have larger standard deviations, (a maximum of 0.55 for $\delta^{13}C$ and 0.73 for $\delta^{18}O$), it further negates the presence of diagenesis at these sites.

Stable Isotopic Compositions

The Variation in Foraminiferal Carbon Isotopes

Data focusing on the conspecific variation in foraminiferal carbonate isotopes are limited, particularly within active seep environments. Within non-seep environments, the carbon isotopic composition of most species of foraminifera varies little downcore, despite changes in the isotopic composition of pore water (McCorkle et al., 1997). Live *U. peregrina* from two non-seep sites, the North Carolina margin and the California margin (south of Pt. Sur), were analyzed and found to have $\delta^{13}C$ variations less than 0.5‰ over the length of a core (McCorkle et al., 1997). Accompanying pore water $\delta^{13}C_{DIC}$ values for these cores, which were 14.5 cm or shorter, ranged from 1.10 to

–3.43‰ (McCorkle et al., 1997). A slightly larger variation was seen in *G. pacifica*, which is characterized as a deeper infaunal species, compared to *U. peregrina*; Live *G. pacifica* displayed $\delta^{13}C$ variations up to 0.98‰ in pore waters with $\delta^{13}C_{DIC}$ ranging between –0.32 and –2.54‰ (McCorkle et al., 1997). However, live *G. pacifica* from the California borderlands, a low-oxygen environment, showed less variation in $\delta^{13}C$ downcore, with an intraspecies variation of 0.28‰ (Mackensen and Douglas, 1989). Fossil *G. pacifica* from the California borderlands showed slightly more variability in $\delta^{13}C$ than live specimens, with variations up to 0.33‰ over 8-cm (Mackensen and Douglas, 1989). No accompanying pore water data was available.

The lack of intraspecific variation at non-seep sites has been attributed to growth within a narrow depth range, growth within microenvironments characterized by relatively constant $\delta^{13}C$ values and food preferences (McCorkle et al., 1990; 1997; Rathburn et al., 1996). Most individuals within a core would have a similar test composition if growth took place within a specific microenvironment during short-lived episodes, such as during an increase in food availability (McCorkle et al., 1997).

At Clam Flats, foraminifera found living at the same depth had isotopic compositions that differed by as much as 1.95‰. These differences imply either that calcification occurred during significantly different pore water conditions for the foraminifera for at least a portion of their tests, perhaps in different microenvironments, or that variations in the amounts of metabolic carbon dioxide incorporated into the test may be causing variation in test $\delta^{13}C$ values. These two factors could be linked; a larger amount of bacteria would be sustained during times of increased methane seepage, leading to isotopically lighter pore water DIC. In addition, deposit-feeding foraminifera,

such as *U. peregrina* and *G. pacifica*, are known to ingest a large amount of sediment, as well as algal cells, bacteria, and organic detritus (Goldstein, 1999). Bacteria in particular seem to comprise an important role in the diet of deposit- feeding foraminifera (Goldstein and Corliss, 1994). Growth should be encouraged during these times of increased food availability, leading to variations in test composition not only by the occasional ingestion of bacteria, which oxidize isotopically light methane, but also by the incorporation of isotopically light DIC from the pore waters. This would, however, likely decrease isotopic variability because all foraminifera would end up with light isotopic compositions if the majority of growth occurred under these conditions.

Variations in foraminiferal carbonate among different species could be enhanced by methane seepage due to increased variations in pore water $\delta^{13}C$ with depth. The interspecific variation in the isotopic composition of foraminifera is much larger than the intraspecific variation. Fractionation linked to growth rate may account for some of the interspecies variation (McCorkle et al., 1997), with sporadic growth occurring during times of increased bacterial activity related to methane release. However, differences in the isotopic composition between species of foraminifera have verified that microhabitat (environmental) effects influence the carbon isotopic composition of benthic foraminifera (McCorkle et al., 1990; 1997). Variations in $\delta^{13}C$ values up to 3 or 4‰ have been documented between species of benthic foraminifera living within the same core simultaneously (McCorkle et al., 1990; 1997; Rathburn et al., 1996). These disparities were enhanced at seep sites, where deeper infaunal taxa were subjected to more depleted pore waters compared to shallow infaunal and epifaunal species.

The difference in the $\delta^{13}C$ composition between epifaunal and deep infaunal species of foraminifera from south of Pt. Sur varies up to 1.68‰ (McCorkle et al., 1997). The epifaunal species, *Cibicidoides wuellerstorfi* had $\delta^{13}C$ values ranging from –0.01 to –0.20‰, compared to shallow infaunal *Uvigerina species*, which ranged from –0.49 to –0.97‰, and the deep infaunal species, *G. pacifica*, which had $\delta^{13}C$ values between –1.34 and –1.67‰ (McCorkle et al., 1997). Epifaunal species at Clam Flats, such as *Planulina*, have $\delta^{13}C$ values ranging from –0.22 to +0.45‰, compared to the shallow infaunal species, *U. peregrina*, which ranges from –0.10 to –2.05‰, and *G. pacifica*, a deep infaunal species, which has $\delta^{13}C$ values ranging from –3.49 to –4.56‰. The maximum variation seen between infaunal and epifaunal species at Clam Flats was 5.01‰, compared to 1.68‰ for the non-seep site south of Pt. Sur. This increased variation is likely a result of the isotopically light $\delta^{13}C_{DIC}$ found at seep sites, which influences the infaunal foraminifera to a larger extent.

The Relationship between Methane, Pore Water $\delta^{13}C$, and Foraminiferal Carbonate

The oxidation of methane produces bicarbonate that retains methane's isotopically light carbon signature. Foraminifera, which primarily use inorganic oxygen-carbon compounds (Grossman, 1987) to calcify their tests, could incorporate this bicarbonate into their tests preserving the source's signature. However, when comparing two Monterey Bay seep sites, the Clam Flats site and the Invertebrate Cliffs site, isotopic differences are not as large as expected based on the differences in the values of pore water $\delta^{13}C_{DIC}$ at these sites. Pore waters at Clam Flats were characterized by isotopically lighter DIC than at Invertebrate Cliffs (Figure 3-4). Live *U. peregrina* from Invertebrate Cliffs range in $\delta^{13}C$ values from -0.04 to -0.85‰. Live *U. peregrina* from Clam Flats,

where $\delta^{13}C$ DIC values were four to six times lighter than at Invertebrate Cliffs, range from –0.1 to –2.05‰, only approximately 2 times lighter than Invertebrate Cliffs. Other species of foraminifera, specifically live *E. pacifica* and live *B. mexicana*, inhabiting both sites had mean $\delta^{13}C$ values that were more depleted (by ~0.30‰) at Clam Flats relative to Invertebrate Cliffs. In all cases, although foraminifera from the site with the isotopically lighter DIC had isotopically lighter tests (Table 4-2), the isotopic differences were not the magnitude expected based upon prior fossil benthic foraminiferal analyses. Even though the foraminifera appear to respond to and incorporate a portion of the isotopically light DIC into their tests, a more significant portion of foraminiferal carbonate must come from other carbon-bearing compounds.

Table 4-2. A comparison of the mean $\delta^{13}C$ values and standard deviations of live foraminifera from Clam Flats (PC31) and Invertebrate Cliffs (PC30).

Species	**Invertebrate Cliffs 1780 PC30**		**Clam Flats 1781 PC31**	
	Mean $\delta^{13}C$	**$\pm\sigma$**	**Mean $\delta^{13}C$**	**$\pm\sigma$**
U. peregrina	-0.50	0.18	-0.91	0.45
E. pacifica	-0.68	0.10	-0.98	0.04
B. mexicana	-0.80	0.08	-1.09	0.07
G. pacifica	-1.39	0.49	-3.97	0.55

It would be expected that deep infaunal species, such as *G. pacifica*, would be influenced by more isotopically depleted pore waters compared to shallow infaunal taxa, such as *U. peregrina*. As is the case in non-seep sites (McCorkle et al., 1990; 1997), this expectation appears to be true for seep sites as well; the $\delta^{13}C$ of *G. pacifica* from both sites is isotopically lighter than *U. peregrina*. The isotopic values of live *G. pacifica* at Invertebrate Cliffs had average $\delta^{13}C$ values of –1.11‰ and –1.40‰ compared to live *G.*

pacifica from the same depths (2.25 cm and 4.5 cm) at Clam Flats, which had $\delta^{13}C$ values of –3.49‰ and –4.56‰.

A Comparison of the Isotopic Composition of Seep and Non-seep Foraminifera

A comparison of foraminifera from known seep sites, with very different pore water chemistries did not create the carbon isotopic differences expected based on prior fossil foraminifera research. However, much of this early research (Wefer et al., 1994; Dickens et al., 1995; Kennett et al., 2000) was looking at older fossil foraminifera, i.e., some from the Pleistocene, where it is unsure what type of environment was present when these foraminifera were alive. The sites sampled for this study, however, are from true seep sites, where evidence of seepage, such as bubbling, authigenic carbonate crusts and chimneys, and cold seep communities, such as clams and bacterial mats, are present.

Nonetheless, the seep sites have different isotopic compositions compared to non-seep sites. For instance, from cores in the Atlantic and the Pacific Oceans, McCorkle et al. (1990) collected data confirming a shallow infaunal habitat for *U. peregrina*. Additionally, the $\delta^{13}C$ of *U. peregrina* was found to be nearly equal to the $\delta^{13}C_{DIC}$ from the top few millimeters of the cores, values typically between –0.6 and –1.2‰ (McCorkle et al., 1990). At Clam Flats live *U. peregrina* have $\delta^{13}C$ values no lighter than –2.05‰ although the $\delta^{13}C_{DIC}$ of pore water at 0.5 cm sediment depth was -36‰. In addition, even Invertebrate Cliffs, which at present shows little sign of methane seepage, has a pore water $\delta^{13}C_{DIC}$ value of –4.78‰ at 0.5 cm sediment depth compared to live *U. peregrina* isotope values no lighter than –0.85‰.

McCorkle et al. (1990; 1997) and Rathburn et al. (1996) determined that in order to compare living foraminifera from different regions, the $\delta^{13}C_{DIC}$ of bottom water (b.w.)

must be subtracted from the foraminiferal $\delta^{13}C$ value, yielding a value termed $\Delta\delta^{13}C$. Actual bottom water samples were not collected during dives for this study; however, the supernatant fluid from the core tops was removed and analyzed for $\delta^{13}C_{DIC}$. The supernatant fluid has $\delta^{13}C_{DIC}$ values that range from –3.72 to –6.42‰ (Table 3-1), which could indicate that methane oxidation is occurring in the water column above seeps at Monterey Bay and Eel River sites. An alternative explanation for the isotopically light values of supernatant is that diffusion or advection of isotopically light DIC from the sediments could enrich the water in ^{12}C. Nonetheless, methanotrophic activity does occur above seep sites in the Eel River basin and bacteria seem to oxidize methane soon after it is released from the sediment (Valentine et al., 2001).

Bottom water $\delta^{13}C_{DIC}$ values (collected 0.5 m above active seeps) ranged from –2.26 to –4.53‰ for cold seeps in the Gulf of Mexico (Aharon et al., 1992); these values are similar to the supernatant values reported here, indicating the supernatant values could represent bottom water values. Water samples were collected using a rosette, deployed from the deck of the R/V Atlantis II, containing remote–tripping water sampling bottles (Aharon et al., 1992). In contrast, bottom water values reported from non-seep sites in the Pacific Ocean south of Pt. Sur varied from –0.19 to –0.29‰ at the two locations sampled (McCorkle et al., 1997). Bottom water samples were collected using small Niskin bottles mounted on the corner of a box corer; the bottles were engineered to close when the corer reached the seafloor (McCorkle et al., 1997).

Since there are few studies (of seep and non-seep sites) reporting both pore water and foraminiferal isotopic data, *U. peregrina* is the species for which the most data is available, among both prior research and this study; therefore it will be the only species

whose isotopic data is substituted into the equation for $\Delta\delta^{13}C$. In addition, because bottom water was not sampled for this study, when determining the value of $\Delta\delta^{13}C$, both estimated values of bottom water and values obtained using supernatant fluid are compared for the Eel River and Monterey Bay cores.

Although no supernatant fluid was analyzed for the Invertebrate Cliffs or the Clam Flats clam beds, supernatant fluid is available from other environments sampled at these sites. At Invertebrate Cliffs, supernatant fluid was analyzed from the yellow bacterial mat (located within the clam ring (Figure 2-1)); the fluid has a $\delta^{13}C_{DIC}$ value of –3.72‰, whereas supernatant fluid from a reference site at the Clam Flats clam bed has a $\delta^{13}C_{DIC}$ value of –3.93‰. If these two values are substituted for bottom water in the equation for $\Delta\delta^{13}C$, resulting values for *U. peregrina* are approximately 3‰ heavier than values reported from other sites (Figure 4-4a). All *U. peregrina* show enrichment in ^{13}C relative to the supernatant DIC. If, however, an estimated bottom water value of –0.3‰ is used, the $\Delta\delta^{13}C$ values of the *U. peregrina* fall mostly within the range of reported values, where *U. peregrina* are depleted in ^{13}C relative to bottom water DIC (Figure 4-4b). Still, the variation in the carbon isotopic composition of *U. peregrina* from methane seeps at Monterey Bay is greater than that reported from non-seep sites.

Supernatant fluid for Eel River cores has $\delta^{13}C_{DIC}$ values of -5.18 and -5.72‰ (Table 3-1), which contrasts markedly with estimated bottom water $\delta^{13}C$ values based on Geosecs data, which Rathburn et al. (2000) report to be about –0.58‰ for the Eel River basin. When the $\delta^{13}C_{DIC}$ values of the supernatant fluid from Eel River (Long Core (LC) 4 and LC 5) were substituted for bottom water and compared to *U. peregrina* carbon isotopic compositions, $\Delta\delta^{13}C$ values varied significantly from those reported in the

literature. All *U. peregrina* had a positive $\Delta\delta^{13}C$ (Figure 4-5a); the values were approximately between 1.75 and 6‰, compared to those reported in the literature, which range from approximately –0.25 to -2‰ (McCorkle et al., 1990; 1997; Rathburn et al., 2000). The fossil *U. peregrina* from Clam bed 4, which had an average $\Delta\delta^{13}C$ that is significantly lighter than those reported in the literature (as well as a much larger standard deviation), were determined to be the result of authigenic carbonate contamination (Rathburn et al., 2000).

When LC 4 and LC5 were replotted using the bottom water $\delta^{13}C_{DIC}$ value (-0.58 ‰) estimated by Rathburn et al (2000) for their sampling site (40˚47.08N, 124˚35.68W), which is near the location of this study's sampling area, the average $\Delta\delta^{13}C$ values are in good agreement with those reported in the literature (Figure 4-5b). Fossil (?) *U. peregrina* from LC4 and LC5 have much larger standard deviations than all cores for which data is available, except fossil *U. peregrina* from clam bed 4.

The Eel River cores analyzed contain some foraminifera, which have been diagenetically altered, based on pore water saturation states, isotopic compositions, and comparison to other seep and non-seep sites. The maximum standard deviation for all species of foraminifera is 7.00‰. This value is larger than the excursions documented by Dickens et al. (1995) who document a –2 to -3‰ shift in $\delta^{13}C$ and $\delta^{18}O$ values in benthic foraminifera during the Paleocene, or the -5‰ excursions during the Quaternary documented by Wefer et al. (1994) and Kennett et al. (2000) off the coast of Peru and in the Santa Barbara Basin, respectively. These large excursions may also include a diagenetic component. The findings from this study show that the relationship between methane and the $\delta^{13}C$ of foraminifera is not characterized by large excursions. Instead,

foraminifera from seepage sites have more variable carbon isotopic compositions, which are similar to or approximately a mil or two lighter than foraminifera inhabiting non-seep sites.

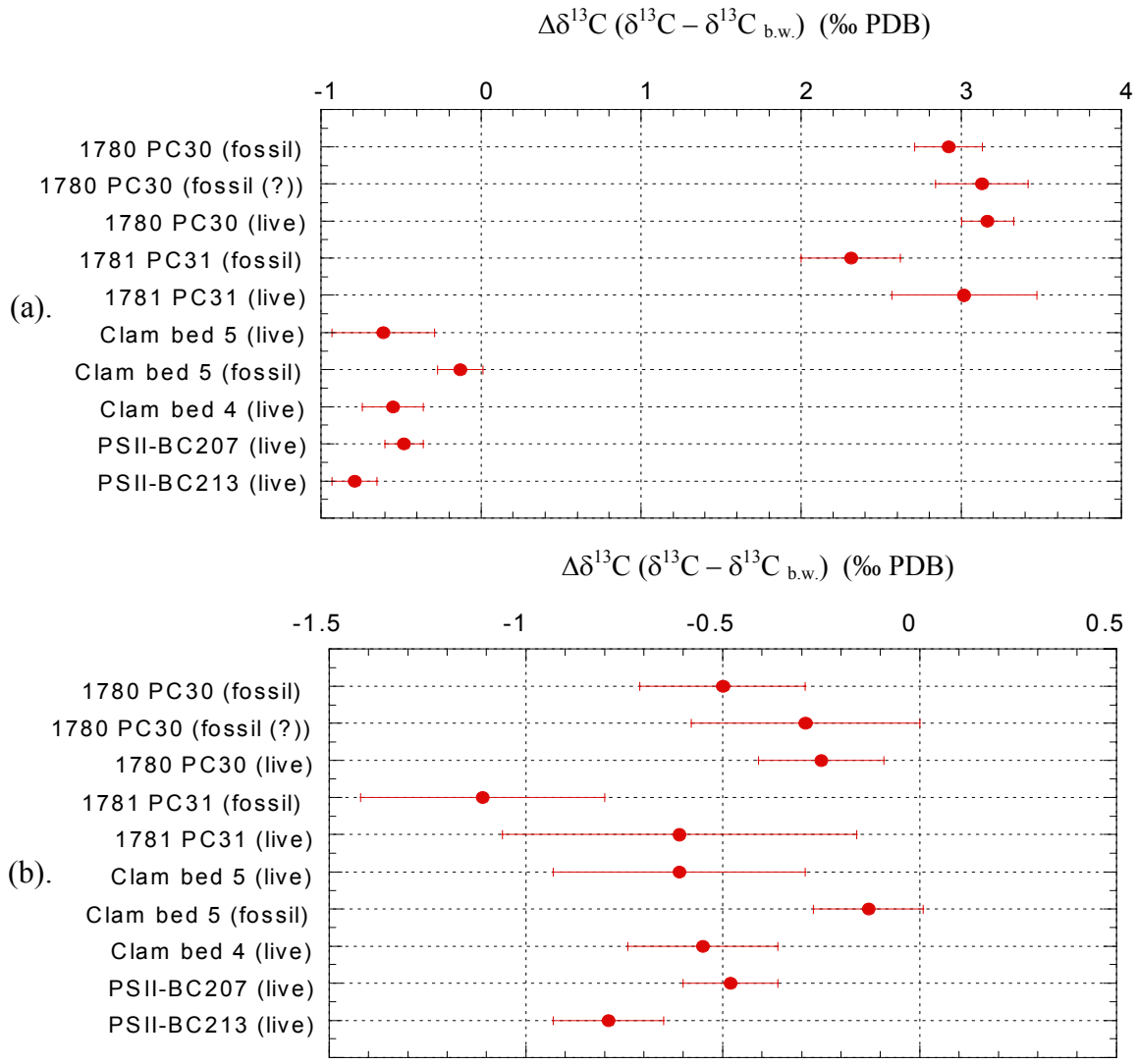

Figure 4-4(a, b). The average $\Delta\delta^{13}C$ and standard deviation (σ) of *U. peregrina* from Invertebrate Cliffs (1780 PC30) and Clam Flats (1781 PC31) compared to values reported in the literature. (a). Actual bottom water $\delta^{13}C$ is not used; instead, the supernatant fluid from the core tops is substituted for bottom water (See text for discussion). Clam bed 5 and Clam bed 4 are seep sites in the Eel River Basin sampled by Rathburn et al (2000). PSII cores are non-seep sites off the coast of California, south of Pt. Sur (McCorkle et al., 1997). (b). An estimated bottom water value of –0.3‰ is used for the calculation of the average $\Delta\delta^{13}C$ from Clam Flats and Invertebrate Cliffs. Note the difference in the scale of the x-axis from (a).

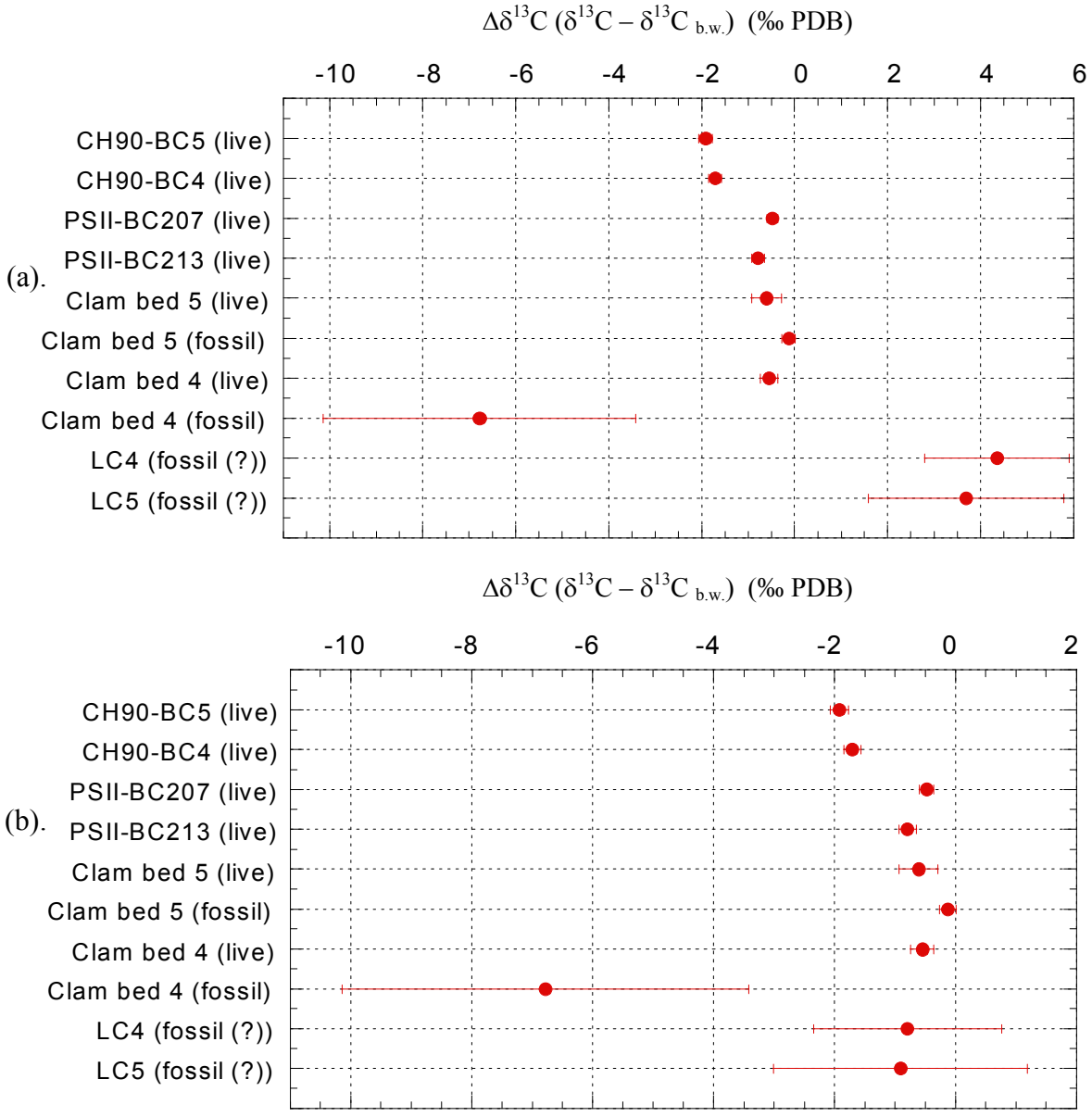

Figure 4-5(a, b). The average $\Delta\delta^{13}C$ and standard deviation of *U. peregrina* from Eel River's Long core (LC) 4 (clam bed) and LC5 (bacterial mat), compared to those reported in the literature. (a). LC4 and LC5 are plotted using $\delta^{13}C_{DIC}$ values obtained from supernatant fluid (see text for discussion). All PSII cores are from the Pacific Ocean south of Pt. Sur, whereas CH90 cores are taken from the North Carolina slope north of Cape Hatteras (McCorkle et al., 1997). Clam bed 5 and Clam bed 4 cores were collected in the Eel River basin by Rathburn et al. (2000). (b) LC4 and LC5 are replotted using Rathburn et al.'s (2000) bottom water $\delta^{13}C_{DIC}$ value of –0.58‰.

Foraminiferal $\delta^{18}O$ Compositions

Within Clam Flats, fossil foraminifera consistently display $\delta^{18}O$ values that are approximately 1.5‰ heavier than live conspecifics (Figure 4-6), whereas the $\delta^{13}C$ values of fossil species are less than 0.5‰ lighter than their live counterparts (Figure 3-14, Figure 3-15). Only a few overlapping oxygen isotopic values are seen and could result from live specimens being inhabited by algae or nematodes, leading to a false 'live' designation. In addition, most of the live foraminifera have oxygen isotopic values that are similar to both live and fossil (?) foraminifera from Invertebrate Cliffs.

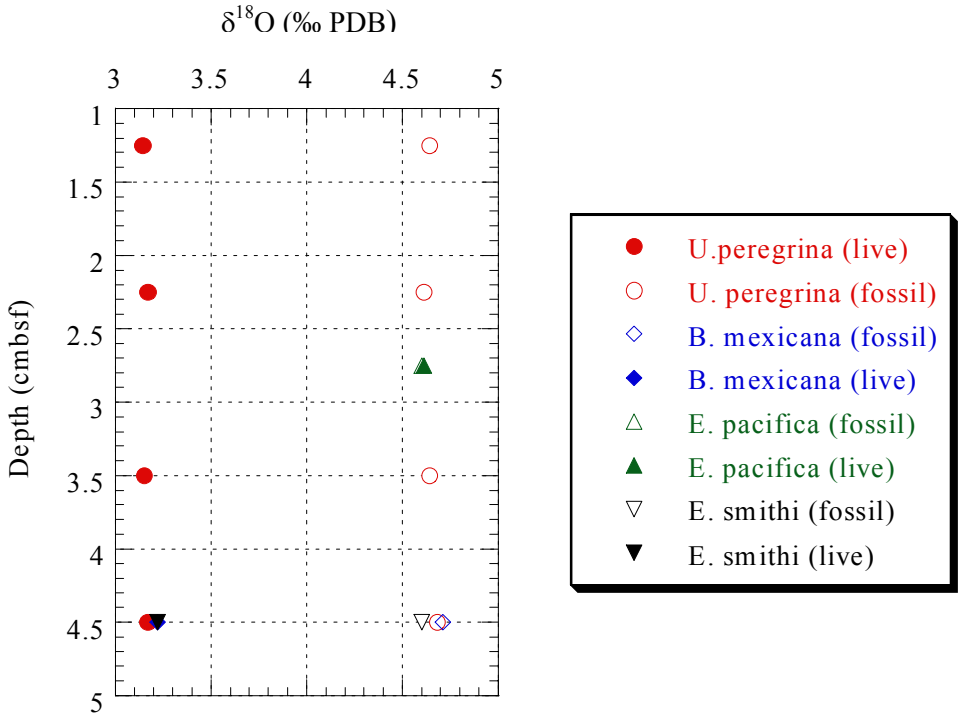

Figure 4-6. A $\delta^{18}O$ comparison of live and fossil conspecific foraminifera from Clam Flats (1781 PC31). Note: *E. pacifica* values from 2.75 cm overlap and the live *B. mexicana* (from 4.5 cm) is clustered with other live species around 3.15‰.

The $\delta^{18}O$ values of the fossil foraminifera from Clam Flats places them within the range of authigenic carbonate analyzed from the Clam Flats area, which Stakes et al. (1999) determined to vary between 4.05 and 5.19‰. The $\delta^{13}C$ values of these same

authigenic carbonates range from –48.82 to –52.60‰ (Stakes et al., 1999). If authigenic carbonate overgrowths, such as those found by Stakes et al. (1999) were to account for the 1.5‰ increase in $\delta^{18}O$, the resulting decrease in $\delta^{13}C$ would be between –13 and –18‰, as somewhere between 28 and 35% of the oxygen isotopic composition would have to be provided by authigenic carbonate. Although pore fluid chemistry could have varied significantly over time, the isotopic composition of numerous fossil foraminifera (of various species) is consistent; therefore, it is unlikely that even multiple stages of authigenic carbonate formation could explain the disparity in $\delta^{18}O$ between live and fossil foraminifera.

One explanation for the disparity between fossil and live foraminifera from Clam Flats is that the fossil foraminifera are remnants from a colder time, perhaps the Last Glacial Maximum (LGM), exposed by an erosional event. Barry et al. (1996) noted the Clam Flats site was characterized by clams inhabiting small shallow depressions. Additionally, clams were noted to form aggregations along the lower edges of small, meter-scale scarps (Barry et al., 1996). As slumping occurs, foraminifera inhabiting the sediment will be displaced. With later recolonization of the site, live foraminifera would inhabit sediment containing older, fossilized foraminifera; these fossilized foraminifera could have secreted their tests under very different temperature conditions, perhaps during glacial times, when deep water was older and had lower $\delta^{13}C$ and cooler temperatures would have contributed to heavier $\delta^{18}O$ compositions. Furthermore, seawater $\delta^{18}O$ would have been heavier due to the glacial sequestering of isotopically light ice. According to Curry et al. (1988), the $\delta^{18}O$ of the deep water in the Pacific Ocean during the LGM was between 3.86 ± 0.06‰ and 4.35 ± 0.02 ‰. In addition, the

oxygen isotopic difference between the LGM and present (expressed as glacial – interglacial) is between 1.33 and 1.67‰ (Curry et al., 1988). Likewise, the LGM had deep-water $\delta^{13}C$ values that were between 0.21 and 0.60‰ lighter than present $\delta^{13}C$ values (Curry et al., 1988). These offsets correlate nicely with the isotopic offsets between fossil and live foraminifera from Clam Flats.

A Comparison of Foraminiferal Oxygen Isotopes from Seep and Non-seep Sites

Living foraminifera from different areas can be compared if calcite in equilibrium with bottom water $\delta^{18}O$ values are subtracted from foraminiferal $\delta^{18}O$ values, yielding a value termed $\Delta\delta^{18}O$ (McCorkle et al., 1990; 1997; Rathburn et al., 1996). For Monterey Bay, the value for calcite in equilibrium with bottom water $\delta^{18}O$ was taken from Stakes et al. (1999), who calculate a $\delta^{18}O$ value of approximately 3.2‰ for a temperature of 4° C, which is approximately the same bottom water temperature as this study. Living foraminifera from both Invertebrate Cliffs and Clam Flats fall within the range of $\Delta\delta^{18}O$ values reported in the literature (Figure 4-7). In addition, fossil foraminifera from Invertebrate Cliffs also fall within the reported range, excluding two *U. peregrina* values. Fossil foraminifera from Clam Flats, however, fall outside the reported range, with values varying from 1.29 to 1.63‰, providing further confirmation that these foraminifera secreted their tests under different bottom water conditions than live foraminifera inhabiting the same sediment.

In the Eel River basin, sites sampled during this study are close to and in similar water depths (~500 m) to those sampled by Rathburn et al. (2000), who estimated a bottom water $\delta^{18}O$ in equilibrium with calcite value of 2.35‰. The average $\Delta\delta^{18}O$ values for Eel River fossil foraminifera are heavier than the fossil values reported by Rathburn et

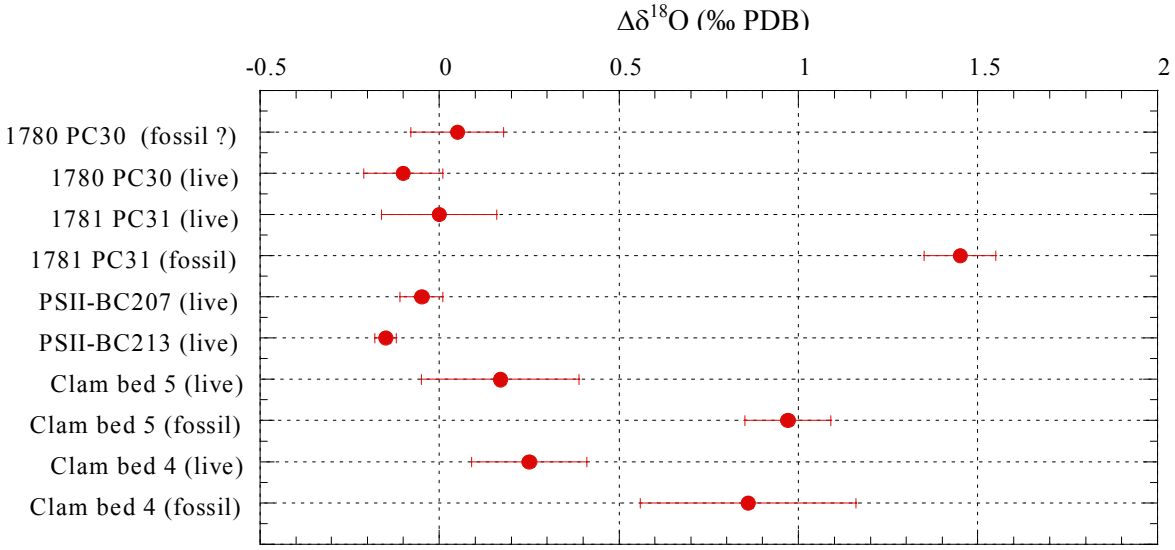

Figure 4-7. A plot of the $\Delta\delta^{18}O$ values of *U. peregrina* from Invertebrate Cliffs (1780 PC30) and Clam Flats (1781 PC31) relative to those values reported in the literature. PSII cores are from south of Pt. Sur (McCorkle et al., 1997). Clam bed 5 and Clam bed 4 are from the Eel River Basin (Rathburn et al., 2000).

al. (2000) (Figure 4-8). In addition, many are heavier than the only $\delta^{18}O$ value reported for authigenic carbonate from the area, which had a $\delta^{18}O$ value of 3.79‰ and a $\delta^{13}C$ value of –33.57‰ (Rathburn et al., 2000).

It has been previously discussed that the isotopic variability found throughout the Eel River cores is in part due to diagenesis, which is also masking variability caused by hydrate dissociation (and the subsequent bacterial oxidation of methane). Because Eel River sites sampled near the boundary of the hydrate stability zone, hydrate dissociation could be causing variations in the $\delta^{18}O$ of pore fluids. The lattice composing methane hydrates preferentially incorporates ^{18}O, therefore, upon dissociation, fluids containing hydrates would be isotopically heavier than fluids not influenced by hydrate dissociation. For instance, Aharon et al. (2001) determined that methane hydrate dissociation has led to a maximum ^{18}O enrichment of 1.7 ‰ in *Bolivina species* in the Gulf of Mexico. The timing of hydrate dissociation and test calcification could create isotopic variability,

however, because live foraminifera were not analyzed, determining the relative contribution of these processes is impossible.

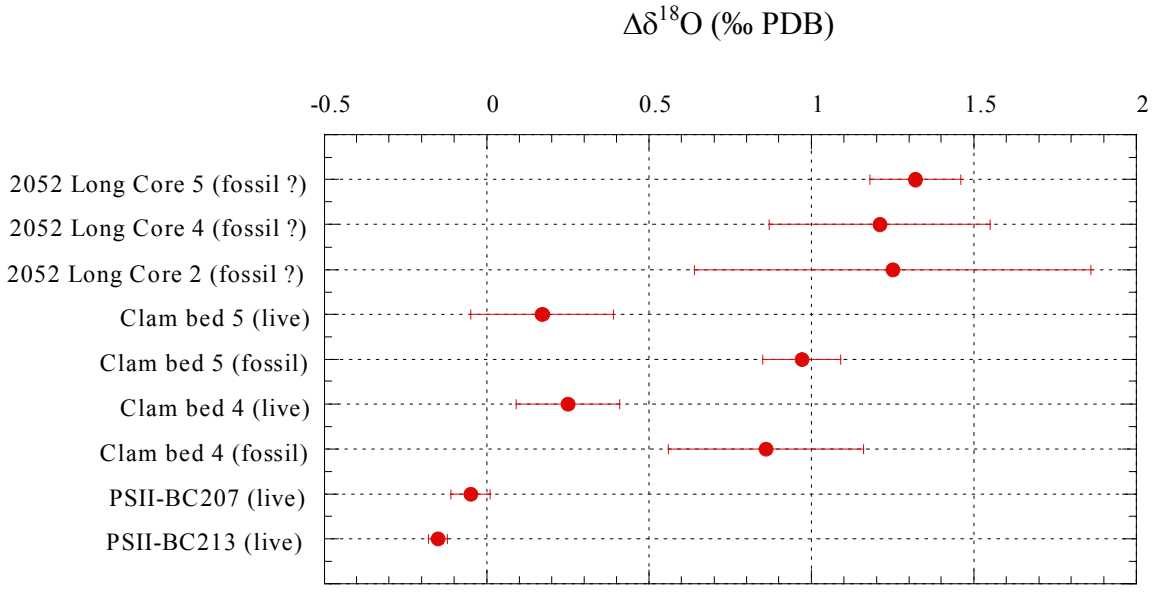

Figure 4-8. A plot of the $\Delta\delta^{18}O$ values of *U. peregrina* from Eel River (2052) LC5 (bacterial mat), LC4 (clam bed) and LC2 (bubble site) relative to those values reported in the literature. PSII cores are from south of Pt. Sur (McCorkle et al., 1997). Clam bed 5 and Clam bed 4 are from the Eel River Basin (Rathburn et al., 2000).

CHAPTER 5
CONCLUSIONS

Methane seepage and its ensuing oxidation by bacteria produces isotopically light DIC in pore waters. In addition, methanotrophic activity creates a favorable environment for the precipitation of authigenic minerals; increases in alkalinity and sulfide could result in the precipitation of carbonate and iron minerals, particularly pyrite. In addition, the degrading protoplasm of dead foraminifera may provide a nucleus for mineral growth (Berner, 1980). Because seepage is likely episodic, pore fluid saturation states could vary temporally, increasing the diversity of isotopic signals found at seep sites. Therefore, careful attention needs to be paid to fossil benthic foraminifera being used to assess the history of methane seepage; as variation in the carbon isotopic composition will be overshadowed by diagenetic effects. Live foraminifera should be analyzed whenever possible to estimate the relative isotopic contribution of methane seepage and possibly diagenesis to fossil foraminiferal carbonate.

This study shows that methane seepage creates carbon isotopic variability in benthic foraminiferal tests; the negative carbon isotopic signal which is imparted on the test is not more than a few per mil. Foraminifera living in the ^{13}C-depleted environment of seeps did not develop $\delta^{13}C$ values in their tests that were similar to pore water values, which had carbon isotopic values as light as -37‰ in the upper 5 cm of a core. Therefore, although methane seepage does create steeper decreases in $\delta^{13}C_{DIC}$ with depth than profiles containing organic matter oxidation alone, isotopic differences between

epifaunal and infaunal species are not enhanced by more than 1 or 2‰ relative to non-seep species. Large negative carbon isotopic excursions, like those seen in Eel River foraminifera, appear to result from authigenic carbonate contamination; however, live foraminifera, which would help quantify the variability contributed by methane seepage, were not analyzed. Additional studies on the variability of foraminiferal carbon isotopes in seep and non-seep environments would enable a more complete characterization of the effects of methane seepage on benthic foraminifera.

Based on the available data from non-seep environments, it appears that the carbon isotopic composition of benthic foraminifera from seep sites is similar or more negative than non-seep foraminifera. However, bottom water samples need to be collected and analyzed for $\delta^{13}C_{DIC}$ to determine if the $\Delta\delta^{13}C$ equation can be used to compare seep and non-seep foraminifera. Additionally, bottom water samples must be collected from seep sites to determine whether DIC values in the waters above seeps are as ^{13}C depleted, up to –4.5‰, as those reported by Aharon et al. (1992). Looking at epifaunal foraminifera, such as *Planulina species*, which are believed to secrete their test in isotopic equilibrium with bottom waters (at least in non-seep environments) would allow for a better characterization of bottom water chemistry and enable conclusions to be drawn on the ability of seep fluxes to alter bottom water composition.

Although a microhabitat effect does exist in seep settings and pore water composition does influence benthic foraminiferal composition, it appears that pore water plays a larger role in creating isotopic variability than it does in imparting negative isotopic signatures on foraminifera. For instance, in non-seep sites, *U. peregrina* had carbon isotopic compositions that were nearly equal to the pore water concentration in

the upper 0.5 cm of the sediment (McCorkle et al., 1997). This, however, was not the case for the seep environments sampled during this study; the $\delta^{13}C$ of *U. peregrina*, on average, was between 4 and 18 times heavier than pore water $\delta^{13}C_{DIC}$. This disequilibrium could indicate that the foraminifera have specific microenvironments where calcification takes place, possibly near the surface or near burrows where seawater DIC ($\delta^{13}C_{DIC}$ approximately 0‰) would contribute more to the DIC pool.

Sediments containing pore waters that have isotopically lighter carbon signatures also contain foraminifera with more variable carbon isotopic compositions. It is, however, impossible to know the pore water conditions under which these foraminifera calcify their tests. Nonetheless, foraminifera are incorporating a portion of DIC derived carbon into their tests, which creates isotopic variability among foraminifera as pore water chemistry changes.

APPENDIX A
PORE WATER CHEMISTRY

Dive Number	Location	Push Core No.	cm-bsf	Alkalinity (mM)	pH	Ca (mM)	Mg (mM)	SO_4 (mM)	HS^- (mM)
1780	Monterey Bay – Invertebrate Cliffs	34	0.5	13.59	7.39	17.1			
			2.0	14.97	7.41	18.9			
			4.0	16.72	7.20	18.3			0.2
			6.0	15.91	7.46	19.1			
			8.0	17.61		17.2			3.0
			10.0	19.89		17.0			1.2
			12.0	17.83	7.92	16.1			
		79	0.5	2.59	7.40	11.8			
			2.0	2.74	7.28	11.3			
			4.0	2.66		11.2			0.2
			6.0	3.01	7.60	11.8			0.5
			8.0	3.14	7.65	11.5			0.6
			10.0	3.38	7.87	11.3			1.1
			12.0	3.61	7.87	11.8			
		31	0.5	3.39		12.9			1.1
			2.0	7.34	7.93	13.3			1.0
			4.0	13.57	8.02	13.0			2.2
			6.0	16.22		14.1			2.3
			8.0	19.57	7.65	15.3			2.2
			10.0	20.03	7.71	17.2			2.3
			12.0	20.56		16.3			1.9
		38	0.5	2.61	7.32	10.7			
			2.0	2.58	7.31	11.3			
			4.0	2.58	7.40	12.0			
			6.0	2.46	7.32	11.7			
			8.0	2.59	7.30	11.1			
			10.0	2.71	7.46	12.1			
			12.0	2.73	7.57	10.8			
			14.0	2.85	7.49	11.2			
			16.0	2.92		11.7			
			18.0	3.01	7.49	11.2			
1781	Monterey Bay- Clam Flats	80	0.5	11.10		11.2			4.3
			2.0	19.47		10.3			7.9
			4.0	31.80		9.0			15.4

Dive Number	Location	Push Core No.	cm-bsf	Alkalinity (mM)	pH	Ca (mM)	Mg (mM)	SO_4 (mM)	HS^- (mM)
1781	Monterey Bay – Clam Flats	80	6.0	34.27		7.7			16.3
			8.0	32.30		6.9			15.5
			10.0	37.55		6.6			18.8
			12.0	38.82		7.7			19.5
			14.0	35.35		7.2			19.5
			16.0	36.92		8.4			18.8
		72	0.5	2.82		11.8			0.7
			2.0	2.81		10.7			
			4.0						3.8
			6.0	2.90		10.1			
			11.0	3.09		11.4			0.8
			16.0	2.27		10.7			
			21.0	4.03		10.6			0.3
		38	0	2.50	7.59				
			0.5	2.92	7.66	11.3			0.5
			2.0	2.94	7.55	11.1			
			4.0	2.77	7.73	10.6			0.6
			6.0	2.74	7.99	10.8			
			11.0	3.52	8.18	12.9			
			13.0						1.4
		28	0.5	3.03	7.70	14.4			0.4
			2.0	4.60		10.9			1.8
			4.0	22.93	8.34	9.2			5.4
			6.0	28.68		8.1			5.0
			8.0	25.28	8.47	7.5			5.7
			10.0	24.77	8.45	7.4			4.8
			12.0	30.07	8.47	8.5			6.6
			14.0	28.93		8.6			7.5
2052	Eel River Basin	8	0	2.50	–	9.9	51.6	27.9	–
			0.5	3.90	7.67	9.7	49.1	27.1	0.0
			1.5	4.40	7.73	9.8	48.7	26.6	0.3
			2.5	5.80	8.00	9.4	48.8	25.4	0.5
			3.5	6.80	7.93	9.3	48.7	24.5	1.3
			4.5	8.30	8.07	9.2	49.4	23.9	1.8
			5.5	11.20	8.05	9.3	51.7	22.5	3.7
			6.5	17.30	8.05	6.8	45.4	14.5	6.9
		16	0	2.50	–	9.8	51.6	–	–
			0.5	3.20	7.52	9.5	49.6	29.5	0.0
			1.5	–	–	9.1	49.2	28.2	0.0
			2.5	4.80	8.43	8.7	50.7	27.5	0.0
			5.5	–	–	5.5	46.3	–	–
			6.5	15.40	8.23	7.1	47.2	22.2	5.4
			8.5	25.30	8.14	5.8	47.2	18.5	7.6
			11.5	32.60	–	3.9	46.7	10.5	11.9

Dive Number	Location	Push Core No.	cm-bsf	Alkalinity (mM)	pH	Ca (mM)	Mg (mM)	SO_4 (mM)	HS^- (mM)
2052	Eel River Basin	16	13.5	30.80	8.21	1.4	46.4	9.3	13.1
			15.5	32.10	8.21	2.1	46.1	5.2	13.5
			17.5	32.40	8.29	1.3	46.1	4.1	12.7
			19.5	33.70	8.34	0.9	51.4	3.4	13.8
		19	0	2.50	–	9.6	50.9	27.5	–
			0.5	4.60	7.78	9.6	50.4	26.3	0.5
			1.5	9.60	7.90	9.0	49.0	22.1	3.7
			2.5	14.00	8.12	10.8	61.5		6.0
			3.5	18.30	8.10	8.4	48.6	15.1	8.4
			4.5	22.10	8.24	5.9	45.7	10.4	8.5
			6.5	28.00	8.22	3.2	45.2	4.5	11.3
			10.5	36.10	8.22	2.0	42.5	0	16.1
			12.5	35.60	8.19	1.5	45.3	0	–
			14.5	36.50	8.22	0.9	45.0	0	14.7
			16.5	35.00	8.34	0.7	45.9	0	15.6
2054	Eel River Basin	2	0	2.50	–	9.6	50.3	–	0.0
			0.5	17.60	–	9.0	47.8	23.3	6.2
			1.5	20.90	8.44	9.3	52.2	19.1	6.9
			2.5	24.50	8.61	4.8	53.3	–	6.9
			3.5	22.30	8.34	6.8	45.4	19.6	7.5
			4.5	25.30	8.37	3.0	44.2	14.4	7.6
			5.5	29.50	8.36	2.8	48.6	9.3	8.4
			6.5	31.50	8.46	1.5	44.9	6.3	6.5
			7.5	29.40	8.18	1.0	45.0	6.4	6.4
		40	0	2.27	-	10.3	52.7	28.2	0.0
			0.5	2.70	7.27	9.8	49.4	28.7	0.0
			1.5	3.00	7.59	9.4	48.7	28.7	0.0
			2.5	5.40	7.95	9.4	48.0	28.3	0.8
			3.5	7.40	7.98	9.3	47.8	26.9	1.6
			4.5	9.80	8.10	9.1	47.5	24.4	3.2
			5.5	11.00	8.15	7.9	46.6	26.7	2.2
			6.5	16.40	8.20	6.8	46.0	21.7	5.0
			7.5	17.20	8.29	5.5	54.5	23.3	4.9

Dive Number	Location	Push Core	Site Description	Interval (cmbsf)	$\delta^{13}C_{DIC}$
1780	Monterey Bay- Invertebrate Cliffs	38	Reference- (clam bed)	0-1	-4.60
				1-3	-3.63
				3-5	-4.42
				5-7	-4.49
				7-9	-4.48
				9-11	-4.69
				11-13	-4.91
				11-13	-4.87
				15-17	-6.09
		31	Yellow Bacterial Mat	Core top supernatant	-3.72
				0-1	-7.60
				1-3	-15.22
				3-5	-18.55
				5-7	-21.07
				7-9	-22.79
				9-11	-22.69
				11-13	-22.00
		34	White/gray Bacterial Mat	0-1	-12.77
				1-3	-13.33
				3-5	-15.09
				5-7	-15.98
				7-9	-18.68
				9-11	-21.00
				11-13	-21.16
		79	Clam Bed	0-1	-4.78
				1-3	-4.12
				3-5	-4.44
				3-5	-4.40
				5-7	-5.75
				7-9	-6.48
				9-11	-7.52
				11-13	-8.58
1781	Monterey Bay- Clam Flats	38	Reference- (clam bed)	Core top supernatant	-3.93
				0-1	-5.46
				1-3	-6.85
				3-5	-6.99
				17-19	-21.62
		28	Bacterial Mat	0-1	-13.79
				3-5	-58.15
				5-7	-56.80
				9-11	-49.54
				11-13	-47.65
				13-15	-47.06
		80	Clam Bed	0-1	-36.47
				1-3	-45.73
				9-11	-41.48

Dive Number	Location	Push Core	Site Description	Interval (cmbsf)	$\delta^{13}C_{DIC}$
1781	Monterey Bay-Clam Flats	80	Clam Bed	9-11	-43.95
				15-17	-42.39
		72	Reference-(bacterial mat)	1-3	-8.21
				3-5	-5.81
				5-7	-7.06
				10-12	-11.24
				15-17	-13.20
				20-22	-10.95
2052	Eel River Basin	8	Clam Bed	Core top supernatant	-5.72
				0-1	-13.51
				2-3	-22.36
				4-5	-27.09
				6-7	-33.95
		16	Bacterial Mat	Core top supernatant	-5.18
				0-1	-9.16
				2-3	-24.06
				6-7	-37.36
				8-9	-38.47
				13-14	-39.08
				15-16	-37.85
				19-20	-38.81
		19	Bubble Site	0-1	-17.83
				2-3	-31.97
				4-5	-37.78
				10-11	-33.49
				12-13	-32.03
				16-17	-30.83
2054		2	Clam Bed	Core top supernatant	-6.42
				0-1	-25.17
				2-3	-23.86
				4-5	-23.19
				6-7	-19.58
				7-8	-18.15
		40	Bacterial Mat	0-1	-9.02
				2-3	-18.91
				4-5	-25.76
				6-7	-30.57
				7-8	-32.06

APPENDIX B
FORAMINIFERAL ISOTOPE DATA

DIVE NUMBER	SITE	TUBE-CORE	DEPTH (cm-bsf)	SPECIES	$\delta^{13}C$	$\delta^{18}O$	NO. OF INDIVIDUALS RUN	LIVE/ FOSSIL
1781	CLAM FLAT	31	0-1	*Gyroidinoides altiformis*	-0.70	3.15	2	LIVE
				Uvigerina peregrina	-1.36	3.09	2	
				Uvigerina peregrina	-1.18	4.04	2	
				Bulimina mexicana	-1.03	3.80	5	
			1 - 1.5	*Uvigerina peregrina*	-1.34	4.63	0.5	FOSSIL
				Uvigerina peregrina	-1.03	4.83	0.5	
				Uvigerina peregrina	-1.35	4.62	1	
				Uvigerina peregrina	-1.85	4.49	1	
				Bulimina mexicana	-1.04	4.89	2	
				Bulimina mexicana	-2.24	4.65	3	
				Uvigerina peregrina	-0.89	3.11	1	LIVE
				Uvigerina peregrina	-0.62	3.21	1	
				Uvigerina peregrina	-0.43	3.12	1	
				Uvigerina peregrina	-0.69	3.12	1	
				Globobulimina pacifica	-3.87	3.42	1	
				Planulina sp.	-0.22	2.63	1	
			1.5- 2	*Epistominella pacifica*	-1.09	4.61	2	FOSSIL
				Epistominella pacifica	-1.11	4.65	2	
				Uvigerina peregrina	-0.55	3.16	0.5	LIVE
				Uvigerina peregrina	-0.49	3.28	1	
				Uvigerina peregrina	-0.74	3.21	1	
				Uvigerina peregrina	-0.22	3.25	1	
				Uvigerina peregrina	-0.21	3.21	0.5	
				Uvigerina peregrina	-0.57	3.15	1	
				Uvigerina peregrina	-0.97	3.10	0.5	
				Gyroidinoides altiformis	-0.83	3.14	2	
				Gyroidinoides altiformis	-0.66	3.11	1	
			2 - 2.5	*Uvigerina peregrina*	-1.57	4.58	1	FOSSIL
				Uvigerina peregrina	-1.04	4.65	1	
				Uvigerina peregrina	-1.31	4.58	1	
				Bulimina mexicana	-1.19	4.72	3	
				Uvigerina peregrina	-2.05	3.04	1	LIVE
				Uvigerina peregrina	-1.13	3.17	1	
				Uvigerina peregrina	-0.81	3.21	0.33	
				Uvigerina peregrina	-1.14	3.07	0.33	
				Uvigerina peregrina	-0.94	3.12	0.33	
				Uvigerina peregrina	-0.10	3.43	0.5	

DIVE NUMBER	SITE	TUBE-CORE	DEPTH (cm-bsf)	SPECIES	$\delta^{13}C$	$\delta^{18}O$	NO. OF INDIVIDUALS RUN	LIVE/ FOSSIL
1781	CLAM FLAT	31	2-2.5	*Epistominella smithi*	-0.92	3.57	3	LIVE
				Globobulimina pacifica	-3.49	3.30	1	
				Epistominella pacifica	-0.92	3.15	2	
			2.5 - 3	*Epistominella pacifica*	-1.20	4.59	3	FOSSIL
				Epistominella pacifica	-1.19	4.61	2	
				Uvigerina peregrina	-1.82	3.18	1	LIVE
				Uvigerina peregrina	-1.12	3.15	1	
				Uvigerina peregrina	-0.25	3.21	1	
				Uvigerina peregrina	-0.75	3.25	0.5	
				Uvigerina peregrina	-1.39	3.27	0.5	
				Epistominella smithi	-0.60	3.11	5	
				Gyroidinoides altiformis	-0.66	3.11	2	
				Gyroidinoides altiformis	-0.45	3.13	1	
				Epistominella pacifica	-0.99	4.56	1	
				Epistominella pacifica	-1.02	4.63	1	
				Epistominella pacifica	-1.01	4.66	1	
			2 .5-3	*Planulina sp.*	0.06	2.60	0.5	LIVE
				Planulina sp.	0.45	2.86	1.0	
				Planulina sp.	0.07	2.60	0.5	
			3 - 4	*Uvigerina peregrina*	-2.03	4.62	2	FOSSIL
				Uvigerina peregrina	-1.40	4.73	1	
				Uvigerina peregrina	-1.30	4.58	1	
				Bolivina spissa	-1.80	4.55	3	
				Bolivina spissa	-1.54	4.75	3	
				Uvigerina peregrina	-1.17	3.15	1	LIVE
				Uvigerina peregrina	-0.83	3.22	1	
				Uvigerina peregrina	-1.82	3.09	1	
				Uvigerina peregrina	-1.30	3.14	0.5	
				Uvigerina peregrina	-0.72	3.16	0.5	
				Uvigerina peregrina	-1.04	3.12	0.5	
				Gyroidinoides altiformis	-0.85	3.06	1	
				Bulimina mexicana	-1.06	3.30	4	
			4-5	*Epistominella smithi*	-1.00	4.57	2	FOSSIL
				Epistominella smithi	-1.89	4.64	3	
				Uvigerina peregrina	-1.40	4.64	1	
				Uvigerina peregrina	-1.21	4.78	1	
				Uvigerina peregrina	-1.04	4.82	1	
				Uvigerina peregrina	-1.36	4.58	1	
				Uvigerina peregrina	-1.92	4.59	3	
				Bulimina mexicana	-1.18	4.71	3	
				Bulimina mexicana	-1.51	4.71	2	
				Gyroidinoides altiformis	-0.67	3.18	2	
				Epistominella smithi	-0.63	3.22	4	LIVE
				Gyroidinoides neosoldani	-0.67	3.12	2	
				Gyroidinoides neosoldani	-0.57	3.28	1	
				Gyroidinoides neosoldani	-0.49	3.40	1	

DIVE NUMBER	SITE	TUBE-CORE	DEPTH (cm-bsf)	SPECIES	$\delta^{13}C$	$\delta^{18}O$	NO. OF INDIVIDUALS RUN	LIVE/ FOSSIL
1781	Clam Flats	31	4-5	*Globobulimina barbata*	-5.36	4.52	2	LIVE
				Globobulimina barbata	-2.77	4.47	2	
				Globobulimina pacifica	-4.56	3.20	2	
				Uvigerina peregrina	-0.95	3.14	2	
				Uvigerina peregrina	-1.53	3.14	2	
				Uvigerina peregrina	-0.78	3.07	2	
				Uvigerina peregrina	-0.78	3.28	1	
				Uvigerina peregrina	-1.05	3.23	1	
				Uvigerina peregrina	-0.86	3.23	1	
				Uvigerina peregrina	-0.51	3.13	1	
				Bulimina mexicana	-1.17	3.22	6	
				Buliminella tenuata	-2.76	4.40	3	
1780	INVERTEBRATE CLIFF CLAM BED - CLAM RING #1	30	0 - 1	*Uvigerina peregrina*	-0.85	2.83	1	LIVE
				Uvigerina peregrina	-0.54	3.01	1	
				Uvigerina peregrina	-0.32	3.19	1	
				Uvigerina peregrina	-0.71	3.06	1	
				Globobulimina pacifica	-0.92	3.28	1	
				Globobulimina pacifica	-1.36	3.28	1	
				Globobulimina pacifica	-0.74	3.30	1	
				Globobulimina pacifica	-1.46	3.28	1	
				Epistominella pacifica	-0.79	3.09	4	
				Epistominella pacifica	-0.73	3.10	3	
				Bulimina mexicana	-0.82	3.26	3	
			1 - 1.5	*Uvigerina peregrina*	-0.43	3.01	1	LIVE
				Uvigerina peregrina	-0.76	3.16	1	
				Uvigerina peregrina	-0.57	3.25	1	
				Globobulimina pacifica	-1.29	3.45	1	
				Globobulimina pacifica	-1.84	3.33	2	
				Globobulimina pacifica	-1.43	3.25	1	
				Globobulimina pacifica	-0.91	3.49	1	
				Epistominella pacifica	-0.78	3.30	3	
				Epistominella pacifica	-0.53	3.11	4	
				Bulimina mexicana	-0.70	3.26	2	
			1.5 - 2	*Uvigerina peregrina*	-0.56	3.09	1	LIVE
				Uvigerina peregrina	-0.51	3.03	1	
				Uvigerina peregrina	-0.49	3.07	1	
				Epistominella pacifica	-0.50	3.22	3	
				Epistominella pacifica	-0.72	3.23	4	
				Globobulimina pacifica	-2.14	3.39	2	
				Globobulimina pacifica	-2.17	3.35	2	
				Bulimina mexicana	-0.72	3.29	2	
			2 - 2.5	*Uvigerina peregrina*	-0.47	3.20	1	LIVE
				Uvigerina peregrina	-0.50	3.01	1	
				Epistominella pacifica	-0.73	3.14	3	
				Epistominella pacifica	-0.63	3.17	2	
				Epistominella pacifica	-0.59	3.15	2	
				Globobulimina pacifica	-1.98	3.33	2	

DIVE NUMBER	SITE	TUBE-CORE	DEPTH (cm-bsf)	SPECIES	$\delta^{13}C$	$\delta^{18}O$	NO. OF INDIVIDUALS RUN	LIVE/ FOSSIL
1780	INVERTEBRATE CLIFF CLAM BED - CLAM RING #1	30	2-2.5	*Globobulimina pacifica*	-1.15	3.38	1	LIVE
				Globobulimina pacifica	-0.92	3.34	1	
				Globobulimina pacifica	-0.41	3.38	1	
				Bulimina mexicana	-0.80	3.30	3	
				Planulina sp.	0.04	2.80	1	
			2.5 - 3	*Uvigerina peregrina*	-0.57	3.23	1	LIVE
				Uvigerina peregrina	-0.77	3.23	1	
				Uvigerina peregrina	-0.27	3.11	1	
				Epistominella pacifica	-0.53	3.15	2	
				Epistominella pacifica	-0.63	3.29	2	
				Epistominella pacifica	-0.60	3.21	2	
				Globobulimina pacifica	-1.20	3.33	1	
				Globobulimina pacifica	-1.68	3.41	1	
				Globobulimina pacifica	-2.23	3.27	2	
				Bulimina mexicana	-0.70	3.29	3	
				Planulina sp.	0.09	2.95	1	
				Globobulimina affinis	-0.90	3.29	1	
			3-4	*Epistominella smithi*	-0.59	3.15	2	LIVE
				Epistominella smithi	-0.76	3.19	4	
				Bulimina mexicana	-0.85	3.28	4	
				Globobulimina pacifica	-1.06	3.28	1	
				Globobulimina pacifica	-0.91	3.29	2	
				Globobulimina pacifica	-1.72	3.25	3	
				Globobulimina pacifica	-1.22	3.27	2	
				Uvigerina peregrina	-0.33	2.97	1	
				Uvigerina peregrina	-0.78	2.87	1	
				Uvigerina peregrina	-0.36	3.26	1	
				Uvigerina peregrina	-0.59	2.98	1	
			4-5	*Epistominella smithi*	-0.40	3.18	1	FOSSIL
				Epistominella smithi	-0.45	3.30	1	
				Epistominella smithi	-0.35	3.18	1	
				Uvigerina peregrina	-0.65	3.06	2	
				Uvigerina peregrina	-0.95	3.20	2	
				Bulimina mexicana	-0.83	3.33	3	
			4-5	*Epistominella smithi*	-0.58	3.06	3	LIVE
				Epistominella smithi	-0.43	3.16	2	
				Epistominella smithi	-0.70	3.20	3	
				Epistominella smithi	-0.48	3.16	2	
				Epistominella smithi	-0.76	3.07	4	
				Epistominella smithi	-0.77	3.06	6	
				Bulimina mexicana	-0.92	3.36	3	
				Bulimina mexicana	-0.81	3.20	4	
				Bulimina mexicana	-0.89	3.28	3	
				Globobulimina pacifica	-0.93	3.30	2	
				Globobulimina pacifica	-1.81	3.23	1	
				Globobulimina pacifica	-1.34	3.26	2	
				Globobulimina pacifica	-1.47	3.33	3	

DIVE NUMBER	SITE	TUBE-CORE	DEPTH (cm-bsf)	SPECIES	$\delta^{13}C$	$\delta^{18}O$	NO. OF INDIVIDUALS RUN	LIVE/ FOSSIL
1780	INVERTEBRATE CLIFFS CLAM BED - CLAM RING #1	30	4-5	*Uvigerina peregrina*	-0.59	2.59	1	LIVE
				Uvigerina peregrina	-0.04	3.11	1	
				Uvigerina peregrina	-0.45	2.91	1	
				Uvigerina peregrina	-0.43	3.14	1	
				Uvigerina peregrina	-0.36	3.40	1	
				Uvigerina peregrina	-0.37	3.15	1	
				Uvigerina peregrina	-0.36	3.10	1	
				Uvigerina peregrina	-0.49	2.66	1	
	INVERTEBRATE CLIFF GRAY BACTERIAL MAT - CLAM RING # 1	67	0-1	*Epistominella smithi*	-0.72	3.31	4	LIVE
				Globobulimina pacifica	-1.22	3.34	3	
			1-1.5	*Epistominella smithi*	-0.66	3.19	3	FOSSIL
				Uvigerina peregrina	-0.61	3.13	3	
			1.5-2	*Uvigerina peregrina*	-0.80	3.16	1	LIVE
				Globobulimina pacifica	-1.12	3.19	2	
				Globobulimina pacifica	-1.50	3.25	2	
			2 - 2.5	*Epistominella pacifica*	-0.59	3.21	4	
				Uvigerina peregrina	-1.04	3.14	1	
			2.5 - 3	*Epistominella pacifica*	-0.62	3.19	2	

Dive No.	Site	Hydraulic Push Core No.	Depth (cm-bsf)	Species (all are fossil (?))	$\delta^{13}C$	$\delta^{18}O$	No. of individuals run
1780	Monterey Bay - Invertebrate Cliffs Clam bed	5	0.5	*Planulina sp.*	0.13	2.55	1
				Bulimina mexicana	-0.72	3.26	3
				Uvigerina peregrina	-0.70	3.26	1
				Uvigerina peregrina	-0.95	3.17	4
				Epistominella pacifica	-0.50	3.22	1
				Epistominella pacifica	-0.41	3.47	1
				Epistominella pacifica	-0.47	3.48	1
			1.5	*Uvigerina peregrina*	-0.30	3.06	0.5
				Uvigerina peregrina	0.01	3.22	0.5
				Uvigerina peregrina	-0.12	3.27	0.5
				Epistominella pacifica	-0.64	3.34	2
				Epistominella pacifica	-0.52	3.24	2
			2.5	*Epistominella pacifica*	-0.42	3.35	1
			4	*Epistominella pacifica*	-0.33	3.23	1
				Epistominella pacifica	-0.52	3.20	1
				Bulimina mexicana	-1.04	3.28	2
				Bulimina mexicana	-1.00	3.05	2
				Globobulimina pacifica	-0.73	3.33	3
				Globobulimina pacifica	-0.78	3.38	3

Dive No.	Site	Hydraulic Push Core No.	Depth (cm-bsf)	Species (all are fossil (?))	$\delta^{13}C$	$\delta^{18}O$	No. of individuals run
1780	Monterey Bay - Invertebrate Cliffs Clam bed	5	4	*Buliminella tenuata*	-1.59	2.98	1
				Uvigerina peregrina	-0.35	3.33	1
			5.5	*Uvigerina peregrina*	-0.60	3.36	1
				Buliminella tenuata	-1.85	3.03	2
				Bulimina mexicana	-0.91	3.72	2
				Epistominella pacifica	-0.52	3.26	2
			7.5	*Epistominella pacifica*	-1.06	3.03	3
			8.5	*Epistominella pacifica*	-0.78	3.51	1
			9.5	*Epistominella pacifica*	-0.43	3.24	1
			10.5	*Epistominella pacifica*	-0.50	3.20	1
				Epistominella pacifica	-0.27	3.19	1
				Uvigerina peregrina	-0.22	3.12	0.5
				Globobulimina pacifica	-1.37	3.36	2
				Uvigerina peregrina	-0.25	3.25	1
			11.5	*Globobulimina pacifica*	-1.04	3.31	1
				Globobulimina pacifica	-1.03	3.40	1
				Epistominella pacifica	-0.41	3.28	1
				Epistominella pacifica	-0.27	3.27	1
				Uvigerina peregrina	-0.75	3.24	1
				Uvigerina peregrina	-0.83	3.34	2
				Uvigerina peregrina	-0.44	3.09	0.5
				Uvigerina peregrina	-0.66	3.22	0.5
			12.5	*Uvigerina peregrina*	-1.00	3.15	3
				Epistominella pacifica	-0.47	3.19	1
				Epistominella pacifica	-0.39	3.22	1
			13.5	*Globobulimina pacifica*	-1.17	3.61	2
				Uvigerina peregrina	-0.28	3.48	1
				Uvigerina peregrina	-0.51	3.24	1
				Bulimina mexicana	-0.84	3.68	3
				Epistominella pacifica	-0.40	3.19	1
				Epistominella pacifica	-0.43	3.34	1
			14.5	*Uvigerina peregrina*	-0.94	3.23	2
				Uvigerina peregrina	-0.50	3.36	1
				Uvigerina peregrina	-0.62	3.22	0.5
				Uvigerina peregrina	-0.51	3.12	0.5
				Bulimina mexicana	-0.73	3.51	2
				Bulimina mexicana	-0.71	3.49	2
				Epistominella pacifica	-0.36	3.21	1
				Epistominella pacifica	-0.13	3.54	1
				Epistominella pacifica	-0.47	3.16	2
				Globobulimina pacifica	-1.08	3.37	2
				Globobulimina pacifica	-1.11	3.40	2
			15.5	*Globobulimina pacifica*	-1.03	3.26	1
				Uvigerina peregrina	-0.25	3.20	1

Dive No.	Site	Hydraulic Push Core No.	Depth (cm-bsf)	Species (all are fossil (?))	$\delta^{13}C$	$\delta^{18}O$	No. of individuals run
1780	Monterey Bay - Invertebrate Cliffs Clam bed	5	15.5	*Uvigerina peregrina*	-0.08	3.10	0.5
				Epistominella pacifica	-0.33	3.35	1
				Epistominella pacifica	-0.51	3.46	1
				Buliminella tenuata	-1.36	3.54	1
			16.5	*Buliminella tenuata*	-1.09	3.50	2
				Uvigerina peregrina	-0.91	3.22	1
				Epistominella pacifica	-0.39	3.29	1
				Epistominella pacifica	-0.31	3.40	1
				Epistominella pacifica	-0.46	3.43	1
				Epistominella pacifica	-0.47	3.29	1
				Epistominella pacifica	-0.45	3.32	1
				Epistominella pacifica	-0.54	3.07	1
				Epistominella pacifica	-0.44	3.46	1
				Epistominella pacifica	-0.39	3.36	1
				Epistominella pacifica	-0.57	3.13	2
				Epistominella pacifica	-0.34	3.37	1
			17.5	*Epistominella pacifica*	-0.50	2.31	1
				Epistominella pacifica	-0.31	3.60	1
			18.5	*Epistominella pacifica*	-0.50	3.23	1
				Epistominella pacifica	-0.39	3.40	1
				Epistominella pacifica	-0.39	3.34	1
			19.5	*Epistominella pacifica*	-0.39	3.25	1
				Epistominella pacifica	-0.42	3.34	1
				Bulimina mexicana	-0.56	3.52	1
			20.5	*Uvigerina peregrina*	-0.72	3.40	1
				Uvigerina peregrina	-0.87	3.32	3
				Epistominella pacifica	-0.26	3.27	1
				Epistominella pacifica	-0.40	3.53	1
				Buliminella tenuata	-1.05	3.29	2
			21.5	*Buliminella tenuata*	-1.45	3.39	2
				Buliminella tenuata	-0.81	3.41	1
				Buliminella tenuata	-0.93	3.43	1
				Buliminella tenuata	-1.54	3.25	4
				Planulina sp.	0.22	2.70	0.5
				Planulina sp.	0.26	2.50	0.5
				Epistominella pacifica	-0.41	3.29	1
				Epistominella pacifica	-0.23	3.36	1
				Uvigerina peregrina	-0.82	3.36	1
				Uvigerina peregrina	-0.77	3.08	1
				Bulimina mexicana	-0.97	3.28	3
				Bulimina mexicana	-0.69	3.14	3
				Globobulimina pacifica	-1.35	3.37	1
				Globobulimina pacifica	-1.07	3.30	2
				Globobulimina pacifica	-0.90	3.40	1

Dive No.	Site	Hydraulic Push Core No.	Depth (cm-bsf)	Species (all are fossil (?))	$\delta^{13}C$	$\delta^{18}O$	No. of individuals run
1780	Monterey Bay - Invertebrate Cliffs Clam bed	5	21.5	*Globobulimina pacifica*	-0.81	3.49	3
				Globobulimina pacifica	-1.08	3.37	1
				Globobulimina pacifica	-0.97	3.40	1
			22.5	*Uvigerina peregrina*	-0.55	3.15	1
				Uvigerina peregrina	-0.71	3.25	1
				Bulimina mexicana	-0.87	3.49	2
				Bulimina mexicana	-0.56	3.42	2
				Globobulimina pacifica	-0.61	3.38	1
				Globobulimina pacifica	-1.07	3.33	1
				Buliminella tenuata	-1.82	3.64	1
				Epistominella pacifica	-0.34	3.31	1
			23.5	*Bulimina mexicana*	-0.57	3.64	1
				Bulimina mexicana	-0.69	3.39	3
				Epistominella pacifica	-0.44	3.22	1
				Epistominella pacifica	-0.21	3.16	1
				Buliminella tenuata	-1.35	3.18	3
				Buliminella tenuata	-1.43	3.17	2
				Globobulimina pacifica	-1.69	3.42	1
				Globobulimina pacifica	-1.04	3.29	2
				Uvigerina peregrina	-0.97	3.25	5
			24.5	*Epistominella pacifica*	-0.49	3.24	1
				Epistominella pacifica	-0.51	3.25	2
				Bulimina mexicana	-0.71	3.37	2
			25.5	*Bulimina mexicana*	-0.52	3.89	2
				Uvigerina peregrina	-0.60	3.73	1
				Uvigerina peregrina	-1.05	3.12	1
				Epistominella pacifica	-0.50	3.28	2
				Epistominella pacifica	-0.50	3.34	2
			26.5	*Buliminella tenuata*	-1.27	3.29	2
				Uvigerina peregrina	-0.72	3.28	2
				Epistominella pacifica	-0.32	3.15	1
				Epistominella pacifica	-0.29	3.15	1
				Globobulimina pacifica	-1.09	3.35	1
				Globobulimina pacifica	-1.19	3.42	1
			27.5	*Epistominella pacifica*	-0.32	3.30	1
				Epistominella pacifica	-0.60	3.22	4
			28.5	*Epistominella pacifica*	-0.38	3.47	1
			29.5	*Epistominella pacifica*	-0.34	3.30	1
				Epistominella pacifica	-0.29	3.18	1
				Epistominella pacifica	-0.31	3.27	1
				Epistominella pacifica	-0.56	3.23	1
				Epistominella pacifica	-0.38	3.26	1
				Epistominella pacifica	-0.22	3.28	1
				Epistominella pacifica	-0.40	3.02	1

Dive No.	Site	Hydraulic Push Core No.	Depth (cm-bsf)	Species (all are fossil (?))	$\delta^{13}C$	$\delta^{18}O$	No. of individuals run
1780	Monterey Bay - Invertebrate Cliffs Clam bed	5	29.5	*Epistominella pacifica*	-0.62	3.20	2
				Epistominella pacifica	-0.54	3.23	2
				Bulimina mexicana	-0.66	3.94	2
				Globobulimina pacifica	-0.87	3.30	1
				Globobulimina pacifica	-0.83	3.68	2
				Globobulimina pacifica	-1.02	3.71	3
			31.5	*Epistominella pacifica*	-0.39	3.45	1
				Epistominella pacifica	-0.68	3.26	2
				Epistominella pacifica	-0.80	3.28	3
	Monterey Bay - Invertebrate Cliffs (between yellow and white bacterial mats)	2	29.5	*Globobulimina pacifica*	-1.37	3.52	1
				Epistominella pacifica	-0.37	3.24	1
				Epistominella pacifica	-0.57	3.19	1
			30.5	*Epistominella pacifica*	-0.46	3.26	1
				Epistominella pacifica	-0.35	3.28	1
				Epistominella pacifica	-0.51	3.39	1
				Epistominella pacifica	-0.75	3.26	2
				Epistominella pacifica	-0.66	3.34	1
				Epistominella pacifica	-0.54	3.19	2
				Bulimina mexicana	-0.90	3.41	4
			31.5	*Globobulimina pacifica*	-2.01	3.57	2
				Epistominella pacifica	-0.29	3.33	1
				Epistominella pacifica	-0.45	3.48	3
			36.5	*Globobulimina pacifica*	-1.53	3.46	1
				Bulimina mexicana	-0.71	3.26	1
			38.5	*Epistominella pacifica*	-0.59	3.09	3
			39.5	*Epistominella pacifica*	-0.45	3.41	1
				Epistominella pacifica	-0.38	3.37	1
				Epistominella pacifica	-0.49	3.29	2
				Epistominella pacifica	-0.56	3.24	2
				Epistominella pacifica	-0.59	3.41	2
				Buliminella tenuata	-1.62	3.16	1
			41.5	*Uvigerina peregrina*	-0.85	3.36	1
				Epistominella pacifica	-0.62	3.38	2
				Globobulimina pacifica	-2.19	3.33	1

DIVE NUMBER	SITE	LONG CORE	Depth (cm)	SPECIES (all are fossil (?))	$\delta^{13}C$	$\delta^{18}O$	NO. OF INDIVIDUALS RUN
2052	Bubble Site	Long Core 2	0.5	*Uvigerina peregrina*	-17.01	4.44	1
				Uvigerina peregrina	-1.16	2.99	2
				Uvigerina peregrina	-0.81	2.94	1
			1.5	*Uvigerina peregrina*	-8.90	3.52	2
			3.5	*Uvigerina peregrina*	-0.74	2.93	1
				Uvigerina peregrina	-0.96	3.01	1
			4.5	*Uvigerina peregrina*	-8.03	4.02	1
				Epistominella pacifica	-0.49	3.14	2
			5.5	*Uvigerina peregrina*	-0.65	3.04	1
				Uvigerina peregrina	-0.79	2.92	1
				Uvigerina peregrina	-0.86	2.99	1
				Uvigerina peregrina	-1.23	3.90	1
				Uvigerina peregrina	-1.16	2.93	1
				Epistominella pacifica	-1.87	4.03	2
				Bulimina mexicana	-18.09	4.22	2
			6.5	*Bulimina mexicana*	-18.68	4.06	3
				Epistominella pacifica	-0.66	2.76	1
				Uvigerina peregrina	-15.31	3.84	1
				Uvigerina peregrina	-1.03	3.09	1
			7.5	*Uvigerina peregrina*	-3.07	3.94	1
				Uvigerina peregrina	-14.08	4.76	1
				Epistominella pacifica	-0.75	3.42	2
				Bulimina mexicana	-11.85	3.96	3
			8.5	*Bulimina mexicana*	-19.67	4.21	4
				Epistominella pacifica	-15.24	3.72	5
				Uvigerina peregrina	-11.56	3.96	1
			9.5	*Uvigerina peregrina*	-23.22	4.46	1
				Uvigerina peregrina	-5.37	3.72	1
				Bulimina mexicana	-21.13	4.26	2
				Epistominella pacifica	-0.90	2.94	3
			10.5	*Bulimina mexicana*	-20.48	4.51	1
				Epistominella pacifica	-0.78	2.85	1
				Epistominella pacifica	-0.85	2.85	1
				Epistominella pacifica	-0.98	2.88	1
				Epistominella pacifica	-0.50	3.04	1
				Epistominella pacifica	-0.81	2.99	1
				Uvigerina peregrina	-1.05	2.78	1
				Uvigerina peregrina	-1.80	2.14	1
				Uvigerina peregrina	-13.83	4.00	1
				Uvigerina peregrina	-1.24	2.91	1
				Uvigerina peregrina	-16.63	3.63	1
				Uvigerina peregrina	-21.93	4.27	1

DIVE NUMBER	SITE	LONG CORE	Depth (cm)	SPECIES (all are fossil (?))	$\delta^{13}C$	$\delta^{18}O$	NO. OF INDIVIDUALS RUN
2052	Bubble Site	Long Core 2	11.5	*Uvigerina peregrina*	-0.72	3.86	1
				Epistominella pacifica	-0.48	2.95	1
				Bulimina mexicana	-8.61	3.89	3
			12.5	*Bulimina mexicana*	-15.81	4.19	2
				Epistominella pacifica	-14.14	3.83	4
				Uvigerina peregrina	-11.75	3.98	1
			13.5	*Uvigerina peregrina*	-8.69	3.99	1
				Bulimina mexicana	-10.98	3.87	4
				Bulimina mexicana	-12.62	4.04	3
			14.5	*Bulimina mexicana*	-10.78	3.97	2
				Uvigerina peregrina	-10.81	4.02	1
				Epistominella pacifica	-5.92	3.85	4
			15.5	*Epistominella pacifica*	-5.37	3.91	3
				Uvigerina peregrina	-1.50	3.78	2
				Bulimina mexicana	-7.81	3.85	3
			16.5	*Uvigerina peregrina*	-13.18	4.05	1
				Epistominella pacifica	-11.54	3.93	4
			17.5	*Epistominella pacifica*	-0.78	3.51	6
				Uvigerina peregrina	-0.99	4.09	1
				Bulimina mexicana	-0.71	4.07	1
			18.5	*Bulimina mexicana*	-9.12	3.88	2
				Bulimina mexicana	-4.59	3.83	3
				Uvigerina peregrina	-1.18	3.88	2
				Epistominella pacifica	-0.16	3.83	1
	Clam Bed	Long Core 4	0.5	*Uvigerina peregrina*	-1.05	3.11	1
				Epistominella pacifica	-0.89	3.72	1
			1.5	*Epistominella pacifica*	-19.46	4.27	1
				Uvigerina peregrina	-1.19	2.81	1
				Uvigerina peregrina	-0.65	3.35	1
				Uvigerina peregrina	-0.62	3.12	1
				Uvigerina peregrina	-6.87	3.70	1
				Uvigerina peregrina	-1.09	3.01	2
			2.5	*Uvigerina peregrina*	-0.95	3.02	1
			3.5	*Uvigerina peregrina*	-0.81	2.85	1
				Uvigerina peregrina	-0.86	3.62	1
				Epistominella pacifica	-2.67	3.60	3
				Epistominella pacifica	-0.65	3.22	4
			4.5	*Epistominella pacifica*	-0.96	3.08	2
				Uvigerina peregrina	-2.90	3.84	1
			5.5	*Uvigerina peregrina*	-7.13	4.05	1
			9.5	*Uvigerina peregrina*	-1.11	2.86	1
				Uvigerina peregrina	-1.00	3.64	1

DIVE NUMBER	SITE	LONG CORE	Depth (cm)	SPECIES (all are fossil (?))	$\delta^{13}C$	$\delta^{18}O$	NO. OF INDIVIDUALS RUN
2052	Clam Bed	Long Core 4	9.5	*Epistominella pacifica*	-7.96	4.00	1
				Epistominella pacifica	-2.67	3.69	3
				Epistominella pacifica	-3.44	3.69	3
			10.5	*Epistominella pacifica*	-1.39	3.90	1
				Epistominella pacifica	-1.22	3.73	2
				Epistominella pacifica	-1.34	3.69	3
				Epistominella pacifica	-1.10	3.67	3
				Uvigerina peregrina	-0.78	3.76	1
			11.5	*Uvigerina peregrina*	-0.73	3.72	1
				Uvigerina peregrina	-1.34	3.65	1
				Uvigerina peregrina	-0.80	3.75	1
				Uvigerina peregrina	-0.46	3.89	0.5
				Uvigerina peregrina	-1.11	3.70	0.5
				Uvigerina peregrina	-1.20	3.66	1
				Uvigerina peregrina	-1.29	3.64	1
				Epistominella pacifica	-0.79	3.68	2
			12.5	*Epistominella pacifica*	-0.75	3.62	2
				Epistominella pacifica	-0.81	3.58	3
				Uvigerina peregrina	-0.78	3.58	0.5
				Uvigerina peregrina	-0.51	3.78	0.5
			13.5	*Uvigerina peregrina*	-0.97	3.62	1
				Uvigerina peregrina	-0.85	3.73	1
				Epistominella pacifica	-1.03	3.48	4
			14.5	*Epistominella pacifica*	-0.74	3.71	2
				Uvigerina peregrina	-0.62	4.00	1
				Uvigerina peregrina	-0.52	3.71	1
			15.5	*Uvigerina peregrina*	-0.87	3.80	1
				Uvigerina peregrina	-0.61	3.82	1
				Epistominella pacifica	-0.83	3.59	3
			16.5	*Epistominella pacifica*	-1.27	3.69	3
				Uvigerina peregrina	-2.04	3.67	2
			17.5	*Epistominella pacifica*	-8.86	4.30	1
			18.5	*Uvigerina peregrina*	-1.38	3.61	1
				Uvigerina peregrina	-0.74	3.70	1
	Bacterial Mat	Long Core 5	0.5	*Uvigerina peregrina*	-0.95	3.57	3
			1.5	*Uvigerina peregrina*	-1.16	2.99	1
				Uvigerina peregrina	-6.97	3.70	2
				Epistominella pacifica	-0.32	3.46	3
			2.5	*Epistominella pacifica*	-0.55	3.37	3
				Uvigerina peregrina	-0.65	3.85	1
				Uvigerina peregrina	-1.03	3.61	1
			3.5	*Uvigerina peregrina*	-1.18	3.93	1
			9.5	*Uvigerina peregrina*	-1.22	3.66	2

DIVE NUMBER	SITE	LONG CORE	Depth (cm)	SPECIES (all are fossil (?))	$\delta^{13}C$	$\delta^{18}O$	NO. OF INDIVIDUALS RUN
2052	Bacterial Mat	Long Core 5	9.5	*Epistominella pacifica*	-0.48	3.82	1
			11.5	*Epistominella pacifica*	-1.01	3.60	4
			12.5	*Uvigerina peregrina*	-1.13	3.60	1
			13.5	*Uvigerina peregrina*	-0.58	3.77	2
			14.5	*Uvigerina peregrina*	-0.49	3.71	1
				Epistominella pacifica	-0.74	3.72	3
			15.5	*Epistominella pacifica*	-0.94	3.66	4
				Uvigerina peregrina	-0.65	3.78	1
				Uvigerina peregrina	-0.73	3.70	1
				Uvigerina peregrina	-0.86	3.64	1
			16.5	*Uvigerina peregrina*	-1.08	3.58	2
			17.5	*Uvigerina peregrina*	-1.12	3.67	2
				Epistominella pacifica	-0.87	3.70	3
			18.5	*Epistominella pacifica*	-0.77	3.73	3
				Epistominella pacifica	-0.88	3.67	3
				Uvigerina peregrina	-0.67	3.83	1
				Uvigerina peregrina	-1.24	3.62	3
			19.5	*Uvigerina peregrina*	-1.12	3.66	2
				Uvigerina peregrina	-1.29	3.60	3
				Epistominella pacifica	-0.85	3.57	5
			20.5	*Epistominella pacifica*	-0.83	3.69	3
				Epistominella pacifica	-0.99	3.97	4
				Uvigerina peregrina	-0.88	3.72	1
				Uvigerina peregrina	-0.78	3.81	1
				Uvigerina peregrina	-0.91	3.73	1
			21.5	*Uvigerina peregrina*	-1.00	3.60	4
				Epistominella pacifica	-0.92	3.57	4
			22.5	*Epistominella pacifica*	-0.85	3.61	4
				Uvigerina peregrina	-0.73	3.71	1
				Uvigerina peregrina	-0.71	3.96	1
				Uvigerina peregrina	-0.41	3.79	0.5
			23.5	*Uvigerina peregrina*	-1.77	3.84	1
				Uvigerina peregrina	-0.82	3.69	1
				Epistominella pacifica	-0.65	3.70	2
			24.5	*Uvigerina peregrina*	-0.90	3.66	1
				Uvigerina peregrina	-1.24	3.53	4
				Uvigerina peregrina	-1.21	3.71	4
			25.5	*Uvigerina peregrina*	-0.93	3.65	1
				Uvigerina peregrina	-0.68	3.97	1
				Epistominella pacifica	-0.57	3.75	3
			26.5	*Epistominella pacifica*	-0.50	3.73	2
				Uvigerina peregrina	-4.48	3.79	0.5
				Uvigerina peregrina	-0.67	3.72	1
			27.5	*Uvigerina peregrina*	-11.59	3.91	1

APPENDIX C
SEM PHOTOMICROGRAPHS

For all of the following, the picture on the left will show an overall view of the foraminifera, whereas the picture on the right will be a close-up of an identified region.

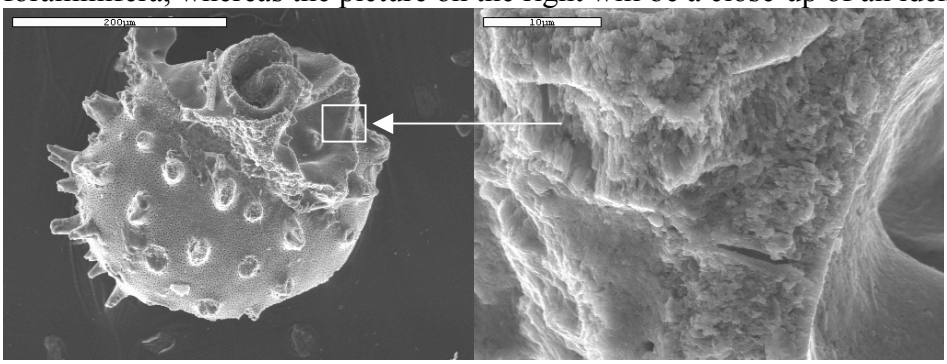

(a). Broken live *Uvigerina peregrina* (top portion near aperture) from Dive 1780 PC30 (Invertebrate Cliffs (IC) clam bed) 0-1 cm.

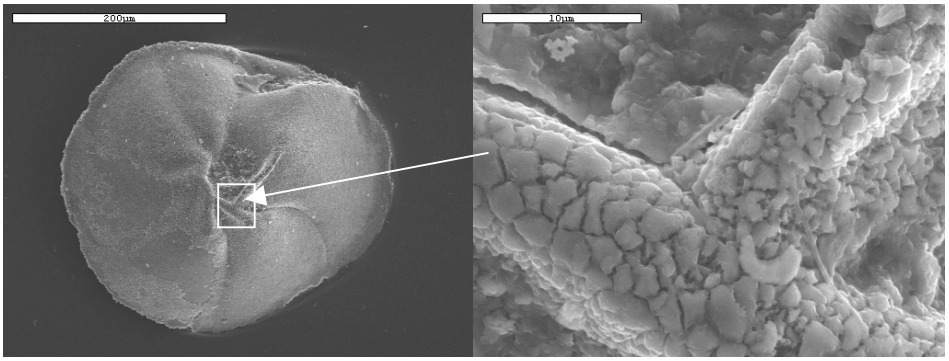

(b). A live *Epistominella smithi* from Dive 1780 PC67 0-1cm (IC gray bacterial mat).

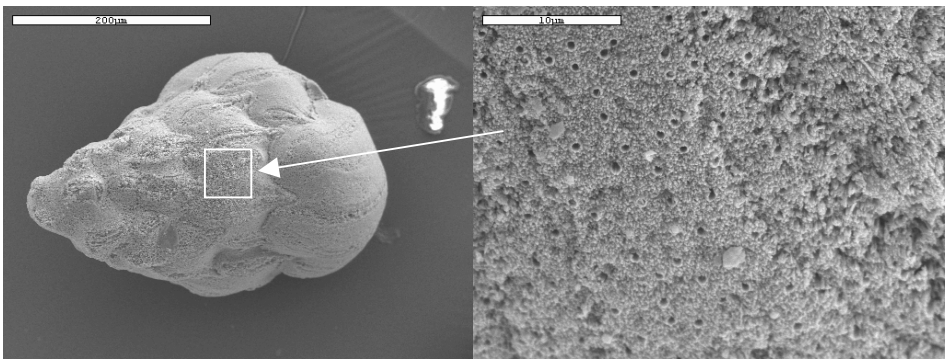

(c). A fossil (?) *U. peregrina* from Dive 1780 HPC5 15-16 cm (IC clam bed).

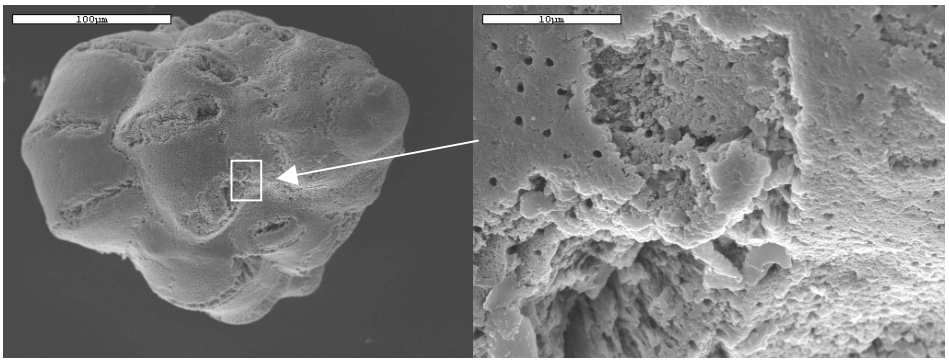

(d). A fossil (?) *U. peregrina* from Dive 1780 HPC5 21-22 cm (IC clam bed).

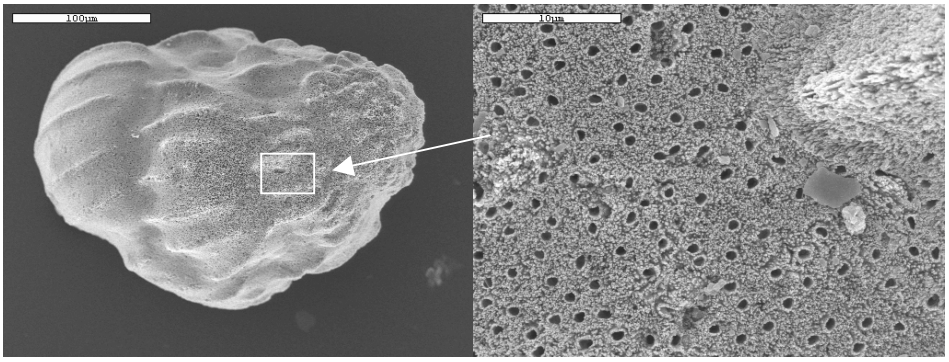

(e). A fossil (?) *U. peregrina* from Dive 1780 HPC5 29-30 cm (IC clam bed).

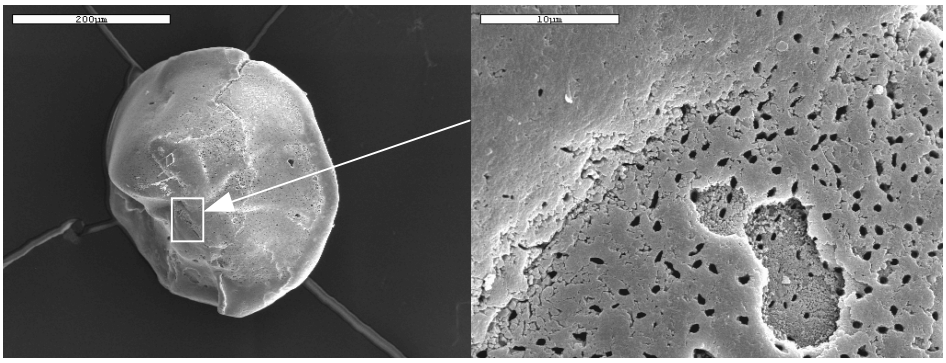

(f). A fossil (?) *E. pacifica* from Dive 1780 HPC5 0-1 cm (IC clam bed).

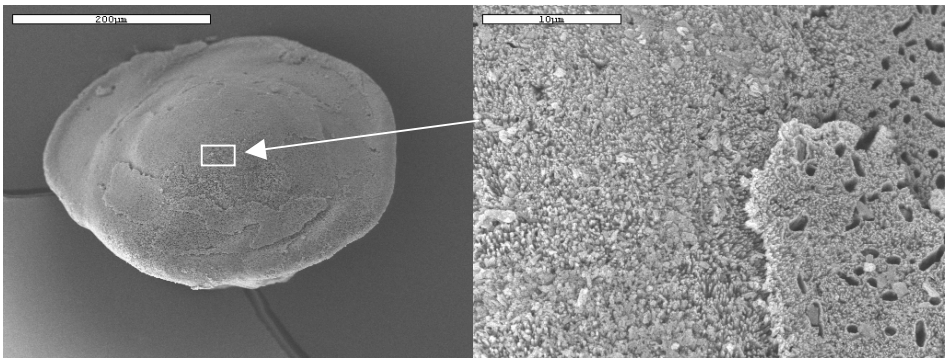

(g). A fossil (?) *E. pacifica* from Dive 1780 HPC5 16-17 cm (IC clam bed). The micrograph shows the dorsal view.

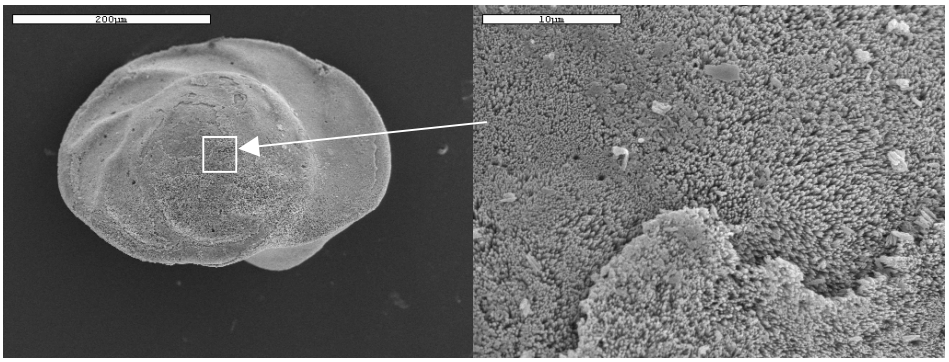

(h). A dorsal view of a fossil (?) *E. pacifica* photographed prior to cleaning from Dive 1780 HPC5 27-28 cm (IC clam bed).

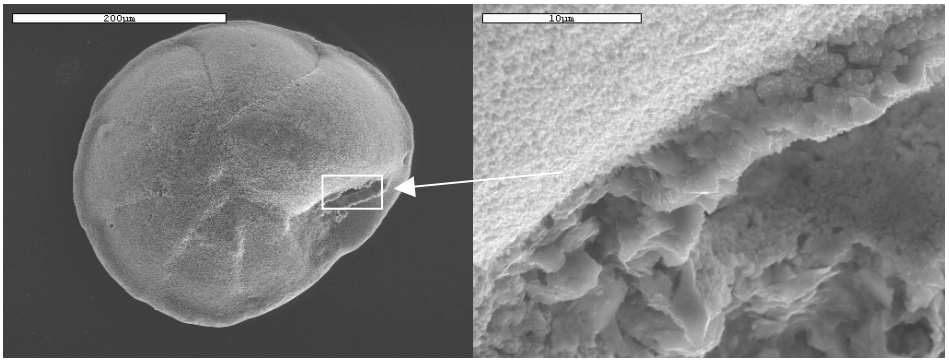

(i). A fossil (?) *E. pacifica* from 2052 LC2 10-11 cm (Eel River Basin (ERB) bubble site).

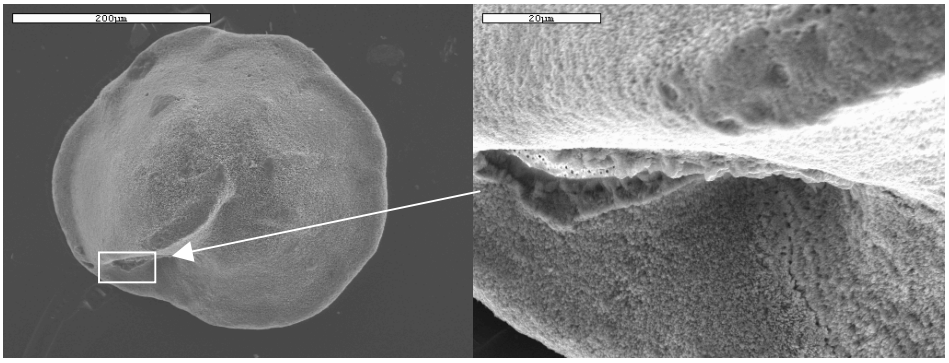

(j). A fossil (?) *E. pacifica* from 2052 LC4 1-2 cm (ERB clam bed). Specimen was not cleaned before photographing.

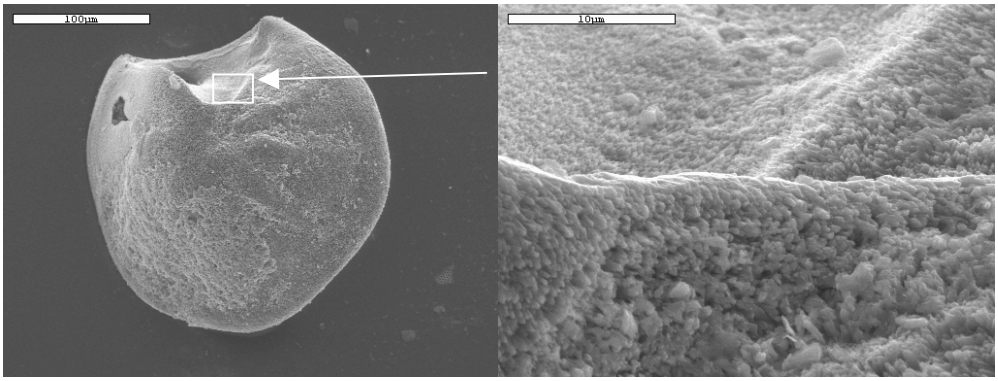

(k). A fossil (?) *E. pacifica* from Dive 2052 LC4 11-12 cm (ERB clam bed) photographed prior to cleaning.

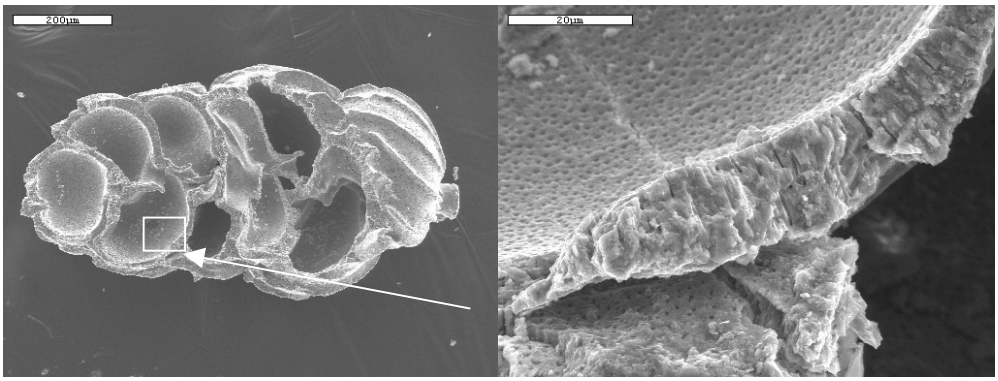

(l). A view inside the test of a fossil (?) *U. peregrina* from Dive 2052 LC4 12-13 cm (ERB clam bed).

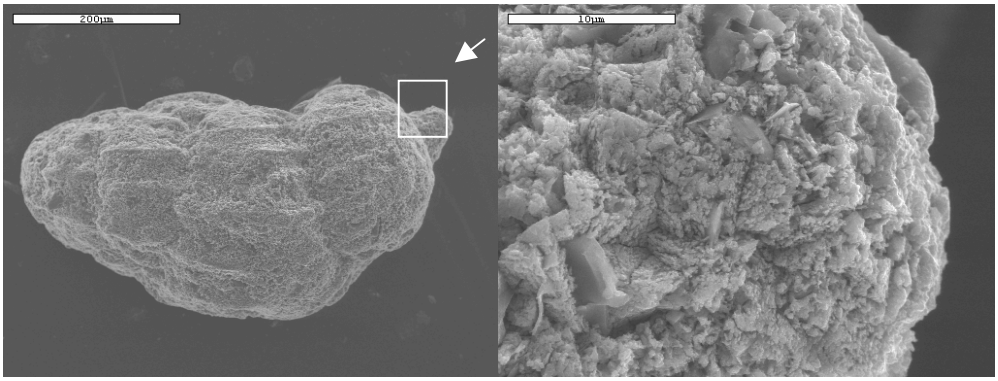

(m). A fossil (?) *U. peregrina* from Dive 2052 LC4 17-18 cm (ERB clam bed).

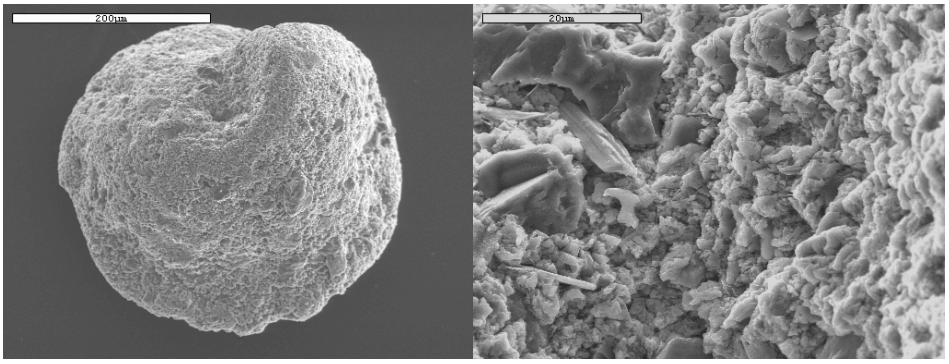

(n). A fossil (?) *E. pacifica* (?) from Dive 2052 LC4 18-19 cm (ERB clam bed).

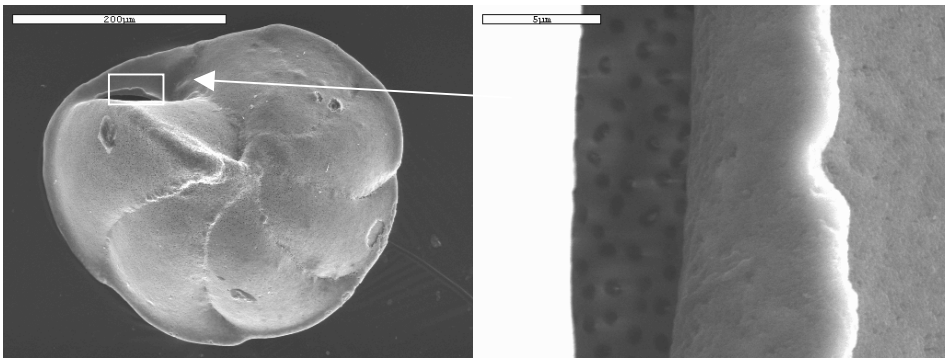

(o). A fossil (?) *E. pacifica* from Dive 2052 LC5 0-1 cm (ERB bacterial mat).

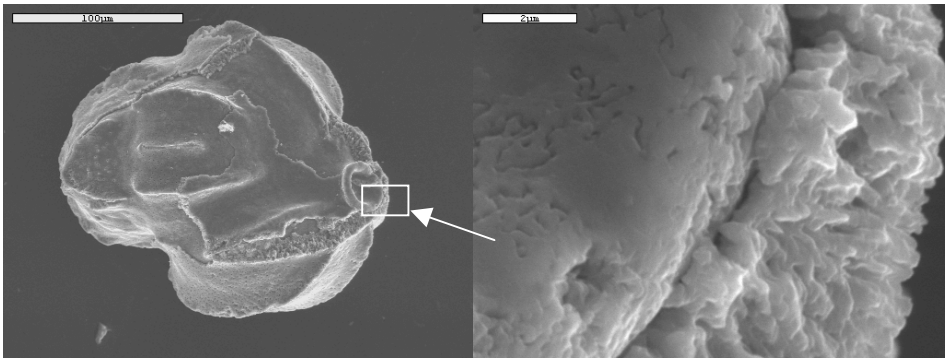

(p). A fossil (?) *U. peregrina* from Dive 2052 LC5 1-2 cm (ERB bacterial mat).

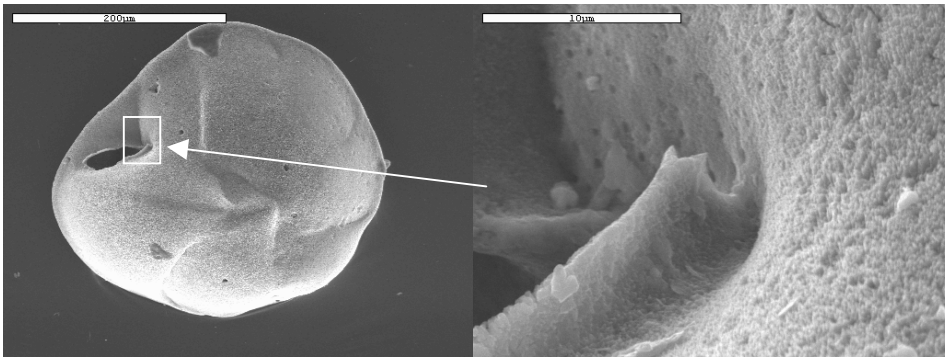

(q). A fossil (?) *E. pacifica* from Dive 2052 LC5 12-13 cm (ERB bacterial mat).

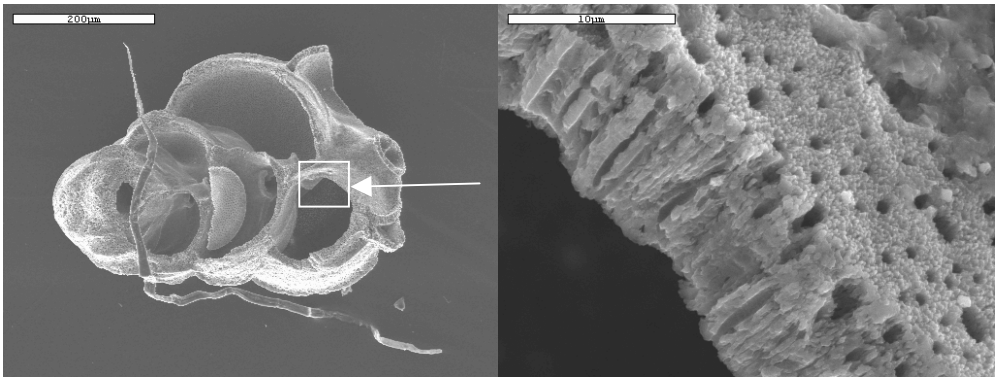

(r). A fossil (?) *U. peregrina* from Dive 2052 LC5 15-16 cm (ERB bacterial mat). A hair and possibly a fragment of a diatom were transferred to the foram during SEM preparation.

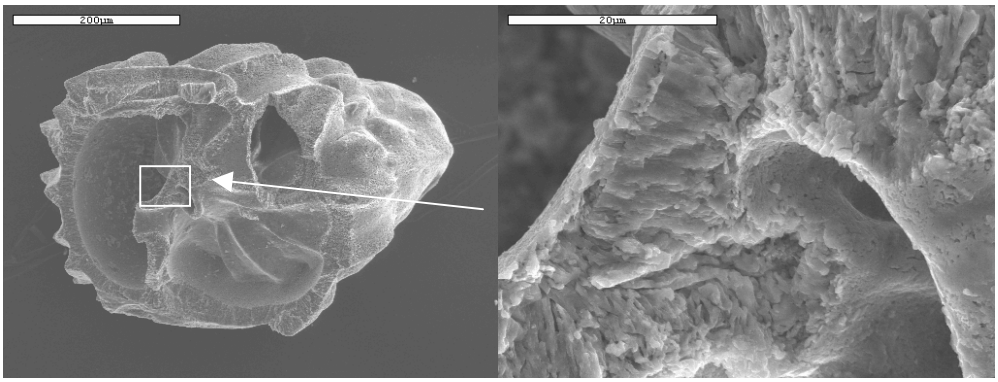

(s). A broken fossil (?) *U. peregrina* from Dive 2052 LC5 25-26 cm (ERB bacterial mat).

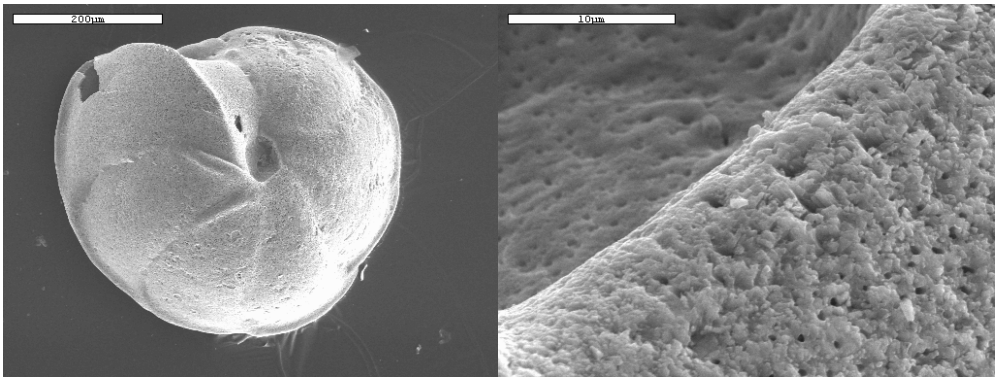

(t). A fossil (?) *E. pacifica* from Dive 2052 LC1 4-5 cm (ERB reference core) photographed prior to cleaning.

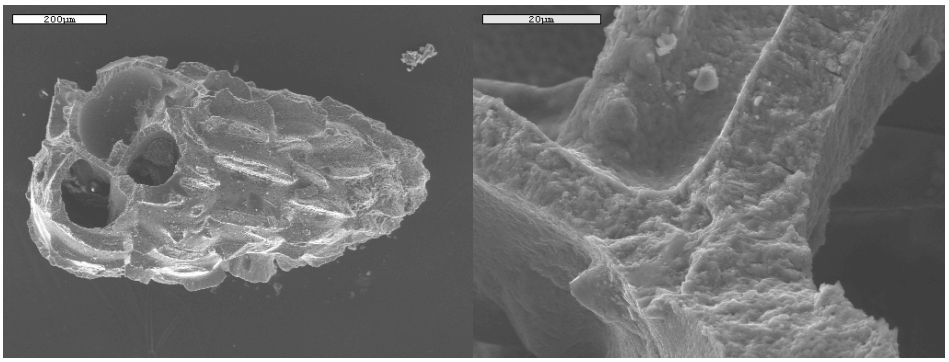

(u). A broken fossil (?) *U. peregrina* from Dive 1781 HPC5 0-1 cm (Clam Flats clam bed). Photographed before cleaning.

LIST OF REFERENCES

Aharon, P., E.R. Graber, and H.H. Roberts, 1992. Dissolved carbon and $\delta^{13}C$ anomalies in the water column caused by hydrocarbon seeps on the northwestern Gulf of Mexico slope. Geo-Marine Letters, 12: 33-40.

Aharon, P. M. Hackworth, E. Platon, C. Wheeler, and B. Sen Gupta, 2001. Isotope records of recent benthic foraminifera from hydrate-bearing sediments: methane-hydrate dissociation effects. GSA Abstracts with Programs, 33: A162.

Barry, J.P., H.G. Greene, D.L. Orange, C.H. Baxter, B.H. Robison, R.E. Kochevar, J.W. Nybakken, D.L. Reed, and C.M. McHugh, 1996. Biologic and geologic characteristics of cold seeps in Monterey Bay, California. Deep-Sea Research, 43 (11-12): 1739-1762.

Barry, J.P., R.E. Kochevar, and C.H. Baxter, 1997. The influence of pore-water chemistry and physiology on the distribution of vesicomyid clams at cold seeps in Monterey Bay: Implications for patterns of chemosynthetic community organization. Limnology and Oceanography, 42 (2): 318-328.

Berner, R.A., 1980. *Early Diagenesis: A Theoretical Approach*. Princeton University Press, Princeton, New Jersey.

Bernhard, J.M., 1988. Postmortem vital staining in benthic foraminifera: duration and importance in population and distributional studies. Journal of Foraminiferal Research, 18 (2): 143-146.

Bernhard, J.M., K.R. Buck, and J.P. Barry, 2001. Monterey Bay cold-seep biota: Assemblages, abundance, and ultrastructure of living foraminifera. Deep-Sea Research I, 48: 2233-2249.

Blair, N.E., and R.C. Aller, 1995. Anaerobic methane oxidation on the Amazon shelf. Geochimica et Cosmochimica Acta, 59 (18): 3707-3715.

Blunier, Thomas. 2000. "Frozen" methane escapes from the seafloor. Science, 288: 68-69.

Boltovskoy, E., and R. Wright, 1976. *Recent Foraminifera*. Dr. W. Junk Publishers, The Hague.

Brewer, P.G., F.M. Orr, G. Friederich, K.A. Kvenvolden, D.L. Orange, J. McFarlane, and W. Kirkwood, 1997. Deep-ocean field test of methane hydrate formation from a remotely operated vehicle. Geology, 25 (5): 407-410.

Brooks, J.M., M.E. Field, and M.C. Kennicutt II, 1991. Observations of gas hydrates in marine sediments, offshore northern California. Marine Geology, 96: 103-109.

Burger, R.L., C.S. Fulthorpe, J.A. Austin Jr., and S. P.S. Gulick, 2002. Lower Pleistocene to present structural deformation and sequence stratigraphy of the continental shelf, offshore Eel River Basin, northern California. Marine Geology, 185: 249-281.

Cavagna, S., P. Clari, and L. Martire, 1999. The role of bacteria in the formation of cold seep carbonates: geological evidence from Monferrato (Tertiary, NW Italy). Sedimentary Geology, 126: 253-270.

Corliss, B.H., 1985. Microhabitats of benthic foraminifera within deep-sea sediments. Nature, 314 (4): 435-438.

Corliss, B.H. and S. Emerson, 1990. Distribution of Rose Bengal stained deep-sea benthic foraminifera from the Nova Scotian continental margin and Gulf of Maine. Deep-Sea Research, 37 (3): 381-400.

Curry, W.B., J.C. Duplessy, L.D. Labeyrie, and N.J. Shackleton, 1988. Changes in the distribution of $\delta^{13}C$ of deep water ΣCO_2 between the last glaciation and the Holocene. Paleoceanography, 3 (3): 317-341.

DeLong, E.F., 2000. Resolving a methane mystery. Nature, 407: 577-579.

Dickens, Gerald R., 2001. The potential volume of oceanic methane hydrates with variable external conditions. Organic Geochemistry, 32: 1179-1193.

Dickens, G.R., J.R. O'Neil, D.K. Rea, and R.M. Owen, 1995. Dissociation of oceanic methane hydrate as a cause of the carbon isotope excursion at the end of the Paleocene. Paleoceanography, 10: 965-971.

Furlong, K.P. and R. Govers, 1999. Ephemeral crustal thickening at a triple junction: the Mendocino crustal conveyor. Geology, 27: 127-130.

Gieskes, J.M., T. Gamo, and H. Brumsack, 1991. Chemical methods for interstitial water analysis on JOIDES Resolution. ODP Technical Note 15, 60 p.

Goldstein, S.T., 1999. "Foraminifera: A biological overview." *Modern Foraminifera*. Ed. B.K. Sen Gupta. Kluwer Academic Publishers, London, England. 37-55.

Goldstein, S.T., and B.H. Corliss, 1994. Deposit feeding in selected deep-sea and shallow-water benthic foraminifera. Deep-Sea Research, 41: 229-241.

Greene, H.G., D.L. Orange, and J.P. Barry, 1993. Geologic diversity of cold seep communities, Monterey Bay region, central California, USA. Transactions, American Geophysical Union, 74: 578.

Greene, H.G., W.L. Stubblefield, and A.E. Theberge Jr., 1989. Geology of the Monterey submarine canyon system and adjacent areas offshore central California. USGS Open File Report, 89-221.

Grossman, E.L., 1987. Stable isotopes in modern benthic foraminifera: a study of vital effect. Journal of Foraminiferal Research, 17(1): 48-61.

Houghton, J.T., G.J. Jenkins and J.J Ephraums, (eds.), 1990. *Climate Change: The IPCC Scientific Assessment*. Cambridge Univ Press, New York, New York.

Jorrisen, F.J., 1999. "Benthic foraminiferal microhabitats below the sediment-water interface." *Modern Foraminifera*. Ed. B.K. Sen Gupta. Kluwer Academic Publishers, London, England. 37-55.

Kennett, J.P., I.L. Hendy, and R. J. Behl, 1996. Late Quaternary foraminiferal carbon isotopic record in Santa Barbara Basin: Implications for rapid climate change. Eos Trans. AGU 77 (46): 294.

Kennett, J.P., K.G. Cannariato, I.L. Hendy, and R.J. Behl, 2000. Carbon isotopic evidence for methane hydrate instability during quaternary interstadials. Science, 288: 128-133.

Kvenvolden, K., 1988. Methane hydrates and global climate change. Global Biogeochemical Cycles, 2: 221-229.

Kvenvolden, K.A., and M.E. Field, 1985. Gas hydrates on the northern California continental margin. Geology, 13: 517-520.

Kvenvolden, K.A, G.D. Ginsburg, and V.A. Soloviev, 1993. Worldwide distribution of subaquatic gas hydrates. Geo-Marine Letters, 13: 32-40.

LaRock, P.A., J.-H. Hyun, and B.W. Bennison, 1994. Bacterioplankton growth and production at the Louisiana hydrocarbon seeps. Geo-Marine Letters, 14: 104-109.

Lewis, R.C., K.H. Coale, B.D. Edwards, M. Marot, J. N. Douglas, and E.J. Burton, 2002. Accumulation rate and mixing of shelf sediments in the Monterey Bay National Marine Sanctuary. Marine Geology, 181: 157-169.

Lorenson, T.D., K.A. Kvenvolden, F.D. Hostettler, R.J. Rosenbauer, D.L. Orange, and J.B. Martin, 2002. Hydrocarbon geochemistry of cold seeps in the Monterey Bay National Marine Sanctuary. Marine Geology, 181: 285-304.

MacDonald, G.J., 1990. Role of methane clathrates in past and future climates. Climatic Change, 16: 247-281.

Mackensen, A., and R.G. Douglas, 1989. Down-core distribution of live and dead deep-water benthic foraminifera in box cores from the Wedell Sea and the California continental borderland. Deep-Sea Research, 36 (6): 879-900.

Martin, J.B., M. Kastner, P. Henry, X. LePichon, and S. Lallement, 1996. Chemical and isotopic evidence for sources of fluids in a mud volcano field seaward of the Barbados accretionary wedge. Journal of Geophysical Research, 101: 20325-20345.

Martin, J.B., D.L. Orange, T.D. Lorenson, and K.A. Kvenvolden, 1997. Chemical and isotopic evidence of gas-influenced flow at a transform plate boundary: Monterey Bay, California. Journal of Geophysical Research, 102: 24903-24915.

McConnaughey, T., 1989. ^{13}C and ^{18}O isotopic disequilibrium in biological carbonates: I patterns. Geochimica et Cosmochimica acta, 53: 151-162.

McCorkle, D.C., L.D. Keigwin, B.H. Corliss, and S.R. Emerson, 1990. The influence of microhabitats on the carbon isotopic composition of deep-sea benthic foraminifera. Paleoceanography, 5: 161-185.

McCorkle, D.C., B.H. Corliss, and C.A. Farnham, 1997. Vertical distributions and stable isotopic compositions of live (stained) benthic foraminifera from the North Carolina and California continental margins. Deep Sea Research I, 44 (6): 983-1024.

Nisbet, E. 1990. Climate change and methane. Nature, 347: 23.

Orange, D.L., H.G. Greene, D. Reed, J.B. Martin, C.M. McHugh, W.B.F. Ryan, N. Maher, D. Stakes, and J.P. Barry, 1999. Widespread fluid expulsion on a translational continental margin: Mud volcanoes, fault zones, headless canyons, and organic-rich substrate in Monterey Bay, California. GSA Bulletin, 111 (7): 992-1009.

Parkhurst, D.L. and Appelo, C.A.J., 1999, User's guide to PHREEQC (Version 2)—A computer program for speciation, batch-reaction, one-dimensional transport, and inverse geochemical calculations: U.S. Geological Survey Water-Resources Investigations Report 99-4259, 310 p.

Page, B.M., 1970. Sur-Nacimiento fault zone of California: Continental margin tectonics. GSA Bulletin, 81: 667-690.

Rathburn A.E., and B.H. Corliss, 1994. The ecology of living (stained) deep-sea benthic foraminifera from the Sulu Sea. Paleoceanography, 9 (1): 87-150.

Rathburn, A.E., B.H. Corliss, K.D. Tappa, and K.C. Lohmann, 1996. Comparisons of the ecology and stable isotopic compositions of living (stained) deep-sea benthic foraminifera from the Sulu and South China Seas. Deep-Sea Research 43 (10): 1617-1646.

Rathburn, A.E., L. Levin, Z. Held, and K.C. Lohmann, 2000. Benthic foraminifera associated with cold methane seeps on the northern California margin: Ecology and stable isotopic composition. Marine Micropaleontology, 38: 247-266.

Reeburgh, W.S., 1976. Methane consumption in Cariaco Trench waters and sediments. Earth and Planetary Science Letters, 28: 337-344.

Reimers, C.E., K.C. Ruttenberg, D.E. Cannfield, M.B. Christiansen, and J.B. Martin, 1996. Pore water pH and authigenic phases formed in the uppermost sediments of the Santa Barbara Basin. Geochimica et Cosmochimica Acta, 60 (21): 4037-4057.

Seigle, G.A., 1973. Pyritization in living foraminifers. Journal of Foraminiferal Research, 3(1): 1-6.

Sen Gupta, B.K., and P. Aharon, 1994. Benthic foraminifera of bathyal hydrocarbon vents of the Gulf of Mexico: Initial Report on communities and stable isotopes. Geo-marine Letters, 14: 88-96.

Sen Gupta, B.K., E. Platon, J.M. Bernhard, and P. Aharon, 1997. Foraminiferal colonization of hydrocarbon-seep bacterial mats and underlying sediment, Gulf of Mexico slope. Journal of Foraminiferal Research, 27 (4): 292-300.

Severinghaus, J.P., T. Sowers, E.J. Brook, R.B. Alley, and M.L. Bender, 1998. Timing of abrupt climate change at the end of the Younger-Dryas interval from thermally fractionated gases in polar ice. Nature, 391 (6663): 141-146.

Sommerfield, C.K., and C.A. Nittrouer, 1999. Modern accumulation rates and a sediment budget for the Eel Shelf: A flood-dominated depositional environment. Marine Geology, 154: 227-241.

Stakes, D.S., D.L. Orange, J.B. Paduan, K.A. Salamy, and N. Maher, 1999. Cold-seeps and authigenic carbonate formation in Monterey Bay, California. Marine Geology, 159: 93-109.

Stott, L.D. W. Berelson, R. Douglas, and D. Gorsline, 2000. Increased dissolved oxygen in Pacific intermediate waters due to lower rates of carbon oxidation in sediments. Nature, 407 (6802): 367-370.

Stott, L.D., T. Bunn, M. Prokopenko, C. Mahn, J. Gieskes, and J.M. Bernhard, 2002. Does the oxidation of methane leave an isotopic fingerprint in the geologic record? Geochemistry Geophysics Geosystems, 3(2), 10.1029/2001GC000196, 2002.

Valentine, D.L., D.C. Blanton, W.S. Reeburgh, and M. Kastner, 2001. Water column methane oxidation adjacent to an area of active hydrate dissociation, Eel River Basin. Geochimica et Cosmochimica Acta, 65 (16): 2633-2640.

Wallman, K., P. Linke, E. Suess, G. Bohrmann, H. Sahling, M. Schlüter, A. Dahlmann, S. Lammers, J. Greinert, and N. Von Mirbach, 1997. Quantifying fluid flow, solute mixing, and biogeochemical turnover at cold vents of the eastern Aleutian subduction zone. Geochimica et Cosmochimica Acta, 61: 5209-5219.

Walton, W.R., 1952. Techniques for recognition of living foraminifera. Cushman Foundation for Foraminiferal Research, 3 (2): 56-60.

Wefer, G., P.M. Heinze, and W.H. Berger, 1994. Clues to ancient methane release. Nature, 369: 282.

Whiticar, Michael J., 1999. Carbon and hydrogen isotope systematics of bacterial formation and oxidation of methane. Chemical Geology, 161: 291-314.

Williams, David, A. Duncan, A. Backherms, E.M. Perez, A.E. Rathburn, J.B. Martin, S. Day, J. Gieskes, C. Mahn, and W. Ziebes, 2002. Stable isotopic compositions of living methane seep foraminifera: Applications for paleoceanography. GSA Abstracts with Programs, 34 (6): 31.

BIOGRAPHICAL SKETCH

Shelley Day was born December 30, 1976 in Boynton Beach, Florida. She graduated from the University of Florida in August of 2000, with a Bachelor of Science degree in geology and a minor in chemistry. She continued her education at the University of Florida, where she received her Master of Science degree in May 2003.